Regulation of MYC Activity by the Ubiquitin-Proteasome System

Regulation der MYC Aktivität durch das Ubiquitin-Proteasom-System

Doctoral thesis

for a doctoral degree
at the Graduate School of Life Sciences,
Julius-Maximilians-Universität Würzburg,
Section Biomedicine

submitted by

Laura Annika Jänicke
from Berlin

Würzburg 2015

Members of the Thesis Committee

Chairperson: Prof. Alexander Buchberger

Primary Supervisor: Prof. Martin Eilers
Second Supervisor: Prof. Hermann Schindelin
Third Supervisor: Prof. Thomas Sommer
Fourth Supervisor: Nikita Popov, PhD

Submitted on:

Date of Public Defence:

Date of Receipt of Certificates:

Table of content

Summary 5

Zusammenfassung 6

1 Introduction 8

1.1 Ubiquitin-proteasome system (UPS) 8

1.2 The ubiquitin-proteasome system in transcriptional regulation 11

1.3 The oncogenic transcription factor MYC 16

1.4 Objectives of the thesis 28

2 Materials 29

2.1 Chemicals 29

2.2 Buffers and solutions 29

2.3 Standards, enzymes and kits 34

2.4 Nucleic acids 35

2.5 Antibodies 39

2.6 Peptides 40

2.7 Strains and cell lines 40

2.8 Cultivation media and supplements 41

2.9 Consumables 42

2.10 Equipment and membranes 42

2.11 Software and online programs 44

3 Methods 45

3.1 Cell biology methods 45

3.2 Molecular biology methods 51

3.3 Biochemical methods 57

3.4 Next-generation sequencing 65

4 Results 67

4.1 MYC is a ubiquitinated protein 67

4.2 K-less MYC retains significant biological activity 69

4.3 K-less MYC is unable to induce proliferation and apoptosis in immortalized mammary epithelial cells 74

4.4 K-less MYC binds to known MYC-regulated promoters 79
4.5 K-less MYC is a weaker transcriptional regulator 84
4.6 Distinct lysine residues can restore K-less MYC function 87
4.7 Proteasomal activity is required for MYC target gene induction 94
4.8 Release of elongating RNAPII is impaired in K-less MYC expressing cells 100
4.9 K-less MYC is impaired in the recruitment of cofactors to MYC-regulated promoters 106
4.10 Identification of a MYC-PAF-complex as an intermediate in transcriptional activation 109

5 Discussion 114

5.1 MYC ubiquitination occurs on multiple lysines 114
5.2 K-less MYC, a tool to study effects of MYC ubiquitination 116
5.3 MYC function can be mediated by diverse ubiquitin acceptor sites 122
5.4 Proteasomal activity is required for MYC target gene induction 124
5.5 K-less MYC is impaired in promoting efficient elongation 128
5.6 Ubiquitination of MYC is required for cofactor recruitment 131
5.7 Impaired MYC turnover enables the identification of an intermediate step in MYC-dependent transcription 134
5.8 Cancer-associated mutations stabilize MYC – how does that fit to the model? ... 136
5.9 Cooperation of MBI and MBII in transcriptional activation 138

6 Bibliography 139

7 Appendix 159

7.1 Abbreviations 159
7.2 Acknowledgements 164
7.3 Publications 165
7.4 Curriculum vitae 166
7.5 Affidavit 167

Summary

The oncogenic MYC protein is a transcriptional regulator of multiple cellular processes and is aberrantly activated in a wide range of human cancers. MYC is an unstable protein rapidly degraded by the ubiquitin-proteasome system. Ubiquitination can both positively and negatively affect MYC function, but its direct contribution to MYC-mediated transactivation remained unresolved.

To investigate how ubiquitination regulates MYC activity, a non-ubiquitinatable MYC mutant was characterized, in which all lysines are replaced by arginines (K-less MYC). The absence of ubiquitin-acceptor sites in K-less MYC resulted in a more stable protein, but did not affect cellular localization, chromatin-association or the ability to interact with known MYC interaction partners.

Unlike the wild type protein, K-less MYC was unable to promote proliferation in immortalized mammary epithelial cells. RNA- and ChIP-Sequencing analyses revealed that, although K-less MYC was present at MYC-regulated promoters, it was a weaker transcriptional regulator. The use of K-less MYC, a proteasomal inhibitor and reconstitution of individual lysine residues showed that proteasomal turnover of MYC is required for MYC target gene induction. ChIP-Sequencing of RNA polymerase II (RNAPII) revealed that MYC ubiquitination is dispensable for RNAPII recruitment and transcriptional initiation but is specifically required to promote transcriptional elongation. Turnover of MYC is required to stimulate histone acetylation at MYC-regulated promoters, which depends on a highly conserved region in MYC (MYC box II), thereby enabling the recruitment of BRD4 and P-TEFb and the release of elongating RNAPII from target promoters. Inhibition of MYC turnover enabled the identification of an intermediate in MYC-mediated transactivation, the association of MYC with the PAF complex, a positive elongation factor, suggesting that MYC acts as an assembly factor transferring elongation factors onto RNAPII. The interaction between MYC and the PAF complex occurs via a second highly conserved region in MYC's amino terminus, MYC box I.

Collectively, the data of this work show that turnover of MYC coordinates histone acetylation with recruitment and transfer of elongation factors on RNAPII involving the cooperation of MYC box I and MYC box II.

Zusammenfassung

Der Transkriptionsfaktor MYC ist an der Regulation einer Vielzahl biologischer Prozesse beteiligt ist und spielt bei der Tumorentstehung und des Tumorwachstum eine entscheidende Rolle. MYC ist ein kurzlebiges Protein, das durch das Ubiquitin-Proteasom-System abgebaut wird. Die Ubiquitinierung von MYC hat auch einen stimulierenden Einfluss auf dessen transkriptionelle Aktivität. Dabei blieb jedoch der Mechanismus, der dieser Beobachtung zugrunde liegt, bislang ungeklärt.

Um den direkten Einfluss von Ubiquitinierung auf die Aktivität von MYC zu untersuchen, wurde in der vorliegenden Arbeit eine MYC Mutante analysiert, in der alle Lysine zu Argininen mutiert wurden (K-less MYC). Die Mutation der Ubiquitin-Verknüpfungsstellen resultierte in einem stabileren Protein, hatte jedoch keinen Einfluss auf die zelluläre Lokalisation oder Assoziation mit bekannten Interaktionspartnern. Im Vergleich zu Wildtyp (WT) MYC war K-less MYC jedoch in der Vermittlung MYC-induzierter biologischer Phänotypen stark beeinträchtigt. Mittels RNA- und ChIP-Sequenzierungen konnte gezeigt werden, dass K-less MYC zwar an MYC-regulierte Promotoren bindet, in der transkriptionellen Aktivität aber stark beeinträchtigt ist und diese Zielgene nicht aktivieren kann. Dabei war K-less MYC noch in der Lage, RNA Polymerase II (RNAPII) zu den Zielpromotoren zu rekrutieren und die Transkription dort zu initiieren, jedoch war der Übergang zur Elongation blockiert. Die Verwendung eines Proteasom-Inhibitors sowie die Rekonstitution einzelner Lysine in K-less MYC zeigten, dass der proteasomale Abbau von MYC für die Aktivierung von Zielgenen benötigt wird. Der proteasomale Abbau ist für die Histon-Acetylierung von Bedeutung, die von einer hoch konservieren Region in MYC, der MYC Box II, abhängt. Durch die WT MYC-vermittelte Induktion der Histon-Acetylierung können folglich die Proteine BRD4 und P-TEFb an die Promotoren rekrutiert werden. Diese Proteine spielen bei dem Übergang der initiierenden RNAPII zur elongierenden RNAPII eine essentielle Rolle.

Darüber hinaus ermöglichte die Inhibition des MYC Abbaus die Identifizierung eines Zwischenschritts der MYC-abhängigen Transaktivierung: die Assoziation von MYC mit dem positiven Elongationskomplex, dem PAF-Komplex. Dieser wird über eine zweite hochkonservierte Region in MYC, der MYC Box I, rekrutiert. Somit kann angenommen werden, dass MYC als eine Verbindungsstelle fungiert, die positive Elongationsfaktoren auf die RNAPII transferiert.

Zusammenfassend resultieren die Daten dieser Arbeit in einem Model, nach dem der proteasomale Abbau von MYC die Histon-Acetylierung mit der Rekrutierung und dem Transfer von Elongationsfaktoren auf die RNAPII koordiniert, was der Kooperation von MYC Box I und MYC Box II bedarf.

1 Introduction

1.1 Ubiquitin-proteasome system (UPS)

1.1.1 Ubiquitin-conjugation cascade

Ubiquitin is a highly conserved small protein consisting of 76 amino acids. It can be covalently attached to its substrate protein via a peptide bond between the C-terminal glycine of ubiquitin and a free amino group of the target protein. Typically, ubiquitin is attached to the ε-amino group of an internal lysine, but it can also be conjugated to a free α-amino group of the N-terminal amino acid of a substrate protein (Breitschopf et al., 1998; Ciechanover and Ben-Saadon, 2004).

The conjugation of ubiquitin is a multistep reaction involving at least three types of enzymes (E1, E2 and E3). First, an E1 ubiquitin-activating enzyme activates ubiquitin in an ATP-dependent manner. This process results in an energy-rich thioester bond formed between the cysteine in the active center of the E1 enzyme and the C-terminal glycine of ubiquitin. Subsequently, the activated ubiquitin is transferred to a cysteine of a ubiquitin-conjugating enzyme (E2). During the third step ubiquitin is transferred to its actual substrate protein. This process is catalyzed by an ubiquitin ligase (E3), which is largely responsible for the substrate specificity of the system (Hershko and Ciechanover, 1998) (Fig. 1.1).

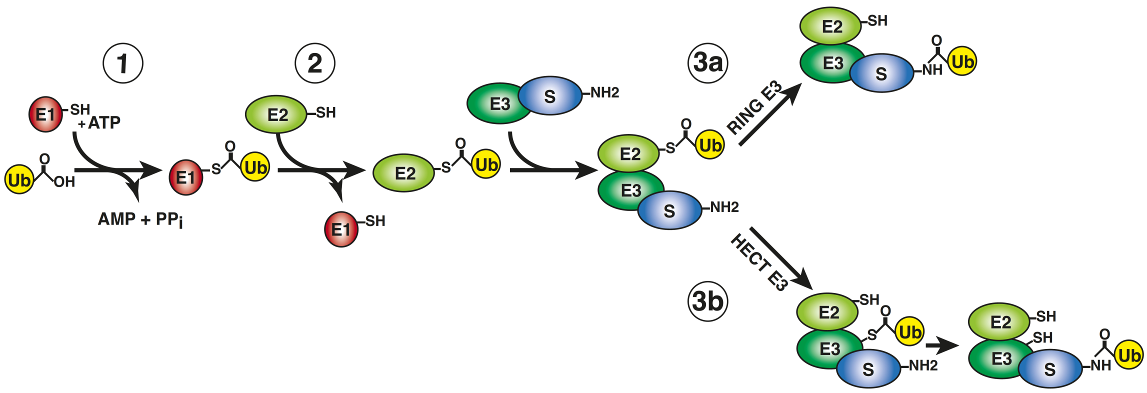

Figure 1.1: Schematic illustration of the ubiquitin-conjugation cascade
Ubiquitination of a substrate involves at least three enzymes. The ubiquitin-activating enzyme E1 activates ubiquitin (Ub) in an ATP-dependent reaction (1) and transfers the activated ubiquitin to the ubiquitin-conjugating enzyme (E2) (2). The third step involves the action of the ubiquitin ligase (E3), which either catalyzes the transfer from the E2 directly to the substrate protein (RING-type E3 ligases) (3a) or via a covalent ubiquitin-E3 intermediate (HECT-E3 ligases) (3b).

When a single ubiquitin molecule is attached to a single site of the target protein, the substrate is monoubiquitinated. Further ubiquitin molecules can be attached to the first one in order to build a polyubiquitin chain. Under certain circumstances, an ubiquitin-chain elongation factor (E4) is required for the extension of an existing short ubiquitin chain (Hoppe et al., 2004; Koegl et al., 1999).

Ubiquitin itself possesses seven internal lysine residues (K6, K11, K27, K29, K33, K48 and K63) and an amino-terminal methionine, which can all serve as attachment sites. This leads to a broad range of chain formations with eight different homotypic and several possible heterotypic chains. The types of chains differ in topology and determine the biological outcome of ubiquitination (Komander and Rape, 2012). K48-linked ubiquitin chains of at least four ubiquitin moieties are considered to be a degradation signal for the 26S proteasome, a multiprotein complex with proteolytic capacity (see also 1.1.2). K63-linked chains are implicated in DNA repair and regulation of protein activity and K29-linked chains participate in lysosomal protein degradation (Ikeda and Dikic, 2008). Recently, several studies have challenged the classical view that distinct chain types mediate exclusively a specific process in the cell. For instance, K48-linked chains do not necessarily result in proteasomal degradation while non-K48-linked ubiquitin chains can also mediate proteasome-dependent turnover (Flick et al., 2004; Kim et al., 2011; Kirkpatrick et al., 2006).

The ubiquitin-conjugation cascade has a hierarchical structure, which is reflected by the encoded enzymes. The human genome encodes for two ubiquitin-activating enzymes, around 40 ubiquitin-conjugating enzymes and more than 600 ubiquitin ligases (Jin et al., 2007; Li et al., 2008; Pickart and Eddins, 2004).

The E3 ubiquitin ligases can be subdivided into two major classes characterized by their structural domains and the resultant distinct mechanisms. The HECT (homologous to the E6-AP carboxyl terminus) E3 ligases contain a conserved cysteine in their HECT domain that forms a thioester with activated ubiquitin of the ubiquitin-E2 conjugate. This results in a covalent ubiquitin-E3 intermediate before the ubiquitin is transferred to the substrate protein. In contrast, the RING (really interesting new gene) and U-box (UFD2 homology) E3 ligases transfer ubiquitin directly from the E2 to the target protein by mediating the association between the E2 enzyme and the substrate protein (Fig. 1.1) (Hatakeyama et al., 2001; Lorick et al., 1999; Pickart, 2001).

RING-type E3 ligases can act as monomers, dimers or multi-subunit complexes such as cullin-RING ligases (CRL). One example of a CRL is the SCF-complex (SKP1-CUL1-F-Box), which consist of the scaffolding protein CUL1, the RING-domain containing protein RBX1, which recruits the E2, and the adapter protein SKP1, which binds a member of the F-box protein family. The F-box protein mediates substrate recognition via a protein-protein-interaction domain such as WD40 or leucine-rich repeats. This interaction often occurs in a phosphorylation-dependent manner, whereby the WD40 domain recognizes a phosphorylated motif (phosphodegron) of the substrate. The F-box protein is incorporated into the SCF-complex by binding SKP1 and CUL1 via the F-box domain (Petroski and Deshaies, 2005; Zheng et al., 2002).

Ubiquitination is a reversible process and can be counteracted by deubiquitinating enzymes (DUBs), a specific group of proteases. Some DUBs associate with their substrate and trim the ubiquitin chain, others remove the entire chain, highlighting that ubiquitination is not necessarily a terminal process (Komander et al., 2009).

Several proteins were identified that are structurally very similar to ubiquitin. These ubiquitin-like (Ubl) post-translational modifiers include, amongst others, SUMO (small ubiquitin-related modifier) and NEDD8. SUMO and NEDD8 are also attached to lysine residues of proteins and function as regulators of many cellular processes including DNA repair and signal transduction (Kerscher et al., 2006).

1.1.2 The 26S proteasome

The degradation of polyubiquitinated substrates is mediated by the 26S proteasome, which is located in the cytosol and nucleus of all eukaryotic organisms. The 26S proteasome is a multimeric enzyme complex consisting of the catalytically active 20S core particle capped by either one or two 19S regulatory particles (Voges et al., 1999).

The 20S has a barrel-formed structure built by two α- and two β-heteroheptameric rings. The proteolytic active sites of the proteasome with chymotryptic-, tryptic-, and caspase-like activities are located on the interior surface of the β-rings thereby shielding the protease activity from the environment to prevent unspecific proteolysis. The two α-rings are positioned at the outside and form an antechamber to the central catalytic chamber.

The 19S regulatory particle is composed of a base and a lid. The lid mediates binding and deubiquitination of the substrate whereas the base with its AAA-ATPases (ATPase associated with diverse cellular activities) is important for the unfolding of the substrate and opening of the outer α-ring of the 20S core particle to allow translocation into the catalytic chamber for degradation (Pickart and Cohen, 2004).

1.2 The ubiquitin-proteasome system in transcriptional regulation

Besides its general role in protein turnover, ubiquitination has been implicated in several biological processes such as DNA damage, receptor internalization, ribosome function and transcriptional regulation. Ubiquitination affects transcription on multiple levels thereby regulating, for instance, chromatin structure and transcription factor activity.

1.2.1 Regulation of chromatin structure by ubiquitin

The first identified ubiquitinated protein was the histone H2A (Goldknopf et al., 1975). Monoubiquitination of H2A is a highly abundant modification in mammalian cells and is associated with transcriptional repression. The polycomb protein RING1B was the first identified ubiquitin ligase that modifies H2A at K119 (Wang et al., 2004). Recently, it has been reported that monoubiquitination of H2A (H2Aub) stimulates H3K27 trimethylation on H2Aub nucleosomes, a chromatin mark associated with transcriptional silencing (Kalb et al., 2014).

In contrast to H2Aub, monoubiquitination of H2B (H2Bub) has been mainly implicated in transcriptional activation. In yeast, H2Bub is required for H3K4 di- and trimethylation, an active mark for transcription. Moreover, H2Bub stimulates the activity of the histone chaperone FACT (facilitates chromatin transcription), which displaces H2A/H2B dimers in front of the elongating RNA polymerase II and reassembles them again, enabling efficient transcription (Pavri et al., 2006). Additionally, deubiquitination of H2B, which can be mediated by the DUB activity of the SAGA coactivator complex or the recently described DUB USP42, can stimulate transcription. This results in a model in which active cycling of ubiquitination and deubiquitination of H2B is required for efficient transcriptional activation (Chandrasekharan et al., 2010; Hock et al., 2014; Zhang et al., 2008).

1.2.2 Role of the proteasome and proteasomal subunits in transcriptional regulation

Genome-wide studies in yeast revealed that proteasomal subunits associate with highly transcribed genes (Auld et al., 2006). Interestingly, several genes were either bound by 20S or 19S subunits of the proteasome suggesting that the subcomplexes mediate different functions at different promoters (Sikder et al., 2006).

A role for the 19S particle in transcriptional regulation has been described for the HIV-1 transactivator TAT. Ubiquitination of TAT by HDM2 stimulates its transcriptional activity without leading to proteasomal degradation. Moreover, TAT stimulates dissociation of the proteasome into the 19S and 20S particles and recruits the 19S subunit to the HIV-1 promoter where it facilitates transcriptional elongation (Brès et al., 2003). Other studies in yeast have reported a role of a 19S subcomplex in transcriptional regulation. This subcomplex is called APIS (AAA-ATPases of the proteasome independent of 20S) and consists of the ATPase subunits. APIS is recruited to actively transcribed genes in yeast to stimulate efficient transcriptional elongation (Ferdous et al., 2001; Gonzalez et al., 2002). The 26S proteasome was detected in regions of transcribed genes with an accumulation of RNA polymerase II at the 3'end of genes and at possible pausing sites of RNA polymerase II raising the possibility that the proteasome functions at these sites to resolve stalled RNA polymerase elongation complexes (Gillette et al., 2004).

A more recent study reported that the entire 26S proteasome is recruited to active sites of transcription and that there were no differences in 19S or 20S occupancy. The authors suggested that in some cases the chaperone function of the 19S base is required for gene expression whereas in other cases the proteolytic function of the proteasome is important (Geng and Tansey, 2012). Nevertheless, the proteasome does not seem to mediate the same function at all promoters. Inhibition of proteasomal function in yeast resulted in an activation of genes involved in mitochondrial function and stress response whereas histone genes and genes involved in protein synthesis were downregulated (Auld et al., 2006; Dembla-Rajpal et al., 2004; Fleming et al., 2002).

1.2.3 Proteolytic function

The most obvious way, in which the UPS affects transcription in a proteolytic manner, is by degrading the transcriptional regulator, thereby reducing its abundance in the cell and limiting its transcriptional activity. One example is β-catenin, which becomes phosphorylated and degraded in the absence of WNT signaling. Active WNT signaling leads to loss of this phosphorylation and thus stabilizes β-catenin, leading to the activation of transcription (Hart et al., 1999).

Importantly, ubiquitin-mediated proteolysis of a transcriptional activator can also have a stimulating effect on its activity. This more counterintuitive idea was first based on the observation that several transcriptional activators are unstable proteins whose activities correlate with protein turnover (Molinari et al., 1999; Wang et al., 2010). Moreover, the transactivation domain of an activator often overlaps with its degron, a sequence directing protein degradation (Salghetti et al., 2000).

Activity of the yeast transcriptional activator Gcn4 depends on the E3 ligase SCF-CDC4. Influencing Gcn4 turnover by mutating either the E3 ligase or inhibiting proteasomal activity resulted in a reduced transcriptional activity (Lipford et al., 2005). Interestingly, activator turnover is often mediated by phosphorylation and the corresponding kinases can be subunits of the transcription machinery. The general transcription factor TFIIH, one component of the preinitiation complex, phosphorylates the androgen receptor (AR). This phosphorylation is a key step in transactivation, leading to ubiquitination and proteasomal degradation of AR at promoters. The turnover of AR is required for efficient transcription and mutations of the phosphorylation site disrupted its transactivation potential (Chymkowitch et al., 2011).

What is the biological significance of coupling proteasomal turnover to efficient transactivation? Degradation of a transcriptional activator could ensure that an activator stimulates only one round of transcription. Turnover could also limit the time an activator spends at a promoter and at the same time ensure that only a persistent signal can lead to multiple rounds of activation (Geng et al., 2012). A similar mechanism has been described for SRC-3, a coactivator of nuclear receptors. SRC-3 is ubiquitinated by SCF-FBW7 in a phosphorylation-dependent manner. Monoubiquitination of SRC-3 initially stimulates transcriptional activity, but it becomes degraded once the ubiquitin is extended to an ubiquitin chain. It was suggested that the ubiquitination functions as a "transcriptional time clock", defining a certain time window in which the coactivator functions (Wu et al., 2007).

But why is turnover in some cases required to stimulate transcription? Deshaies and colleagues described some mechanisms how degradation might be necessary for gene expression. First, activator turnover could help to disrupt the preinitiation complex (PIC) and enable RNA polymerase II to leave the promoter and transcribe the gene (Fig. 1.2 B). Second, a preinitiation complex needs to be reassembled after each round of transcription and activator turnover helps to clear the promoter (Fig. 1.2 A) (Lipford and Deshaies, 2003). Tansey and colleagues extended this model by including phosphorylation of the activator. The phosphorylation by kinases of the transcriptional machinery could mark the activator as “used up”, keeping it inactive and unable to stimulate further rounds of transcription. The removal by proteasomal degradation would clear the promoter making it accessible for a new preinitiation complex (Geng et al., 2012) (Fig. 1.2).

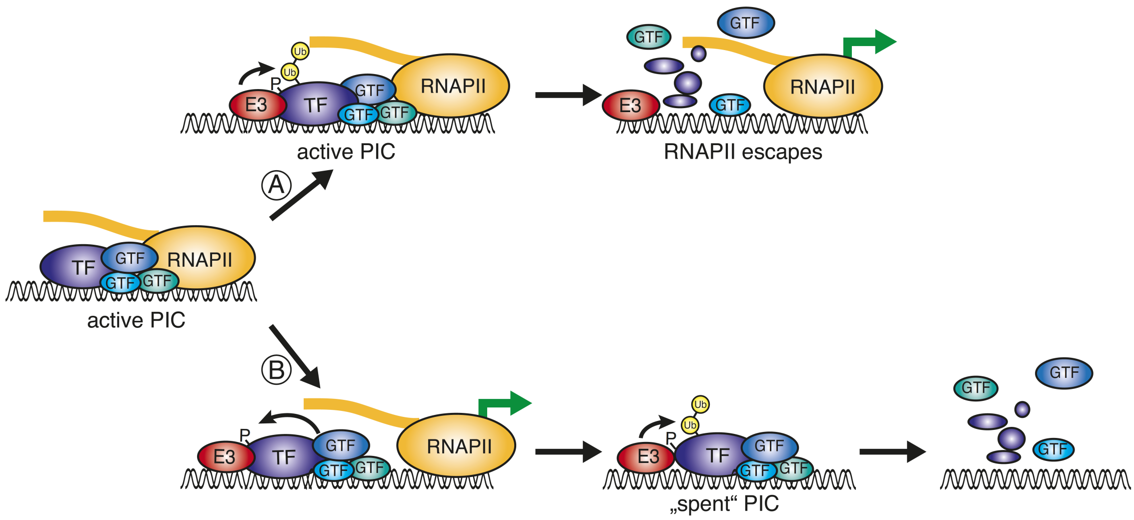

Figure 1.2: Model for stimulation of gene expression by activator turnover
Proteasomal turnover of a transcriptional activator can help to release RNA polymerase II by disrupting the preinitiation complex (PIC) (1). Activator turnover can help to clear the promoter from a “spent” PIC (2). In both scenarios, phosphorylation of the activator by kinases of the transcription machinery can induce the turnover. (GTF, general transcription factor; TF, transcription factor; RNAPII, RNA polymerase II) Adapted from (Geng et al., 2012; Lipford and Deshaies, 2003).

1.2.4 Non-proteolytic function

Ubiquitination of a transcription factor can influence its activity independently of its proteasomal turnover. Several studies have established that ubiquitination affects cellular localization and chromatin association of transcription factors. One example is the transcription factor FOXO4, which becomes monoubiquitinated after oxidative stress, resulting in nuclear translocation and activation of FOXO4-dependent genes. Interestingly, oxidative stress also enhances the binding of the DUB USP7 to FOXO4, leading to its deubiquitination and nuclear exclusion. FOXO4 is then available for another round of activating monoubiquitination (van der Horst et al., 2006). In this way, the cells ensure that only a persistent signal leads to multiple rounds of activation, highlighting how the interplay between ubiquitination and deubiquitination tightly regulates a cellular response.

Several different mechanisms have been described for the negative control of transcription factor activity by ubiquitination. One transcription factor, for which different mechanisms have been established, is the yeast transcription factor Met4. Met4 regulates a set of genes involved in sulfur metabolism (MET genes), when methionine levels are low. During culture in rich medium, when sufficient organic sulfur sources are present, Met4 becomes ubiquitinated and MET genes are not activated. However, this ubiquitination does not result in proteasomal degradation. Instead, the ubiquitin chain blocks recruitment of a cofactor thereby inhibiting the function of Met4 (Kaiser et al., 2000). Another group proposed a different mechanism how ubiquitination of Met4 prevents activation of MET genes. Kuras et al. demonstated that Met4 ubiquitination triggers its recruitment to a different set of promoters resulting in the expression of SAM genes. The SAM genes are required for the synthesis of S-adenosylmethionine, which is not present in rich medium but can be produced from methionine (see Fig. 1.3 A) (Kuras et al., 2002). Recently, a mechanism has been described, how ubiquitination of Met4 might prevent it from binding to promoters of MET genes to maintain repression. Cdc48 is an ubiquitin-selective chaperone that belongs to the AAA-ATPase protein family. It possesses segregase activity and uses the energy of ATP hydrolysis to remove ubiquitinated proteins from binding partners or cellular structures (Dantuma and Hoppe, 2012; Rape et al., 2001). Cdc48 is involved in regulation Met4 promoter occupancy by stripping ubiquitinated Met4 off the MET gene promoters. With this non-proteolytic mechanism, the cell keeps Met4 level constant and is thereby able to quickly respond to changes in methionine levels (Ndoja et al., 2014) (see Fig. 1.3 B).

How Cdc48 regulates promoter occupancy of ubiquitinated transcription factors was first described for the yeast transcriptional repressor MATα2, an important regulator of mating type switching. Upon the signal for mating type switching, MATα2 becomes polyubiquitinated leading to removal of the transcriptional repressor from chromatin and subsequent proteasomal degradation. Extraction of MATα2 terminates its repressive function and mating type switching can occur (Wilcox and Laney, 2009).

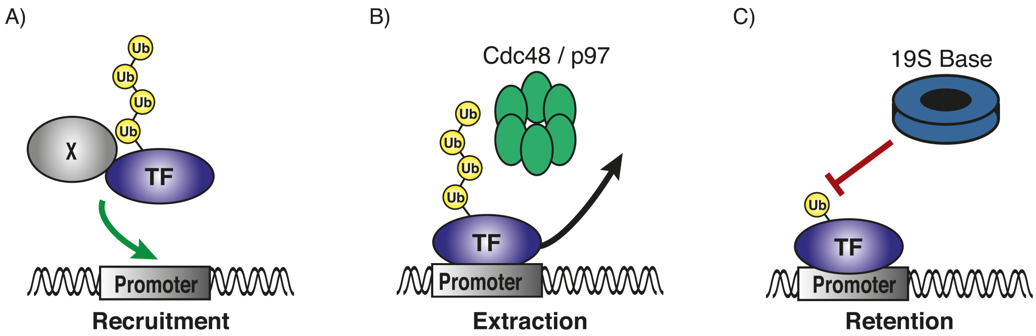

Figure 1.3: Mechanisms how ubiquitination of a transcription factor affects its chromatin association

Ubiquitination of a transcription factor can affect its chromatin association in multiple ways. It can help to recruit it to certain promoters (A), it can lead to extraction of the activator from chromatin by the AAA-ATPase p97 (B) or monoubiquitination can prevent the removal from chromatin by the 19S base particle of the proteasome (C).

In human cells it was described that p97 (the mammalian Cdc48 orthologue) prevents DNA-binding of ubiquitinated receptor-activated SMADs (R-SMADs) thereby attenuating TGF-β signaling. Upon TGF-β signaling, R-SMADs get deubiquitinated by USP15. This prevents the ubiquitin-dependent extraction from chromatin and transcriptional activation of TGF-β-R-Smad target genes (Inui et al., 2011).

In contrast to ubiquitin-dependent removal of transcription factors from promoters, monoubiquitination of the yeast transcriptional activator Gal4 is required to retain it on chromatin highlighting the diverse effects of transcription factor ubiquitination on chromatin association (see Fig. 1.3 C) (Archer et al., 2008).

1.3 The oncogenic transcription factor MYC

The proto-oncogene *c-MYC* was originally identified as a cellular homolog of the viral oncogene *v-myc*, which induces myelocytomatosis in chickens (Sheiness and Bishop, 1979). c-MYC is highly conserved during evolution and expressed in all vertebrates as well as Drosophila melanogaster and the Northern sea star Asterias vulgaris (Gallant et al., 1996; Walker et al., 1992).

In addition to c-MYC, the MYC protein family includes N-MYC and L-MYC. The gene encoding for L-MYC was identified as a *c-MYC*-related gene being amplified in small cell lung cancer whereas the N-MYC encoding gene is amplified in neuroblastoma cell lines and primary tumors (Nau et al., 1985; Schwab et al., 1983).

The majority of *c-MYC* transcripts are initiated at two promoters (Wierstra and Alves, 2008). The alternative translation initiation start sites result in the expression of different isoforms. Translation starting from a CUG start codon produces the minor isoform p67 with 454 amino acids whereas translation at the AUG in the second exon results in the expression of the shorter isoform p64 with 439 amino acids (Blackwood et al., 1994; Hann et al., 1988). The c-MYC p64 isoform is the predominant form and will be hereafter referred to as “MYC”.

MYC expression is deregulated in a wide variety of, if not all, human cancers. In Burkitt’s lymphoma, chromosomal translocation of the *MYC* gene to one of the immunoglobulin enhancer loci leads to elevated MYC expression (Taub et al., 1982). Amplifications of the *MYC* gene have been observed in different solid tumors such as prostate and mammary carcinoma (Escot et al., 1986; Jenkins et al., 1997). Moreover, activation of upstream pathways can lead to increased expression of MYC. In colorectal cancer for example, activation of the WNT/β-catenin pathways results in an increased *MYC* transcription (He et al., 1998). Furthermore, MYC protein stability is increased in several malignancies (see 1.3.5), highlighting that different mechanism can result in deregulated MYC expression.

1.3.1 Structural and functional domains of MYC

MYC is a member of the basic helix-loop-helix leucine zipper transcription factor family with an amino-terminal acidic-type transregulatory and a carboxy-terminal DNA-binding and dimerization domain. MYC contains several conserved domains, called MYC boxes (MB), which are also found in the related proteins N- and L-MYC.

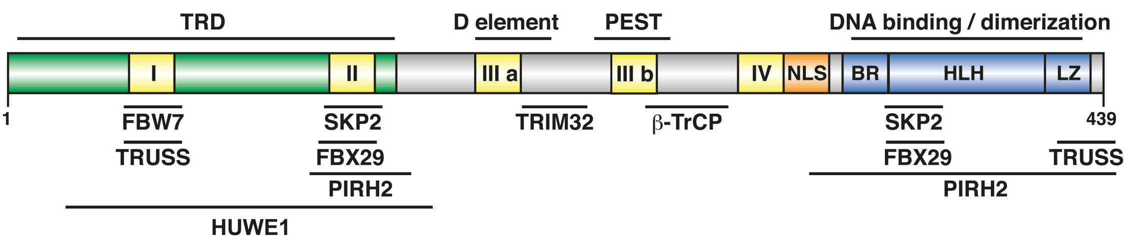

Figure 1.4: Schematic domain structure of MYC

MYC contains a N-terminal transregulatory domain (TRD, green box), several conserved MYC boxes (yellow boxes, MYC box I – IV) and a nuclear localization signal (NLS). The C-terminal basic region helix-loop-helix/leucine zipper domain (BR-HLH/LZ, blue boxes) mediates DNA-binding and dimerization. The PEST sequence and D element are located in the central part of the protein. Identified interaction sites of E3 ligases or their substrate recognition subunits targeting MYC are illustrated in the lower part of the figure. Adapted from (Farrell and Sears, 2014).

MBI and MBII are located within the N-terminal transregulatory domain (TRD), which is required for transcriptional activation and repression (Kato et al., 1990; Lee et al., 1996). One important function of MBI is the regulation of MYC stability. Phosphorylation of threonine-58 and serine-62 within MBI mediate proteasomal degradation of MYC (Sears et al., 1999; 2000). MBII serves as an interaction platform for multiple proteins important for MYC-mediated gene regulation. Cofactors like TRRAP (transactivation/transformation-associated protein), an adaptor protein that recruits the histone acetyltransferase GCN5 to MYC, interact with MYC via MBII (McMahon et al., 1998; 2000). MBIIIa is important for transcriptional repression by MYC and inhibits apoptosis thereby increasing transformation capability (Herbst et al., 2005). MBIIIb was recently described to be important for the interaction with WDR5, a protein that mediates MYC recruitment to chromatin (Thomas et al., 2015). The so-called D-element, a region important for ubiquitin-independent proteolysis of MYC, overlaps with MBIIIa (Herbst et al., 2004). In addition to the D-element, MYC contains the central PEST sequence, which is also important for MYC degradation. The PEST sequence is rich in the amino acids proline (P), glutamic acid (E), serine (S) and threonine (T) and deletion of this element stabilizes MYC without affecting its ubiquitination (Gregory and Hann, 2000). For N-MYC it has been reported that MBIV is involved in the regulation of apoptosis, DNA binding and transformation capability (Cowling et al., 2006). Moreover, MYC carries a canonical lysine-rich nuclear localization signal (NLS) (Dang and Lee, 1988). The carboxy-terminal basic region (BR) is important for sequence-specific DNA-binding and the helix-loop-helix/leucine zipper domain (HLH/LZ) mediates dimerization with other HLH/LZ containing proteins like MAX (MYC-associated factor X) (Blackwood and Eisenman, 1991). In addition, this region also mediates interaction with the transcription factor MIZ1 (MYC-interacting zinc finger protein 1) and the histone acetyltransferases p300 and CBP (Peukert et al., 1997; Vervoorts et al., 2003).

1.3.2 Biological functions and transcriptional regulation by MYC

MYC is required for normal embryonic development. Homozygous deletion of MYC is embryonically lethal, probably due to defects in the placenta (Davis et al., 1993; Dubois et al., 2008). Conditional MYC deletion in the epiblast revealed a requirement for MYC in the hematopoietic system underlining the importance of MYC for normal development (Dubois et al., 2008).

MYC can activate and repress gene expression and thereby affects many different biological processes. Moreover, MYC regulates transcription by all three RNA polymerases. Besides regulating RNA polymerase II targets, MYC can promote expression of ribosomal RNAs transcribed by RNA polymerase I and of tRNAs and 5S rRNA transcribed by RNA polymerase III (Arabi et al., 2005; Gomez-Roman et al., 2003; Grandori et al., 2005; Steiger et al., 2008).

Thus, MYC regulates a huge set of target genes and thereby affects many different biological processes ranging from proliferation and cell growth to apoptosis (Eilers and Eisenman, 2008).

Recently, it was described that, rather than being a specific transcriptional regulator, MYC functions as a general transcriptional amplifier that globally enhances transcription (Lin et al., 2012; Nie et al., 2012).

1.3.2.1 Transcriptional activation by MYC

In order to activate gene transcription MYC heterodimerizes with its partner protein MAX and the MYC/MAX dimer binds to specific DNA sequences, the E-boxes, which can be either canonical (CACGTG) or non-canonical (CANNTG, where N can be any nucleotide) (Blackwell et al., 1993; Blackwood and Eisenman, 1991). MYC occupies almost all open promoters and binding correlates with trimethylated H3K4 (Guccione et al., 2006). Recently, it has been demonstrated that the interaction of MYC with WDR5 is important for recruitment of MYC to chromatin (Thomas et al., 2015). To induce transcription, MYC recruits many co-activators, such as p300 or the adaptor protein TRRAP, a core subunit of several macromolecular complexes that contain the histone acetyltransferases (HAT) GCN5 or TIP60 (see Fig. 1.5). The recruitment of HATs by MYC to its target promoters results in an increase of H3 and H4 acetylation that further opens the chromatin structure and enables transcriptional activation (Bouchard et al., 2001; Frank et al., 2003; McMahon et al., 2000). Examples of other MYC-recruited cofactors are the ATPases TIP48 and TIP49, which possess helicase activity and are part of several chromatin remodeling complexes (Wood et al., 2000).

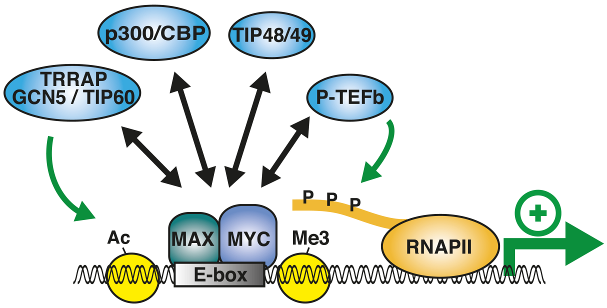

Figure 1.5: Transcriptional activation by MYC
Schematic illustration of MYC-mediated transactivation of target genes. The MYC-MAX heterodimer binds to E-box sequences within open promoters with H3K4 trimethylated histones and recruits coactivators. The coactivors induce H3 and H4 acetylation and chromatin remodeling. The recruitment of P-TEFb leads to RNA polymerase II (RNAPII) Ser2 phosphorylation and subsequent productive elongation.

Moreover, MYC regulates transcriptional activation by interacting with components of the transcription apparatus and thereby affecting different steps in the transcription cycle.

The transcription cycle is a multistep process involving several different proteins and is regulated at multiple steps. First, RNA polymerase II (RNAPII) is recruited to the promoter in a hypophosphorylated state and together with general transcription factors (GTFs) forms the pre-initiation complex. The promoter acquires an open conformation and transcription initiation starts with the transcription of short, unstable transcripts. RNAPII contains a highly repetitive carboxy-terminal domain (CTD) with the conserved motif Tyr1-Ser2-Pro3-Thr4-Ser5-Pro6-Ser7 (YSPTSPS). The mammalian RNAPII contains 52 of these repeats. Early in the transcription cycle, RNAPII gets phosphorylated at Ser7 and Ser5 primarily by the CDK7 subunit of TFIIH. Even though the role of Ser7 phosphorylation is less studied, the function of Ser5 phosphorylation is well understood. Phosphorylation of this site is stimulated by the Mediator complex, a conserved multiprotein complex, triggering promoter clearance. It stimulates the recruitment of the 5'end capping machinery to the nascent mRNA. Once the short transcripts acquire a certain length, the RNAPII escapes from the promoter, defining the transition from intitiation to productive elongation (Heidemann et al., 2013; Shandilya and Roberts, 2012; Svejstrup, 2004).

MYC stimulates the recruitment of RNAPII to promoters and mediates Ser5 phosphorylation of the CTD by recruiting TFIIH and Mediator in a MBII-dependent manner (Bouchard et al., 2004; Walz et al., 2014).

The transition to productive elongation is often delayed by promoter-proximal pausing. RNAPII remains associated with the nascent RNA transcript but requires further signals to resume elongation. The RNAPII is held in the pausing state by the negative elongation factor NELF, a protein with four subunits (A, B, C/D and E) and DSIF (DRB sensitivity-inducing factor), consisting of the proteins SPT4 and SPT5. The paused state of RNAPII may also be maintained by additional proteins (Adelman and Lis, 2012). The release of RNAPII into productive elongation requires phosphorylation of Ser2 within its CTD. In mammals, Ser2 is primarily phosphorylated by the positive elongation factor P-TEFb. Besides phosphorylating RNAPII, P-TEFb also phosphorylates DSIF, leading to the dissociation of NELF from the complex and turning DSIF from a negative into a positive elongation factor, which remains associated with the elongating RNAPII through the gene (Adelman and Lis, 2012). Ser2 phosphorylation functions as a recruitment signal for several positive elongation and splicing factors. Moreover, 3'end processing factors and factors being important for mRNA export are also recruited by the Ser2-phosphorylated polymerase (Heidemann et al., 2013).

MYC regulates transcriptional elongation by interacting with P-TEFb (Eberhardy and Farnham, 2002). The release of elongating RNAPII from a paused state is thought to be a key mechanism for MYC-driven transactivation (Bouchard et al., 2004; Rahl and Young, 2014; Rahl et al., 2010; Walz et al., 2014).

Whether MYC acts as a general amplifier, as it has been described for MYC in activated B-cells, or as a transcription factor with a specific set of target genes might depend on the cellular context and MYC levels.

Recently, it has been described that promoter affinities and MYC level play an important role whether MYC activates gene expression profiles of normal proliferating cells or oncogenic signatures. Promoters with high-affinity binding sites, representing mostly physiological targets, are already saturated in normal proliferating cells. An increase in MYC level leads to an enhanced occupancy of low affinity promoters, which results in activation of oncogenic gene expression profiles (Walz et al., 2014). Moreover, high MYC levels lead to an invasion of enhancers, potentially increasing its transcriptional output (Lin et al., 2012; Sabò et al., 2014b).

1.3.2.2 Transcriptional repression by MYC

In addition to directly activating transcription, MYC can downregulate gene expression either in a direct or indirect manner. A mechanism for indirect MYC-mediated transcriptional repression is the induction of specific microRNAs (miRNAs). MYC regulates the expression of miR17-92, which in turn represses proteins important for induction of senescence or apoptosis, thereby maintaining a survival program (Li et al., 2014).

To directly repress gene expression independent of another transcription factor, MYC recruits the histone deacetylase 3 (HDAC3) in a MBIII-dependent manner to E-box containing promoters, thereby reducing H3 and H4 acetylation (Kurland and Tansey, 2008).

Another mechanism for MYC-mediated transcriptional repression operates via the interaction with other transcription factors like MIZ1 or SP1 (Gartel et al., 2001; Peukert et al., 1997). In this context, MYC displaces co-activators and recruits co-repressors, such as HDACs or DNA methyltransferases (e.g. DNMT3a) (Brenner et al., 2005; Staller et al., 2001).

Interestingly, the repressive MYC-MIZ1 complex does not only lead to repression of MIZ1-induced target genes but also attenuates MYC-mediated activation. The ratio of MYC-MIZ1 complexes at promoters determines the direction of the transcriptional output (Walz et al., 2014). In cellular systems with low levels of MYC, MIZ1 acts as a sequence-specific transcription factor that binds to a MIZ1-binding motif and activates, among others, genes involved in autophagy (Wolf et al., 2013). These MIZ1-binding sites possess a low MYC/MIZ1 ratio, meaning more MIZ1 is bound than MYC and are regulated by MIZ1 but not by MYC. Elevated MYC level lead to the cooperative binding of MIZ1 to many MYC-regulated promoters, which dampens the transcriptional response to MYC (Walz et al., 2014; Wiese et al., 2015; 2013).

1.3.3 Regulation of MYC expression and functionality

Since MYC regulates many different biological processes and can contribute to almost all aspects of tumor development and tumor maintenance it is absolutely critical for a cell to keep MYC function and levels tightly regulated. This regulation occurs on multiple levels ranging from regulation of *MYC* mRNA expression to regulation of MYC function and stability by posttranslational modifications.

1.3.3.1 Transcriptional and post-transcriptional regulation of *MYC*

Transcription of the *MYC* gene is tightly regulated at the level of transcription initiation and elongation and the *MYC* promoter is bound by many different transcription factors, which are regulated by multiple signal transduction cascades including WNT, MAPK and TGFβ (Levens, 2010). Interestingly, BRD4, a BET bromodomain protein, is a transcriptional co-activator of MYC and inhibition of BRD4 leads to downregulation of *MYC* expression (Delmore et al., 2011). BRD4 and Mediator co-occupy many enhancers of actively transcribed genes. A selected group of bound enhancers, the so-called stretch- or super-enhancers, are up to 50 kb large and bind high levels of Mediator and BRD4. Super-enhancers can act on oncogenes including MYC (Lovén et al., 2013). Inhibition of BRD4 preferentially disrupts super-enhancers, making BRD4 inhibitors such as JQ1 attractive drugs to target *MYC* expression (Delmore et al., 2011; Filippakopoulos et al., 2010).

MYC mRNA is relatively unstable with a half-life of approximately 20 min (Dani et al., 1984). Translation of *MYC* is regulated by several mechanisms including IRES-dependent translation and miRNAs-dependent pathways (Carter et al., 1999; Kress et al., 2011; Sachdeva et al., 2009; Sampson et al., 2007).

1.3.3.2 Post-translational regulation of MYC

The MYC protein is targeted by different post-translational modifications, including acetylation, phosphorylation and ubiquitination, which have various effects on MYC function and protein stability.

1.3.3.2.1 Acetylation

For efficient transcriptional activation, MYC recruits different HATs to promoters and induces histone acetylation (see 1.3.2.1). However, MYC does not only recruit these cofactors to promoters but is itself a substrate of HATs, such as GCN5, TIP60 and p300/CBP.

CBP acetylates MYC *in vitro* and in cells and overexpression of CBP leads to reduced ubiquitination of MYC and increased protein stability (Vervoorts et al., 2003). Acetylation of MYC by TIP60 and GCN5 increases the half-life of MYC (Patel et al., 2004). Lysines of mouse MYC, which are acetylated by GCN5, have been mapped *in vivo* and include K149 close to MBII, K323 in the NLS and K417 in the leucine zipper domain. Several lysines of human MYC are acetylated by p300 (K143, K148, K157, K275, K317, K323, K371). In contrast to other HATs, acetylation by p300 increases MYC protein turnover (Faiola et al., 2005; Zhang et al., 2005). Whether acetylation of MYC might mediate protein-protein interactions or influence MYC function in another way is still unknown.

1.3.3.2.2 Sumoylation

Sumoylation is another post-translational modification of proteins, which, similar to ubiquitin, targets lysine residues. Sumoylation of proteins can have various effects. It can affect the cellular localization of a protein, interfere with the binding of another protein or serve as an interaction platform (Geiss-Friedlander and Melchior, 2007). MYC and N-MYC are sumoylated with K349 being the major SUMO-acceptor site in N-MYC and K326 or K323 being the major acceptor site in MYC. Sumoylation of the endogenous N-MYC protein could be detected after heat shock but had no effect on stability or activity of the protein (Sabò et al., 2014a).

The MYC sumoylation site K326 was also identified by mass spectrometry of transfected MYC. However, mutation of the SUMO acceptor site had no effect on MYC half-life or activity (Kalkat et al., 2014). Therefore, it remains unresolved, whether sumoylation of MYC influences its biological activity in some contexts.

1.3.3.2.3 Phosphorylation

MYC is a well-established phosphoprotein and phosphorylation sites in MYC can be found all over the protein. The first identified phosphorylation sites in MYC are clusters of residues that reside within the PEST domain (T247/T248/S249/S250/S252) and near the BR (T343/S344/S347/S348), which are modified by the casein kinase 2 (CK2) (Lüscher et al., 1989). Although the functional relevance of these phosphorylation events remains unclear, it was suggested that CK2 phosphorylation in the PEST domain stabilizes MYC (Channavajhala and Seldin, 2002). Phosphorylation of the cluster close to the BR affects the transformation capability of MYC, since mutation of these sides to alanine result in gain-of-function alleles with increased transforming activity (Wasylishen et al., 2013).

Besides these phosphorylation sites in the central and C-terminal part of MYC, several sites are located within the TRD. The kinase ABL phosphorylates up to five tyrosine residues with the major site being Y74. MYC phosphorylated at Y74 resides in the cytoplasm and its presence correlates with ABL activity in tumors. Nevertheless, the precise function of phospho-Y74 MYC in the cytoplasm remains open (Sanchez-Arévalo Lobo et al., 2013). S62 and S71 can be phosphorylated by c-Jun N-terminal kinase (JNK) and these phosphorylation events promote MYC-induced apoptosis (Noguchi et al., 1999).

Several other phosphorylation sites in MYC have been mapped but the best characterized sites are T58 and S62, which are located in MBI (Alvarez et al., 1991; Henriksson et al., 1993). Different growth-stimulating signal transduction pathways regulate these phosphorylation events and S62 was shown to be phosphorylated by the Ras-activated mitogen-activated kinase (MAPK) (also known as extracellular signal-regulated kinases, ERK), which has a stabilizing effect on MYC (Sears et al., 2000). Whether S62 phosphorylation strictly depends on MAPK *in vivo* remains unclear (Lutterbach and Hann, 1999), since S62 can also be phosphorylated by CDK2 (Hydbring et al., 2010).

T58 and S62 phosphorylation are interdependent because phosphorylation of T58 by the glycogen synthase kinase 3 β (GSK3β) requires the priming phosphorylation at S62 (Gregory et al., 2003; Lutterbach and Hann, 1994). The prolyl isomerase PIN1 isomerizes MYC, enabling the protein phosphatase 2A (PP2A) to dephosphorylate MYC at S62 (Yeh et al., 2004). The dephosphorylation of S62 is required for subsequent proteasomal degradation of T58-phosphorylated MYC, because this phosphorylation site functions as a phosphodegron and is recognized by the ubiquitin ligase SCF-FBW7 (Welcker et al., 2004b; Yada et al., 2004).

1.3.3.2.4 Ubiquitination

Several different ubiquitin ligases have been identified that target MYC (Farrell and Sears, 2014). Ubiquitination can have various effects and either inhibit or promote proteasomal degradation and either stimulate or inhibit MYC transcriptional activity.

FBW7 (F-box and WD40 repeat domain-containing 7) is a substrate specificity factor of the SCF ubiquitin ligase complex and one of the best-studied ubiquitin ligases targeting MYC. As mentioned previously, FBW7 is a tumor suppressor protein that recognizes phosphorylated T58 in MBI leading to MYC ubiquitination and subsequent proteasomal degradation (Welcker et al., 2004a; Yada et al., 2004). FBW7 was also shown to ubiquitinate MYC in vitro (Welcker et al., 2004b). Mutations in the phosphodegron recognized by FBW7 (T58) are found in Burkitt's lymphomas and are associated with increased MYC stability (Bahram et al., 2000; Gregory and Hann, 2000). FBW7 exists in three isoforms (α, β, γ) that differ in their cellular localization. FBW7α is a nuclear protein and FBW7γ is present in the nucleolus. Both isoforms mediate proteasomal degradation of MYC. FBW7β is cytosolic and not involved in MYC degradation (Welcker et al., 2004a).

Several other ubiquitin ligases were identified that target MYC for proteasomal degradation, including FBX29, TRIM32, TRUSS, PIRH2 and CHIP (Farrell and Sears, 2014). FBX29 is a substrate recognition factor of an SCF-like ubiquitin ligase, consisting of the scaffold protein CUL7, the RING finger protein ROC1 and SKP1 (Dias et al., 2002).

It was identified as a MYC-interacting protein using a mass spectrometry approach. Overexpression of FBX29 reduces MYC level and inhibits MYC transcriptional activity (Koch et al., 2007). TRIM32 is a RING-finger ubiquitin ligase promoting MYC proteasomal turnover in neuronal progenitor cells to induce neuronal differentiation (Schwamborn et al., 2009). Another ubiquitin ligase for MYC identified in a proteomic approach is TRUSS (tumor necrosis factor receptor-associates ubiquitous scaffolding and signaling protein), an adaptor protein for the CUL4-DDB1 (damage-specific DNA-binding protein 1) ubiquitin ligase complex (Lee and Zhou, 2007). Initially identified as a binding partner for N-MYC, TRUSS ubiquitinates both, MYC and N-MYC. As FBW7 and TRIM32, TRUSS appears to be a negative regulator of MYC activity, leading to its ubiquitination and proteasomal degradation (Choi et al., 2010). The ubiquitin ligase PIRH2 also mediates MYC ubiquitination and proteasomal degradation. (Hakem et al., 2011). Recently, the carboxyl terminus of HSC70-interacting protein (CHIP) has been described as an ubiquitin ligase targeting MYC for proteasomal degradation, resulting in decreased MYC target gene induction (Paul et al., 2013).

Ubiquitination of MYC by SCF-β-TrCP does not mediate proteasomal turnover but instead stabilizes MYC (Popov et al., 2010). Ubiquitination and thus stabilization of MYC by β-TrCP is required for a cell-cycle reentry after S-phase arrest. PLK1 (polo-like kinase 1) phosphorylates MYC in a region between amino acids 278 to 283, creating a phosphodegron that is bound by β-TrCP. Moreover, β-TrCP assembles heterotypic non-proteolytic ubiquitin chains at the amino-terminus of MYC thereby stabilizing MYC and preventing the assembly of degrading K48 ubiquitin chains by FBW7.

The ubiquitin ligase HUWE1 (HECT, UBA and WWE containing 1) belongs to the HECT-E3 ubiquitin ligases and ubiquitinates MYC *in vivo* and *in vitro* (Adhikary et al., 2005). Six lysine residues of MYC, overlapping with the NLS, were shown to be modified by HUWE1 with K63-linked ubiquitin chains. Similar to β-TrCP, this ubiquitination does not lead to proteasomal degradation of MYC but is important for its transcriptional activity by promoting recruitment of the coactivator p300 (Adhikary et al., 2005). HUWE1 does not only ubiquitinate MYC but also N-MYC and MIZ1, leading to their proteasomal degradation (Inoue et al., 2013; Yang et al., 2010; Zhao et al., 2008a). A recent paper demonstrates that HUWE1 antagonizes the assembly of MYC/MIZ1 repressive complexes at MYC-responsive genes by degrading MIZ1 and thereby preventing a decreases in the transcriptional response (see 1.3.2.2) (Peter et al., 2014). In colon carcinoma cell lines, inhibition of HUWE1 by small molecules resulted in a stabilization of MIZ1 and a subsequent accumulation of MYC/MIZ1 repressive complexes at growth associated MYC target genes preventing their activation. This suggests that MYC function can be targeted by inhibition of ubiquitin ligases (Peter et al., 2014; Schaub and Cleveland, 2014).

Another E3 ligase which ubiquitinates MYC without leading to its proteasomal degradation is SCF-FBXO28, whose activity is cell cycle-regulated. Phosphorylation by cyclin-dependent kinase 1/2 (CDK1/2) activates the F-box protein FBXO28 and active SCF-FBXO28 ubiquitinates MYC at the S- and G2/M-phases of the cell cycle and stimulates its transcriptional activity by promoting p300 recruitment (Cepeda et al., 2013).

In contrast to other ligases, which stimulate MYC transcriptional activity, ubiquitination by SCF-SKP2 (S-phase kinase-associated protein 2) leads to proteasomal turnover of MYC but at the same time stimulates its activity (Kim et al., 2003; Lehr et al., 2003). This effect is dependent on the F-box domain of SKP2, suggesting that ubiquitin ligase activity is required for the stimulating effect on MYC function. Furthermore, von der Lehr et al. showed that SKP2 and components of the proteasome are present at MYC-regulated promoter, suggesting that ubiquitination of MYC by SKP2 could occur on chromatin (Lehr et al., 2003). Ubiquitination of the TRD of MYC appears to be specifically required for the SKP2-mediated effects on MYC, since mutation of lysines within this region results in a decreased transforming capacity and canonical target gene induction (Zhang et al., 2013).

Ubiquitination of MYC can be reverted by deubiquitinating enzymes. The ubiquitin specific protease USP28 was identified in an shRNA screen, which was performed to identify genes essential for MYC function (Popov et al., 2007). USP28 was shown to antagonize FBW7□-mediated ubiquitination of MYC and thereby stabilizes the protein. USP28 is highly expressed in colon cancer and deletion of *Usp28* in a murine model of colorectal cancer attenuates tumorigenesis and prolongs survival (Diefenbacher et al., 2014; Popov et al., 2007). USP37 directly deubiquitinates and stabilizes MYC in lung cancer (Pan et al., 2014). Recently, USP36 was identified as a deubiquitinating enzyme that specifically antagonizes FBW7□-mediated ubiquitination thereby stabilizing MYC in the nucleolus (Sun et al., 2015).

1.4 Objectives of the thesis

The oncogenic transcription factor MYC is a central driver of tumorigenesis that is required for sustained tumor growth. However, it has been challenging to target MYC directly for cancer therapy. Therefore, it is important to understand how MYC function and activity is regulated in order to develop new therapeutic strategies.

MYC is an unstable protein that is rapidly turned over by the ubiquitin-proteasome system. Ubiquitination can both, stimulate and inhibit MYC function. Since several ubiquitin ligases seem to redundantly promote MYC ubiquitination and since these ligases have a broad spectrum of other substrates, it has been challenging to investigate the direct contribution of MYC ubiquitination to its transcriptional activity.

To address this problem, we generated a MYC mutant, in which all lysine residues were replaced by arginines: this preserves the positive charge of the amino acid but prevents ubiquitination due to the absence of a free amino group.

The objective of this thesis was to characterize this mutant and investigate how the absence of ubiquitination acceptor sites affects MYC activity. It should be analyzed whether there is a site-preference for ubiquitination that influences MYC activity. Finally, the detailed mechanism for the stimulating effect of MYC ubiquitination on its activity should be elucidated.

2 Materials

2.1 Chemicals

All chemicals were purchased from the companies AppliChem, Calbiochem, Invitrogen, Merck, Roth and Sigma-Aldrich. If not otherwise indicated, solutions and buffers were prepared in ddH_2O.

2.2 Buffers and solutions

Ammonium persulfate (10%)	5.0 g ammonium persulfate were dissolved in 50 ml ddH_2O, aliquots were stored at -20°C
Ampicillin stock solution	10 g ampicillin were solubilized in 100 ml ddH_2O and sterile filtered; aliquots were stored at -20°C
β-galactosidase buffer	60 mM Na_2HPO_4 1 mM $MgSO_4$ 10 mM KCl
Blocking solution for PVDF membrane	5% (w/v) skim milk powder in TBS-T
Blocking solution for ChIP	5 mg/ml BSA in PBS
BCA buffer A	1% BCA-Na_2 2% Na_2CO_3 x H_2O
BCA buffer B	4% $CuSO_4$ x 5 H_2O 0.16% Na-tartrate 0.4% NaOH 0.95% $NaHCO_3$
Bis-Tris (3.5 x)	1.25 M Bis-Tris
Bis-Tris stacking gel	4% (v/v) acrylamide / bisacrylamide 1 x Bis-Tris 0.03% (v/v) APS 0.05% (v/v) TEMED
Bis-Tris separation gel	8-15% (v/v) acrylamide / bisacrylamide 1 x Bis-Tris 0.03% (v/v) APS 0.05% (v/v) TEMED

Bradford reagent	0.01% (w/v) Coomassie Brilliant Blue G250 8.5% phosphoric acid 4.75% ethanol solution was filtered and stored in the dark
Crystal violet solution	0.1% (w/v) crystal violet 20% (v/v) ethanol
ChIP elution buffer	50 mM Tris, pH 8.0 1 mM EDTA 1% SDS 50 mM $NaHCO_3$
ChIP swelling buffer	25 mM HEPES, pH 7.8 1.5 mM $MgCl_2$ 10 mM KCl 0.1% NP-40 1 mM DTT, freshly added 0.5 mM PMSF, freshly added
ChIP high salt buffer	50 mM HEPES, pH 7.9 500 mM NaCl 1 mM EDTA 1% Triton X-100 0.1% Na-deoxycholate 0.1% SDS 0.5 mM PMSF, freshly added
ChIP LiCl buffer	20 mM Tris, pH 8.0 1 mM EDTA 0.5% NP-40 0.5% Na-deoxycholate 0.5 mM PMSF freshly added
ChIP lysis buffer	20 mM Tris, pH 7.5 150 mM NaCl 1% NP-40 1% Na-deoxycholate 0.1% SDS 1 mM EDTA
Denaturing lysis buffer (2 x)	50 mM Tris, pH 8.0 2% SDS 20 mM EDTA 20 mM DTT
DNA loading buffer (6 x)	10 mM EDTA, pH 8.0 0.2% (w/v) Orange G 40% (w/v) sucrose

HBS for transfection (2 x)	280 mM NaCl 1.5 mM Na_2HPO_4 50 mM HEPES adjusted to pH 7.05 with 5N NaOH sterile filtered
HEGN lysis buffer (2 x)	40 mM HEPES pH 7.9 2% NP-40 0.4 mM EDTA 20 mM sodium pyrophosphate 20 mM sodium fluoride
Luciferase substrate solution	25 mM glycylglycine solution 15 mM K_3PO_4 (pH 8.0) 4 mM EGTA 15 mM MgSO4 0.1 mM CoA 75 µM luciferin, freshly added 2 mM ATP, freshly added 1mM DTT, freshly added
Miniprep lysis buffer	0.2 N NaOH 1% SDS
Miniprep precipitation buffer	3 M KOAc, pH 5.2
Nuclease incubation buffer	150 mM HEPES, pH 7.9 1.5 mM $MgCl_2$ 150 mM KOAc
Nucleoplasmic extraction buffer	20 mM HEPES, pH 7.9 3 mM EDTA 10% glycerol 150 mM KOAc 1.5 mM $MgCl_2$
NuPAGE transfer buffer (20 x)	500 mM Bis-Tris 500 mM Bicine 20.5 mM EDTA 0.1 mM chlorobutanol
NuPAGE transfer buffer (ready to use)	1x NuPAGE transfer buffer with 20% methanol
MOPS running buffer (20 x)	1 M MOPS 1 M Tris 20 mM EDTA 2% SDS

MOPS running buffer (ready to use)	1x MOPS running buffer with 5 mM sodium bisulfite
PBS (1 x)	137 mM NaCl 2.7 mM KCl 10.1 mM Na_2HPO_4 1.76 mM KH_2PO_4 the solution was autoclaved
PI-FACS buffer	38 mM sodium citrate 54 µM propidium iodide 24 µg/ml RNase A
Phosphatase inhibitor	Ser/Thr phosphatase inhibitor (Sigma, P0044), Tyr phosphatase inihibitor (Sigma, P5726), used 1:200
Phenylmethylsulfonylfluorid (PMSF)	150 mM in isopropanole
Polyethylenimin (PEI)	450 µl PEI (10%, MW 25,000 g/mol, Sigma) 150 µl HCl (2 N) 49.5 ml ddH_2O
Protease inhibitor	protease inhibitor cocktail (Sigma, P8340), used 1:800
Proteinase K	10 mg/ml in ddH_2O
RIPA lysis buffer	50 mM HEPES, pH 7.9 140 mM NaCl 1 mM EDTA 1% Triton X-100 0.1% Na-deoxycholate 0.1% SDS 1 mM PMSF freshly added protease and phosphatase inhibitors freshly added
RNase A (10 mg/ml)	100 mg RNase A (Roth) in 27 µl 3 M sodium acetate, pH 5.2 9 ml ddH_2O aliquots à 450 µl boiled for 30 min at 100°C to inactivate DNases 50 µl 1M Tris, pH 7.4 added per aliquot stored at -20°C

Sample buffer (6 x)	1.2 g SDS 6 mg bromphenol blue 4.7 ml 100% glycerol 1.2 ml 0.5 M Tris, pH 6.8 2.1 ml ddH_2O the solution was heated up, 0.93 g DTT was dissolved, solution was aliquotted and keep frozen at -20°C
Silver gel fixing solution	30 % (v/v) ethanol 10 % (v/v) acetic acid
Silver gel sensitization solution	6.8 % (w/v) $NaCH_3COO$ 30% (v/v) ethanol 0.2% (w/v) $Na_2S_2O_3$ x 5 H_2O, added before use 0.125% (w/v) glutaraldehyde, added before use
Silver gel staining solution	0.2% (w/v) $AgNO_3$ 0.0074% formaldehyde, added shortly before use, stored protected from light
Silver gel developing solution	3% Na_2CO_3 0.0037% formaldehyde pH<11.5 (titrate with $NaHCO_3$)
Silver gel stopping solution	1% (w/v) glycin
Stripping buffer (10 x)	2 M glycin, pH 2.5 2% Tween-20
Sucrose buffer	10 mM HEPES, pH 7.9 0.34 M sucrose 3 mM $CaCl_2$ 2 mM MgOAc 0.1 mM EDTA
TAE (50 x)	2 M Tris, pH 8.0 5.7% acetic acid 50 mM EDTA
TBS (20 x)	500 mM Tris base 2.8 M NaCl adjusted to pH 7.4 with concentrated HCl
TBS-T	1 x TBS 0.2% Tween-20
TE	10 mM Tris, pH 7.4 1 mM EDTA, pH 8.0

TNT lysis buffer	25 mM Tris, pH 8.0 250 mM NaCl 1% Triton X-100
Ubi-buffer A	6 M guanidine-HCl 0.1 M Na_2HPO_4/NaH_2PO_4 10 mM imidazole
Ubi-buffer B	25 mM Tris-HCl, pH 6.8 20 mM imidazole

2.3 Standards, enzymes and kits

2.3.1 Standards

DNA marker	Gene Ruler 1 kb Plus DNA ladder (Thermo Scientific)
Protein marker	PageRulerTM Prestained Protein Ladder (Thermo Scientific)

2.3.2 Enzymes

Benzonase	Novagene/VWR International
M-MLV Reverse Transcriptase	Promega
Phusion HF DNA polymerase	Thermo Scientific
Restriction endonuclease	Thermo Scientific, New England Biolabs (NEB)
RNase-free DNase	Qiagen
SYBR Green qPCR Master Mix	Thermo Scientific
T4 DNA ligase	Thermo Scientific

2.3.3 Kits

Experion DNA 1K analysis kit	Bio-Rad
Experion RNA StdSense Analysis Kit	Bio-Rad
GeneJET Gel Extraction Kit	Thermo Scientific
GeneJET PCR Purification Kit	Thermo Scientific
Immobilon Western HRP Substrate	Millipore
MinElute PCR Purification Kit	Qiagen
NEBNext® ChIP-Seq Library Prep Master Mix Set for Illumina®	NEB
NEBNext® Multiplex Oligos for Illumina® (Index Primer Set 1)	NEB

NEBNext® Multiplex Oligos for Illumina® (Index Primer Set 2)	NEB
NEBNext® Poly(A) mRNA Magnetic Isolation Module	NEB
NEBNext® UltraTM RNA Library Prep Kit for Illumina®	NEB
PureLinkTM HiPure Plasmid Maxiprep Kit	Invitrogen
QIAquick Purification Kit	Qiagen
QIAquick Gel Extraction Kit	Qiagen
Quanti-iTTM PicoGreen ® dsDNA Assay Kit	Life technologies
RNeasy Mini Kit	Qiagen

2.4 Nucleic acids

2.4.1 Primers

Primers used in this study were synthesized by Sigma-Aldrich or Operon and listed in the following tables.

Table 2.1: Primers used for cloning
fw = forward, rev = reverse

Name	Application	Sequence 5’ to 3’
MYC_BamHI_fw	MYC cloning	CGCGGATCCACCATGCCCCTCAACGTTAGCTT C
MYC_EcoRI_rev	MYC cloning	ATCCGGAATTCTTACGCACAAGAGTTCCGTAG
MYC-HA-EcoRI_rev	MYC cloning	ATCCGGAATTCTTAGGCGTAATCTGGAACATC GTATGGGTACGCACAAGAGTTCCGTAGCTG
MYC_AgeI_fw	MYC cloning	GCTACCGGTATTTAAATATGCCCCTCAACGTT AGCTT
MYC-SpeI_rev	MYC cloning	GCGTTAATTAAACTAGTTTACGCACAAGAGTT CCGTA
MYC-HA_SpeI_rev	MYC cloning	AATGGACTAGTTTAGGCGTAATCTGGAACATC GTATGGGTA CGCACAAGAGTTCCGTAGCTG
MYC_attB1_fw	MYC cloning	GGGGACAAGTTTGTACAAAAAAGCAGGCTTCA CCATGCCCCTCAACGTTAGCTT
HA_attB2_rev	MYC cloning	GGGGACCACTTTGTACAAGAAAGCTGGGTCTT AGGCGTAATCTGGAACAT

Primers used for qRT-PCR were designed with the program Universal ProbeLibrary from Roche. For this prupose, primers were selected to be intron-spanning to avoid amplification of genomic DNA.

Table 2.2: Primers used for qPCR
The name indicates, which mRNA or DNA region was amplified. TSS = transcription start site, TES = transcription end site

Name	Application	Sequence (5' to 3') forward primer	Sequence (5' to 3') reverse primer
FBXW8 TSS	ChIP	GTGATAGGCAGCAGAGCTGA	TGTACGCACGTGGTGGTC
NCL TSS	ChIP	CTACCACCCTCATCTGAATCC	TTGTCTCGCTGGGAAAGG
Ctrl region	ChIP	TTTTCTCACATTGCCCCTGT	TCAATGCTGTACCAGGCAAA
GNL3 TSS	ChIP	GTGACGCTCGTCAGTGG	CATATTGGCTGTAGAAGGAAGC
GNL3 TES	ChIP	GATCAGGCCACAGGTTACAA	TGCTGAATGACTGGAAAGAAGA
U2 promoter	ChIP	TTTGCTCCCACTGCCGTC	CTGAGTCTTTCGGTGCCC
GNL3	qRT-PCR	TATCCATGGGGCTTACAAGG	CTGGACTTCGCAGAGCAAG
PLD6	qRT-PCR	CTCAACGGCTCGCAAATC	GCCTGGGTCTTGATCGTG
TFAP4	qRT-PCR	ACGGAGAGAAGCTCAGCAAG	TGAAGCGCTTGAGCTGTGT
RRP12	qRT-PCR	CCGTGACCCTTCAGGTGTA	GCCCTTGAGGACTGAGCATA
FBW7	qRT-PCR	CAGCAGTCACAGGCAAATGT	GCATCTCGAGAACCGCTAAC
SKP2	qRT-PCR	CTGTCTCAAGGGGTGATTGC	TGTACACGAAAAGGGCTGAA
MYC	qRT-PCR	TCCTACGTTGCGGTCACA	GCTCGGTCACCATCTCCA
b2M	qRT-PCR	GTGCTCGCGCTACTCTCTC	GTCAACTTCAATGTCGGAT

2.4.2 RNA oligonucleotides

siRNA oligonucleotides were purchased from Dharmacon as a pool of four RNA oligonucleotides targeting the corresponding gene (ON-TARGETplus SMARTpool). As a control siRNA, the ON-TAGETplus Non-targeting Pool was used.

siCtrl	ON-TARGETplus Non-targeting Pool	D-001810-10
siSKP2	ON-TARGETplus SMARTpool	L-003324-00
siFBW7	ON-TARGETplus SMARTpool	L-004264-00

2.4.3 Plasmids

Plasmids used in this study are listed in the following tables. All plasmids listed in tables 2.3 – 2.5 were already available in the group of Prof. Martin Eilers.

Table 2.3: Empty vectors used in this study

Vector	Description
pcDNA3.1	eukaryotic expression vector with CMV-promoter
pLEGO-iG2-puro-IRES-GFP	lentiviral expression vector with SFFV-promoter, puromycin resistance and eGFP, obtained from Boris Fehse
pRRL-SFFV-IRES-Hygro	lentiviral expression vector with SFFV-promotor and hygromycin resistance, generated by Katrin E. Wiese
pDONR221	vector to generate entry clone for gateway cloning, Invitrogen
pINDUCER21	Dox-inducible cDNA expression vector with IRES GFP

Table 2.4: Packaging vectors used for lentivirus production

Name	Description
psAX.2	plasmid for lentivirus production, encoding for virion packaging system
pMD2.G	plasmid for lentivirus production, encoding for virion envelope

Table 2.5: Plasmids used in this study, which were already available in the lab of Prof. Eilers

Name	Description
pcDNA3.1-Flag-MYC	eukaryotic expression vector with coding sequence (CDS) of human *MYC* with N-terminal Flag-tag
pcDNA3.1-His6-Ubiquitin	eukaryotic expression vector with CDS of *UBIQUITIN* with N-terminal hexa-histidin (His6)-tag
pcDNA3.1-HA-WT MYC	eukaryotic expression vector with CDS of human *MYC* with N-terminal hemagglutinin (HA)-tag
pcDNA3.1-HA-K-less MYC	eukaryotic expression vector with CDS of human K-less *MYC* with N-terminal HA-tag
pcDNA3.1-HA-K52o MYC	eukaryotic expression vector with CDS of human K52o *MYC* with N-terminal HA-tag
pcDNA3.1-MIZ1	eukaryotic expression vector with CDS of human *MIZ1*
pTK-Ebox	firefly luciferase reporter construct with prothymosin-α promotor containing a canonical E-box (Gaubatz et al., 1995)
CMV-β-Gal	eukaryotic expression vector with CMV-promoter and β-Gal CDS
pRetroSuper-puro-scrambled	retroviral vector for shRNA expression, RNA pol III-dependent H1-RNA promotor, puromycin resistance, non-targeting control shRNA (Brummelkamp et al., 2002)
pRetroSuper puromycin shMax1	retroviral vector for shRNA expression, RNA pol III-dependent H1-RNA promotor, puromycin resistance, shMAX, NKI library
pRetroSuper puromycin shMax2	retroviral vector for shRNA expression, RNA pol III-dependent H1-RNA promotor, puromycin resistance, shMAX, NKI library

Table 2.6: Plasmids generated for this project

Name	Description
pcDNA3.1-WT MYC	eukaryotic expression vector with CDS of human WT *MYC*
pcDNA3.1-K-less MYC	eukaryotic expression vector with CDS of human K-less *MYC*
pcDNA3.1-HA-WT_N-K_C MYC	eukaryotic expression vector with CDS of human WT_N-K_C *MYC* with N-terminal HA-tag
pcDNA3.1-HA-$K_N WT_C$ MYC	eukaryotic expression vector with CDS of human -$K_N WT_C$ *MYC* with N-terminal HA-tag
pLEGO-WT MYC	lentiviral expression vector with CDS of human WT *MYC*
pLEGO-K-less	lentiviral expression vector with CDS of human K-less *MYC*
pLEGO-WT_N-K_C	lentiviral expression vector with CDS of human WT_N-K_C *MYC*
pLEGO-$K_N WT_C$	lentiviral expression vector with CDS of human -$K_N WT_C$ *MYC*
pLEGO-WT-HA	lentiviral expression vector with CDS of human WT *MYC* with C-terminal HA-tag
pLEGO-K-less-HA	lentiviral expression vector with CDS of human K-less *MYC* with C-terminal HA-tag
pLEGO-K52o-HA	lentiviral expression vector with CDS of human K52o *MYC* with C-terminal HA-tag
pRRL-WT MYC	lentiviral expression vector with CDS of human WT *MYC*
pRRL-K-less MYC	lentiviral expression vector with CDS of human K-less *MYC*
pRRL-WT_N-K_C	lentiviral expression vector with CDS of human WT_N-K_C *MYC*
pRRL-$K_N WT_C$	lentiviral expression vector with CDS of human -$K_N WT_C$ *MYC*
pRRL-K52o	lentiviral expression vector with CDS of human K52o *MYC*
pRRL-WT-HA	lentiviral expression vector with CDS of human WT *MYC* with C-terminal HA-tag
pRRL-K-less-HA	lentiviral expression vector with CDS of human K-less *MYC* with C-terminal HA-tag
pINDUCER21-WT-HA	Dox-inducible lentiviral expression vector with CDS of human WT *MYC* with C-terminal HA-tag
pINDUCER21-K-less-HA	Dox-inducible lentiviral expression vector with CDS of human K-less *MYC* with C-terminal HA-tag
pINDUCER21-HA-WT_N-K_C	Dox-inducible lentiviral expression vector with CDS of human WT_N-K_C *MYC* with C-terminal HA-tag
pINDUCER21-HA-WT_N-K_C	Dox-inducible lentiviral expression vector with CDS of human -$K_N WT_C$ *MYC* with C-terminal HA-tag
pINDUCER21-K52o-HA	Dox-inducible lentiviral expression vector with CDS of human K52o *MYC* with C-terminal HA-tag

2.5 Antibodies

Table 2.7: List of primary antibodies
IB = immunoblot, ChIP = chromatin immunoprecipitation, IF = immunofluorescence, IP = immunoprecipitation

Antibody	Host / Isotype	Application	Description / Source of supply
α-TUBULIN	rabbit, polyclonal IgG	IB	E-19-R, Santa Cruz, sc-12462
acetylated histone H3	rabbit, polyclonal IgG	ChIP	#06-599, Millipore
acetylated histone H4	rabbit, polyclonal IgG	ChIP	#06-866, Millipore
acetylated lysine	rabbit, polyclonal IgG	IB	#9441, Cell Signaling
BRD4	rabbit, polyclonal IgG	IB	A301-985A100, Bethyl
CDK2	rabbit, polyclonal IgG	IB	M2, Santa Cruz, sc-163
CDK9	rabbit, polyclonal IgG	ChIP	Santa Cruz, sc-484
CDK9	rabbit, polyclonal IgG	IB	Santa Cruz, sc-8338
cleaved-PARP	mouse, monoclonal IgG1	IB	51-9000017, BD Pharmingen
CTR9	rabbit, polyclonal IgG	ChIP, IB	A301-395, Bethyl
FLAG-tag	mouse, monoclonal IgG1	IP, IB	M2, F3165, Sigma-Aldrich
HA-tag	rabbit, polyclonal IgG	ChIP, IF, IB	Abcam, ab9110
histone H2B	rabbit, polyclonal IgG	IB	Abcam, ab1790
histone H3	rabbit, polyclonal IgG	ChIP	Abcam, ab1791
HELLS	rabbit, polyclonal IgG	IB	produced by Dr. Björn von Eyß
MAX	rabbit, polyclonal IgG	ChIP, IP, IB	C17, Santa Cruz, sc-197
MIZ1	rabbit, polyclonal IgG	IP	H190, Santa Cruz, sc-22837
MIZ1	mouse, monoclonal	IB	10E2, produced by AG Eilers
MNT	rabbit, polyclonal IgG	ChIP, IB	sc-769, Santa Cruz
MYC	mouse, monoclonal IgG1	IB	9E10, produced by AG Eilers
MYC	rabbit, polyclonal IgG	IP, IB	N-262, Santa Cruz, sc-764
MYC	rabbit, polyclonal IgG	IB	Y69, Abcam, ab32072
MYC T58p	rabbit, polyclonal IgG	IB	Abcam, ab28842
MYC S62P	rabbit, polyclonal IgG	IB	Abcam, ab51156
RNAPII total	rabbit, polyclonal IgG	ChIP	N20, sc-899X, Santa Cruz
RNAPII Ser2p	rabbit, polyclonal IgG	ChIP	Abcam, ab5095
RNAPII Ser5p	mouse, monoclonal IgG1	ChIP	CTD4H8, MMS-128P, Covance
SPT5	mouse, monoclonal IgG1	IB	A-3, sc-133097
VINCULIN	mouse, monoclonal IgG1	IB	V9131, Sigma-Aldrich

Table 2.8: List of secondary antibodies
IB = immunoblot, IF = immunofluorescence

Antibody	Host	Application	Description / Source of supply
Alexa Fluor® 647 anti-rabbit IgG	goat	IF	A-21244, Life Technologies
anti-mouse IgG-HRP	donkey	IB	sc-2314, Santa Cruz
anti-rabbit IgG-HRP	donkey	IB	sc-2313, Santa Cruz
anti-rabbit IgG-HRP TrueBlot	mouse	IB	eB182, 18-8816-33, Biomol
FITC mouse anti-BrdU	mouse	FACS	B44, 347583, BD Biosciences

2.6 Peptides

Biotinylated N-MYC peptides were kindly provided by Richard Bayliss and Mark Richards (University of Leicester, UK).

N-MYC$^{28\text{-}89}$,

Biotin-FYPDEDDFYFGGPDSTPPGEDIWKKFELLP**T**PPL**S**PSRGFAEHSSEPPSWVTEMLLENELWG

with the following modifications:

non-phosphorylated

phosphorylated at T58

phosphorylated at S62

phosphorylated at T58 and S62

2.7 Strains and cell lines

2.7.1 Bacterial strains

DH5α — *Escherichia coli*, genotype F– Φ80lacZΔM15 Δ(lacZYA-argF) U169 recA1 endA1 hsdR17 (rK–, mK+) phoA supE44 λ– thi-1 gyrA96 relA1; used for plasmid amplification

XL1 blue — *Escherichia coli*, genotype recA1 endA1 gyrA96 thi-1 hsdR17 supE44 relA1 lac [F´ proAB lacIqZΔM15 Tn10 (Tetr)], used for amplification of lentiviral plasmids

2.7.2 Human cell lines

293TN	human embryonic kidney cell line (ATCC)
HeLa	human cervix carcinoma cell line (ATCC)
IMECs	human immortalized mammary epithelial cell line (kindly provided by Victoria Cowling and Michael Cole)
MCF10A	human immortalized mammary epithelial cell line (kindly provided by Mohamed Bentires-Alj)

2.8 Cultivation media and supplements

2.8.1 Media and antibiotics for bacterial cell culture

LB-medium	10% (w/v) Bacto tryptone 0.5% (w/v) yeast extract 1% (w/v) NaCl
LB-agar	LB-medium with 1.2% (w/v) Bacto agar was first autoclaved, then heated in a microwave oven, cooled down to 50°C, antibiotics were added and 20 ml was poured into 10 cm dishes
Antibiotics	The following antibiotics were added to LB-medium and LB-agar plates: Ampicillin 100 µg/ml Kanamycin 30 µg/ml Chloramphenicol 25 µg/ml

2.8.2 Media for mammalian cell culture

293TN, HeLa	DMEM containing 4.5 g/l glucose and 0.584 g/l L-glutamine (Sigma) 10% (v/v) FBS (Biochrom, heat inactivated for 30 min at 56°C before usage) 1% (v/v) penicillin / streptomycin (Sigma)
IMECs	DMEM/F12 with 365 mg/l L-glutamine (Gibco® Life Technologies) 0.5% (v/v) penicillin / streptomycin (Sigma) 10 µg/ml insulin (Sigma) 0.5 µg/ml hydrocortisone (Sigma) 20 ng/ml EGF (Life technologies)

MCF10A	DMEM/F12 with 365 mg/l L-glutamine (Gibco® Life Technologies) 1% (v/v) penicillin / streptomycin (Sigma) 5% horse serum (Sigma) 10 µg/ml insulin (Sigma) 0.5 µg/ml hydrocortisone (Sigma) 20 ng/ml EGF (Life technologies) 100 ng/ml cholera toxin (Sigma)

2.8.3 Antibiotics for mammalian cell culture

For selection of stably infected cells, the following antibiotics with the indicated concentrations were used:

Puromycin (InvivoGen)	1 µg/ml
Hygromycin (InvivoGen)	80 µg/ml

2.8.4 Additional supplements

	Stock concentration	used concentration
Chloroquine (Sigma)	25 mM in ddH_2O	25 µM
Cycloheximid (CHX, Sigma)	100 µg/µl in EtOH	100 µg/ml
Doxycyclin (Dox, Sigma)	1 mg/ml in EtOH	250 ng/ml
MG-132 (Calbiochem)	20 mM in EtOH	10 µM
Protamine sulfate (Sigma)	4 mg/ml in ddH_2O	5 µg/ml

2.9 Consumables

Consumables such as cell culture dishes, reaction tubes and other disposable plastic items were purchased from the companies Applied Biosystems, Eppendorf, Greiner, Kimberley-Clark, Nunc, Sarstedt and VWR.

2.10 Equipment and membranes

Automated Electrophoresis	Experion™ Automated Electrophoresis System (Bio-Rad)
Chemiluminescence imaging	LAS-4000 mini (Fujifim)
Cell culture incubator	BBD 6220 (Heraeus)
Cell Counter	Casy® cell counter (Innovatis)

Centrifuges	Avanti J-26 XP (Backman Coulter) Eppendorf 5417 R (Eppendorf) Eppendorf 5425 (Eppendorf) Eppendorf 5430 (Eppendorf) Galaxy MiniStar (VWR) Multifuge 1S-R (Heraeus)
Deep-sequencer	Genome Analyzer IIx (Illumina)
Flow cytometer	BD FACS CantoTM II (BD Biosciences)
Heating block	Dry Bath System (Starlab) Thermomixer® comfort (Eppendorf)
Heat Sealing	ALPTM 50V (Thermo Scientific)
Incubator shaker	Model G25 (New Brunswick Scientific)
Luminometer	GloMax 96 Microplate Luminometer (Promega)
Microscopes	Axiovert 40CFL (Zeiss) TCS SP5 (Leica)
PCR thermal cycler	Mastercycler pro S (Ependorf)
Photometer	Multiscan Ascent (Thermo Labsystems) UltrospecTM 3100 pro UV/Visible (Amersham Biosciences) Spectrofluorometer NanoDrop 1000 (Thermo Scientific)
Power supply	Power Pac (Bio-Rad) Consort EV231/EV243 (Roth)
PVDF transfer membrane	Immobilon-P transfer membrane (Millipore)
Quantitative RT-PCR machine	Mx3000P (Stratagene)
SDS-PAGE system	Minigel (Bio-Rad) Mini-PROTEAN Tetra Cell (Bio-Rad)
Sterile bench	HeraSafe (Heraeus)
Ultrasonifier	Digital Sonifier® W-250 D (Branson)
UV fluorescent table	Maxi UV fluorescent table (Peqlab)
Vortex mixer	Vortex-Genie 2 (Scientific Industries)

Water bath	Julabo ED-5M water bath (Julabo) Memmert waterbath (Memmert)
Immunoblot transfer chamber	PerfectBlue Tank Electro Blotter Web S (Peqlab)
Whatman filter paper	Gel Blotting Paper (Schleicher and Schuell)

2.11 Software and online programs

ApE plasmid editor	by M. Wayne Davis
BD FACSDiva 6.1.2	BD Biosciences
Bedtools	(Quinlan and Hall, 2010)
Bowtie v.0.12.8	www.bowtie-bio.sourceforge.net
FlowJo 8.8.6	FlowJo, LLC
Illustrator™, Photoshop™, Acrobat™	Adobe Inc.
Integrated Genome Browser	(Nicol et al., 2009)
LAS AF 2.0	Leica
Mac OS X	Apple Inc.
Multi Gauge	Fujifilm
MSigDB 3.1	(Subramanian et al., 2005) www.broadinstitute.org/gsea/msigdb/index.jsp
MxPro qPCR Software	Stratagene
Office 2011 Mac	Microsoft Inc.
Papers	Mekentosj
Prism4	GraphPad Software Inc.
R 3.1.1	R foundation
Samtools	(Li et al., 2009)
UCSC Genome Bioinformatics	http://genome.ucsc.edu

3 Methods

3.1 Cell biology methods

3.1.1 Cultivation of eukaryotic cell lines

All eukaryotic cell lines were cultivated in a cell incubator at 37°C, 5% CO_2 and a relative humidity of 95%.

3.1.1.1 Passaging of cells

For maintenance of an adherent cell line, cells were passaged every two to three days. The medium was removed, cells were washed with PBS and trypsinized to detach them from the cell culture dish. The enzymatic activity of trypsin was inhibited by addition of serum-containing medium. The cells were transferred into a 15 ml tube and centrifuged at 300 x g for 5 min. Supernatant was removed, the cell pellet resuspended in the appropriate cell culture medium and a fraction of the cell suspension was replated on a new cell culture dish with fresh medium. For plating cells at a specific cell number, the cell number of a suspension was either determined with a Neubauer counting chamber or with the CASY cell counter.

3.1.1.2 Freezing of cells

For long-term storage, cells were frozen and stored in liquid nitrogen. To this end, cells were detached from their cell culture dish by trysinization (see 3.1.1.1), spun down, resuspended in freezing medium and transferred to cryo vials. The cryo vials were first stored in an MrFROSTY freezing container at -80°C to ensure slow freezing (1°C per min) and then transferred to liquid nitrogen storage tanks.

3.1.1.3 Thawing of cells

Frozen cells were quickly thawed in a 37°C water bath and transferred into a medium-filled tube. To remove all traces of DMSO, cells were centrifuged at 300 x g for 5 min, the cell pellet was resuspended in fresh medium and the cells were plated on a cell culture dish.

3.1.2 Synchronization of IMECs by EGF withdrawal

To synchronize immortalized mammary epithelial cells (IMECs), the cells were seeded at a specific cell number obtaining approximately 50% confluence on the next day. Then, cells were washed twice with PBS, medium without EGF was added and the cells were cultivated for 24-48 h.

3.1.3 Transfection of siRNA

Transfection of synthetic siRNAs (Dharmacon) was performed with the transfection reagent Lipofectamine^{TM} RNAiMAX (Invitrogen). First, cells were washed with PBS and provided with medium without antibiotics. For transfection, 20 µM siRNA was diluted with Opti-MEM (Invitrogen) up to 500 µl and, in a separate tube, 10 µl Lipofectamine^{TM} RNAiMAX was diluted with 490 µl Opti-MEM. The reactions were incubated for 5 min at RT, mixed and incubated for another 20 min. The transfection mix was added dropwise to the cells. After 8-10 h, the medium was changed to full medium. The cells were harvested 48 h after transfection for further analysis.

3.1.4 Transfection of plasmid DNA

One of the following methods was used to transfect mammalian cells with plasmid DNA depending on the cell line. 48 h after transient transfection of cDNA expression plasmids, cells were harvested for further analysis.

3.1.4.1 Calcium phosphate transfection

Cells were seeded in an appropriate density one day before transfection. The medium was changed shortly before transfection and 25 µM chloroquine was added. For transfection of a 10 cm dish, 5–30 µg DNA was mixed with 50 µl 2.5 M $CaCl_2$ and filled up to 500 µl with ddH_2O. 500 µl 2x HBS was added drop wise to the reaction while vortexing to generate calcium phosphate-DNA complexes and this mixture was added to the cells. On the next day, cells were washed with PBS to remove DNA precipitates and fresh medium was added.

3.1.4.2 Transfection with polyethylenimin (PEI)

Cells were seeded in an appropriate density 24 h before transfection. On the day of transfection, cells were washed with PBS and transfection medium (DMEM with 2% FCS, without antibiotics) was added. To transfect a 10 cm dish, 10 µg of DNA was diluted with Opti-MEM to 500 µl and in a second tube, 20 µl PEI (1 µg/µl) were mixed with 480 µl Opti-MEM. After incubation for 5 min at RT, the reactions were mixed and incubated for 15 min at RT. The transfection mix was added dropwise to the cells. Cells were washed with PBS 4 to 5 h after transfection and fresh full medium was added.

3.1.5 Production of lentiviruses

One day before transfection, $5x10^6$ 293TN cells were plated on a 10 cm cell culture dish. On the next day, cells were transfected with the calcium phosphate transfection method. For lentivirus production 10 µg of the packaging vector psPAX2, 2.5 µg of the envelope vector pMD2.G and 10 µg lentiviral expression plasmid (such as pRRL, pLEGO or pINDUCER21) was used for transfection. On the next day, the medium was removed and 6 ml fresh medium was added. The first virus containing supernatant was harvested 48 h after transfection. Further virus containing supernatants were collected 60 h and 72 h after transfection. The supernatants were pooled and filtered using a syringe with 0.45 µm filter. The virus supernatant was either used directly for infecting cells or stored in aliquots at -80°C.

3.1.6 Lentiviral infection of cells

To infect a 6 cm dish with lentivirus, 2 ml fresh medium was added to the cells together with 200 µl lentiviral supernatant and 2.67 µl protamine sulfate (4 µg/µl). The amount of virus used for infection was dependent on the lentiviral constructs, virus titer and the cell line that should be infected. Medium was changed approximately 24 h after infection. If applicable, selection with appropriate antibiotics was started 48 h after infection. To determine the time point when the selection was successful, a non-infected control plate was treated with the same selection medium.

3.1.7 Colony formation assay (crystal violet staining)

The crystal violet staining can be used to visualize cell densities on a cell culture dish and therefore determine proliferation of cells. For this purpose cells were plated with the same cell number and cultivated for four to eight days. Then, cells were fixed with 1% formaldehyde for 15 min, washed with PBS and stained for 1 h with the triphenylmethane dye crystal violet. Excess of the dye was washed away with desalted water and the plates were air dried at RT.

3.1.8 Cumulative growth curve

To compare proliferation capability of different stable cell lines a cumultative growth curve was prepared. To this end, cells were plated in equal cell numbers (150,000) in triplicates in 6 cm dishes. Every third day, the cells were trypsinized and the total number of living cells was determined with the CASY cell counter. The original cell number (150,000) was replated. On the basis of the total cell number (X), the increase of the cell number (R) was determined (R=X/150,000), the cumulative cell number (Y) of each passage (p) was calculated ($Y_{(p)}=Y_{(p-1)}xR$) and illustrated in a graph.

3.1.9 Single-color competition experiment (GFP-competition)

For a single-color competition experiment, stable cell lines were generated that expressed the protein of interest and the green fluorescent protein GFP. These cells were mixed with uninfected cells that neither expressed GFP nor the transgene. The mix ratio was 1/5 meaning 20 % were GFP- and transgene positive cells whereas 80% were uninfected cells. The cell mixtures were plated with equal cell number in triplicates on 6 cm dishes. After 3 days, cells were trypsinized, a fraction of the mix was replated and the amount of GFP/transgene positive cells was determined with a flow cytometer. The in- or decrease of GFP-positive cells over time was illustrated in a graph.

3.1.10 Propidium iodide staining for flow cytometry (PI-FACS)

Propidium iodide staining of DNA with subsequent analysis by FACS (fluorescence-activated cell sorting) was used to determine DNA-content and therewith cell cycle distribution of cells. Propidium iodide is a fluorescent dye that intercalates into DNA. On

the basis of the DNA content, it can be determined whether a cell resides in the G1/G0 (DNA content 2N), S (DNA content <2N, <4N) or G2/M (4N) cell cycle phase. Moreover, apoptotic (sub G1, <2N) and polyploid cells (>4N) can be identified.
To include apoptotic cells in the measurement, cell culture supernatant containing floating cells was transferred into tubes and the adherent cells were trypsinized and added to the supernatant. Cells were spun down for 5 min at 400 x g, washed with cold PBS and again centrifuged. The cell pellet was resuspended in 200 µl PBS and cells were fixed by adding 800 µl 100% ice-cold EtOH while vortexing. Fixed cells were stored over night at -20°C. On the next day, cells were spun down for 10 min at 400 x g and washed twice with 5 ml cold PBS. Cell pellets were resuspended in 400 µl 38 mM sodium citrate containing 1 µl RNase A (10 mg/ml stock solution) and 15 µl propidium iodide (1 mg/ml stock solution). After incubation at 37°C for 30 min protected from light, samples were transferred into FACS tubes measured with an excitation wavelengths of 488 nm, a 556 nm longpass- and a 585/42 nm bandpassfilter for propidium iodide (emission at 617 nm). The cell cycle distribution was analyzed using the BD FACSDiva 6.1.2 software.

3.1.11 BrdU-PI-FACS

Bromdesoxyuridin (BrdU) is a thymidine analog, which is incorporated into the DNA during S-phase. Cells that were in S-phase during the labeling can be identified using an anti-BrdU antibody.
For labeling, cells were incubated with 10 µM BrdU for 1 h. Harvesting and ethanol fixation was performed analog to the procedure for the PI-FACS. After the incubation at -20°C over night, cells were pelleted (10 min, 400 x g) and washed with cold PBS. Then, cells were resuspended in 1 ml 2 M HCl / 0.5% Triton X-100 and incubated for 30 min at RT. After pelleting, cells were resuspended in 1 ml 0.1 M $Na_2B_4O_7$ (pH 8.5). Cells were again spun down, resuspended in 100 µl 1% BSA in PBS-T (0,5% Tween-20 in PBS) and 20 µl anti-BrdU-FITC antibody was added. After incubation for 30 min at RT (protected from light), cells were washed with 200 µl 1% BSA in PBS-T and pellets resuspended in 400 µl 38 mM sodium citrate containing 1 µl RNase A (10 mg/ ml stock solution) and 15 µl propidium iodide. After incubation for 30 min at 37°C (in the dark), cells were measured by flow cytometry.

3.1.12 Indirect immunofluorescence

To analyze subcellular localization of proteins, cells were plated on glass cover slips coated with 0.1% gelatin. On the next day, cells were washed with PBS and incubated for 15 min in fixing solutions (4% PFA (w/v) / 2% sucrose (w/v) in PBS). Afterwards, cells were washed with PBS and incubated twice for 10 min in 0.1 M glycine in PBS. Cells were permeabilized by incubating them twice for 5 min in 0.1% NP-40 (v/v) in PBS. The cover slips were transferred into a wet chamber, followed by blocking for 45 min in blocking solution and incubation with primary antibody diluted in blocking solution over night at 4°C. On the next day, the cover slips were washed three times with PBS and incubated for 1 h with fluorescence-labeled secondary antibody at RT in the dark. Cover slips were washed three times with PBS. The second PBS washing solution contained Hoechst (1:10,000) to stain nuclei. The cover slips were mounted with Fluoromount (Sigma) and edges sealed with nail polish. Samples were analyzed with a fluorescence microscope and could be stored at 4°C protected from light.

3.1.13 Luciferase reporter gene assay and ONPG measurement

To determine luciferase activity, cells were plated in 6-well plates and transfected with the reporter constructs and expression plasmids using PEI transfection. 48 h after transfection, cells were washed with PBS and lysed with 250 µl passive lysis buffer (Promega) for 15 min at RT while shaking. Lysates were transferred into a 1.5 ml tube and cleared by centrifugation. 50 µl lysate was pipetted into a clear bottom 96-well plate and the plate was placed in the Glomax 96 Microplate Luminometer. The luminometer automatically added 100 µl luciferase substrate solution per well and measured light emission at 562 nm in relative light units (RLU).

For normalization, the activity of the co-transfected β-galactosidase was determined. To this end, 50 µl lysate was mixed with 50 µl ONPG (5 mg/ml H_2O) and 750 µl β-galactosidase buffer. The samples were incubated at 37°C until a yellow color has developed and absorbance was measured at 420 nm.

3.2 Molecular biology methods

3.2.1 Transformation of competent cells with plasmid DNA and plasmid amplification

Chemically competent bacteria were thawed on ice and mixed with the ligation mix or 1 µg plasmid DNA. The bacteria were incubated on ice for 30 min, followed by a heat shock for 90 s at 42 °C. The reactions were shortly cooled down on ice followed by the addition of 1 ml LB medium. Bacteria were incubated for 30 min at 37°C before plating them on LB-agar plates. Was the transformation performed for plasmid amplification, 50 µl bacteria suspension was plated on LB agar plates containing the appropriate antibiotic for selection. After transformation of a ligation mix, the bacteria suspension was spun down, resuspended in 50 µl LB medium and the complete reaction was plated. LB agar plates were incubated at 37°C over night.

3.2.2 Analytical preparation of plasmid-DNA from bacteria (Miniprep)

The analytical preparation of plasmid DNA was performed using alkaline lysis. 1.5 ml overnight culture was spun down and the bacteria were resuspended in 150 µl TE buffer containing 1.5 µl RNase A (10 mg/ml stock solution). Lysis was performed by addition of 150 µl lysis buffer and incubation for 5 min at RT. The lysis was stopped by adding 150 µl precipitation buffer and the samples were centrifuged for 10 min at 18,000 x g. The supernatant was mixed with 1 ml 100% EtOH and the plasmid DNA was pelleted by centrifugation for 10 min at 18,000 x g and 4°C. The DNA pellet was washed with 70% EtOH, air dried and solubilized in 50 µl ddH_2O.

3.2.3 Preparative isolation of plasmid DNA (Maxiprep)

For preparative isolation of plasmid DNA, 200 ml overnight culture was processed according to the manufacturer's protocol (PureLink® HiPure Plasmid Maxiprep Kit, Life Technologies). The purified plasmid DNA was solubilized in TE and adjusted to a concentration of 1 µg/µl.

3.2.4 Restriction analysis of DNA

Sequence specific hydrolysis of DNA was performed with restriction endonucleases from Fermentas and New England Biolabs using the recommended restriction buffers and enzyme amounts. A control digestion was incubated for 2 h at the recommended temperature and set up according to the following table:

1 µg DNA
0.4 µl restriction endonuclease 1
0.4 µl restriction endonuclease 2
1 µl 10x reaction buffer
ad 10 µl ddH_2O

For a preparative restriction digestion, the amount of DNA, restriction endonucleases, sample volume and digestion time was adjusted.

3.2.5 Gel electrophoretic separation of DNA fragments

The separation of DNA fragments by gel electrophoresis was performed depending on the expected fragment size using a 1-2% agarose gel in a TAE buffer. For this purpose the agarose was boiled in TAE buffer, supplemented with 0.3 µg/ml ethidium bromide and poured into a gel chamber with combs. The samples were mixed with DNA loading buffer and pipetted into the pockets of the gel. To determine the size of the DNA fragment, a DNA ladder (Thermo Scientific) was loaded next to the samples. The separation was preformed at 120 V for one hour and the DNA fragments were visualized due to the intercalated ethidium bromide on a UV transilluminator.

3.2.6 Extraction and purification of DNA fragments and PCR products

For purification of DNA fragments from agarose gels, the fragment was cut out of the gel and extracted with the gel extraction kit according to the manufacturer's protocol (GeneJET Gel Extraction Kit, Thermo Scientific).
Purification of PCR products was performed according to the manufacturer's protocol (GeneJET PCR Purification Kit, Thermo Scientific).

3.2.7 Ligation of DNA fragments

Ligation of DNA fragments was performed with the T4 DNA ligase (Thermo Scientific). The DNA fragment (insert) was used in 3x molar excess to the linearized vector.

Ligation mix:	50 ng linearized vector
	X ng fragment
	1 µl T4 DNA ligase
	1 µl 10x ligation buffer
	ad 10 µl ddH_2O

The ligation mix was incubated for 1-2 h at RT und transformed into competent bacteria.

3.2.8 Gateway® cloning

To clone cDNA into the pINDUCER21 vector, the Gateway® cloning technology from Life technologies was used. This technology is based on the site-specific recombination properties of the bacteriophage lambda, which integrates its DNA into the *E.coli* genome. Cloning was performed according to the manufacture's protocol and includes two recombination reactions (BP and LR reaction). Briefly, primers with an *att*B1 or *att*B2 site were designed to amplify the cDNA of interest. The PCR product with the *att*B sites was recombined into the pDONR™ vector with the BP reaction to generate an entry clone. Using the LR reaction, the cDNA was then transferred from the entry clone into the destination vector, in this case the pINDUCER21 expression vector (Meerbrey et al., 2011).

3.2.9 Nucleic acid quantification

3.2.9.1 Nanodrop

DNA and RNA concentration was typically determined with the NanoDrop 1000. (PeqLab). Absorbance was measured at 260 nm. To assess the purity of the nuclei acid solution, the ratio of absorbance at 260 and 280 nm was determined. A ratio of ~ 1.8 for pure DNA and ~2.1 for pure RNA was expected.

3.2.9.2 PicoGreen

The concentration of double-stranded DNA (dsDNA) was determined with the Quant-iTTM PicoGreen® dsDNA reagent (Invitrogen). PicoGreen intercalates into dsDNA and the fluorescence at a wavelength of 485/535 nm can be determined. The measurement was performed according to the manufacturer's protocol. DNA quantifications with PicoGreen were performed to determine concentrations of chromatin samples after ChIP, which were used for ChIP-Sequencing.

3.2.9.3 Bioanalyzer

RNA, which was used for library preparation for RNA-Sequencing, as well as the prepared DNA-libraries, were quantified with the Experion™ Automated Electrophoresis System from Bio-Rad.

3.2.10 RNA Isolation

3.2.10.1 RNA isolation with TriFAST

Total RNA was typically isolated with peqGOLD TriFast (Peqlab). The cell culture medium was aspirated and cells were lysed directly on the plate with 1 ml Trifast and transferred into a 1.5 ml reaction tube. 200 µl chloroform was added and the suspension was vortexed for 10 s. The reactions were centrifuged (10 min at 20,000 x g, 4°) to separate the phases and the upper aqueous phase containing the RNA (~500 µl) was transferred into a new reaction tube. To precipitate the RNA, 500 µl isopropanol and 1 µl glycogen (20 µg/µl stock solution, Fermentas) were added. The samples were incubated on ice for 10 min followed by centrifugation for 10 min (20,000 x g at 4°). The supernatant was discarded and the RNA pellet washed twice with 75% EtOH. The washed RNA pellet was air-dried and solubilized in 20-50 µl RNAse free ddH_2O. The RNA was used for cDNA synthesis and stored at -80°C.

3.2.10.2 RNA isolation with RNeasy® Mini Columns and DNase digestion (Qiagen)

If RNA was used for RNA-Sequencing (RNA-Seq), isolation was performed with the RNeasy® Mini Columns and additional DNase I digestion according to manufacturer's protocol.

3.2.11 cDNA synthesis

For expression analysis of individual genes, the extracted total RNA was reverse transcribed into complementary DNA (cDNA) with random hexanucleotide primers. For this purpose, 0.5-2 µg total RNA was diluted with nuclease-free water up to 20 µl and incubated for 2 min at 65°C to dissolve secondary structures. The samples were quickly cooled down and 30 µl cDNA synthesis mix was added per reaction. The samples were incubated for 10 min at 25°C, followed by incubation at 37°C for 50 min and 70°C for 15 min.

cDNA synthesis mix:	10 µl 5x First strand reaction buffer (Promega)
	1.25 µl dNTPs (10 mM Stock, Roth)
	2 µl random primers (2 µg/ml Stock, Roche)
	0.2 µl RiboLock RNase Inhibitor (40 U/µl, Fermentas)
	1 µl M-MLV reverse transcriptase (200 U/µl, Promega)
	ad 30 µl nuclease-free water

The cDNA was diluted up to 250 µl with ddH_2O and 5 µl of diluted cDNA was used per quantitative reverse transcriptase PCR reaction (see 3.2.12.2).

3.2.12 Polymerase chain reaction (PCR)

3.2.12.1 PCR to amplify cDNA for cloning

To generate new cDNA expression vectors the gene of interest was amplified from an existing expression vector. This allowed the addition of tags to the gene of interest, insertion of mutations and addition of new restriction sites.

Standard PCR reaction:	5 ng cDNA template
	5 µl 10x Phusion High-Fidelity (HF) reaction buffer
	1 µl dNTPs (10 mM Stock, Roth)
	1.25 µl forward primer (10 µM Stock)
	1.25 µl reverse primer (10 µM Stock)
	1.5 µl DMSO (3% final concentration)
	0.5 µl Phusion HF DNA polymerase (Fermentas)
	ad 50 µl nuclease-free water

Table 3.1: PCR cycling profile for cloning

Cycle step	Temperature	Time	Cycles
Initial denaturation	98°C	30 s	1 x
Denaturation	98°C	10 s	30 x
Annealing	55 – 62 °C	30 s	
Extension	72°C	15 – 30 s per kb	
Final extension	72°C	8 min	1 x

For mutagenesis the desired mutation was included in the primers and the cDNA was amplified by overlapping PCR. First, the N-terminal and C-terminal halves of the cDNA from the introduced mutation were amplified. These fragments were purified, mixed in a molar ratio 1:1 and used as the template for amplification of the complete cDNA that harbors now the desired mutation.

3.2.12.2 Quantitative real-time PCR (qPCR)

Quantitative PCR was performed to analyze abundance of mRNAs or to analyze enrichment of DNA fragments after chromatin immunoprecipitation (see 3.3.11). During amplification of the DNA a fluorescent dye intercalates into the newly synthesized double-stranded DNA, which can be quantified in real time.

qPCR reaction:	5 µl diluted cDNA (see 3.2.11) or chromatin (see 3.3.11)
	10 µl SYBRGreen Mix (Thermo Scientific)
	5 pmol forward primer
	5 pmol reverse primer
	ad 20 µl nuclease-free water

Table 3.2: PCR cycling profile for qPCR

Cycle step	Temperature	Time	Cycles
Initial denaturation	95°C	15 min	1 x
Denaturation	95°C	30 s	38 x
Annealing	60 °C	20 s	
Extension	72°C	15 s	
Melting curve	95°C	1 min	1 x
	60°C	30 s	
	95°C	30 s	

For quantitative reverse transcriptase PCR (analysis of cDNA), the fold induction relative to a control (e.g. control infected or uninduced cells) was calculated. The housekeeping gene *β2-MICROGLOBULIN* (*b2M*) was used for normalization. For calculation, the threshold cycle (CT) was determined, which indicates at which PCR cycle the fluorescence signal was above the background fluorescence.

$\Delta CT = CT^{b2M} - CT^{Gene}$

$\Delta\Delta CT = \Delta CT_{control} - \Delta CT_{sample}$

relative expression = $2^{-\Delta\Delta CT}$

For ChIPs the result was presented as % of input.

% of input $= 2^{CT(1\%\ Input)-CT(IP)} \times 1\%$ (if 1% input was loaded)

The qPCR measurement was always performed in triplicates. The average and standard deviation was calculated.

standard deviation (SD) = $\sqrt{\frac{\Sigma(X-\overline{X})^2}{(n-1)}}$

3.3 Biochemical methods

3.3.1 Preparation of whole cell protein extracts

For whole cell protein extraction cells were washed with ice cold PBS and scraped directly with RIPA lysis buffer containing proteinase and phosphatase inhibitors off the cell culture dish. The suspension was transferred into a 1.5 ml reaction and snap-frozen in liquid nitrogen. The samples were thawed on ice, vortexed in between and cell debris were pelleted by centrifugation at 20,000 x g for 20 min at 4°C. The supernatant was transferred to a fresh tube and protein concentration was determined with the BCA assay (see 3.3.3.1.).

3.3.2 Fractionation of cell extracts

To investigate whether a protein resides in the cytosol, nucleoplasm or is chromatin associated, cell extracts were fractionated. To this end, freshly harvested cells were pelleted by centrifugation at 300 x g for 5 min. The cell pellet was resuspended in sucrose buffer with freshly added 0.5% NP-40 and protease inhibitors and pipetted carefully up and down with a 200 µl pipette to facilitate cytoplasmic lysis. The cell suspension were incubated on ice for 10 min and then centrifuged for 20 min at 3900 x g. The supernatant was transferred into a new tube (containing cytoplasmic proteins) and the white nuclear pellet was washed with sucrose fractionation buffer without any detergent and again centrifuged for 20 min at 3900 x g. The supernatant was discarded, the nuclei were homogenized in nucleoplasmic extraction buffer (2 packed nuclear volumes) and incubated on ice for 20 min. The homogenate was centrifuged for 30 min at 20,000 x g. The nucleoplasmic extract was transferred into a new tube and the pellet was resuspended in nuclease incubation buffer and digested with benzonase. The digested chromatin was cleared by centrifugation at 20,000 x g for 30 min. Protein concentration of all fractions was determined and analyzed by SDS-PAGE and immunoblot.

3.3.3 Total protein quantification by colorimetric assays

Quantification of total protein extracts lysed in RIPA buffer were performed using the BCA assay whereas lysates from HEGN- or TNT-lysis were quantified using the Bradford assay.

3.3.3.1 Bicinchoninic acid assay (BCA) assay

For the BCA assay, 4 µl protein lysate was pipetted into a well of a flat bottom 96-well plate and mixed with 200 µl BCA reagent consisting of buffer A and buffer B (50:1). The reaction was incubated at 37°C for 30 min and the absorbance was measured at a wavelength of 550 nm. A well containing only the lysis buffer with BCA reagent served as the blank. Protein concentration was determined on the basis of a standard curve, which was always included on the plate and prepared in the same lysis buffer as the lysates.

3.3.3.2 Bradford assay

Protein lysates prepared with HEGN- or TNT lysis were quantified according to the Bradford method (Bradford, 1976). 100 µl 150 mM NaCl were pipetted into cuvettes and 2 µl protein lysate was added followed by 900 µl Bradford reagent. The reaction was mixed by vortexing and absorbance was measured at 595nm. A reaction containing 2 µl lysis buffer instead of protein lysate served as the blank. Protein concentration was determined according to the absorbance of the standard curve.

3.3.4 SDS Polyacrylamide gel electrophoresis (SDS-PAGE)

SDS polyacrylamide gel electrophoresis was used to separate proteins according to their molecular weight. Protein lysates were boiled in 6x sample buffer for 5 min at 95°C, spun down and equal protein amounts were loaded on a Bis-Tris polyacrylamide gel consisting of a 8-15% stacking and a 4% resolving gel. The PageRuler Pre-Stained Protein Ladder (Fermentas) was used as a molecular weight marker. Separation of the proteins was performed using SDS-PAGE chambers (Biorad) filled with 1x MOPS running buffer containing freshly added sodium bisulfite at 80-120 V.

3.3.5 Immunoblot

After separating protein lysates by SDS PAGE, proteins were transferred onto a PVDF membrane. To this purpose, a PVDF membrane was incubated in methanol for 1 min and equilibrated, together with the gel and several Whatman filter papers, in transfer buffer. The gel was layered on the PVDF membrane followed by Whatman filter papers on each side and fixed in a tank blot transfer chamber that was filled with 1x transfer buffer containing 20% methanol. The transfer was carried out in the cold room (4°C) at 300 mA for approximately 2-3 h depending on the molecular weight of the proteins. Subsequently, the membrane was blocked for 30 min in blocking buffer followed by incubation in primary antibody at 4°C over night. Afterwards, membranes were washed three times for 10 min with 1x TBS-T and incubated for 1 h with secondary antibody (diluted 1:5000 in blocking solution) followed by additional 3 washing steps with TBS-T. Antibodies were visualized by chemiluminescence using the Immobilon Western Substrate (Millipore) according to manufacturers' protocol and detected with the LAS-4000 imager (Fujifilm Global).

Protein signals were quantified relative to the loading control using the software Multi Gauge.

3.3.6 Stripping of PVDF membranes

To remove antibodies from PVDF membranes, the membranes were incubates for 1 h in stripping buffer. Afterwards, membranes were washed thoroughly with TBS-T before incubating them in blocking buffer. The antibody incubation and detection was performed according to 3.3.5.

3.3.7 Silver staining of proteins in polyacrylamide gels

To visualize immunoprecipitated proteins, which were subjected to mass spectrometric analysis, eluates were loaded on a SDS-PAGE and stained with silver staining. To this end, gels were first incubated for 30 min in fixing solution and then stored for at least 30 min in sensitization solution. After sensitization, gels were washed three times in ddH_2O and proteins were visualized with silver staining for 20 min protected from light followed by incubation in developing solution until protein bands were visible. The developing was stopped by incubation for 10 min in stopping solution and the gels were washed two times in ddH_2O. For long-term storage, gels were dried by vacuum drying.

3.3.8 *In vivo* ubiquitination assay

To detect ubiquitinated proteins in transfected mammalian cells, HeLa cells were transfected with plasmids expressing His-tagged ubiquitin and the protein of interest. 48 h after transfection, cells were harvested, the cell pellet was resuspended in 100 µl PBS and 10 µl was taken as an input control. The input control was adjusted with PBS and sample buffer to a volume of 100 µl, the samples were boiled for 5 min at 95°C and stored at -20°C till further use. The remaining cells were lysed with 1 ml Ubi-buffer A and the lysates were centrifuged at 20,000 x g for 10 min. The supernatant was transferred into a new tube, 50 µl of washed Ni^{2+}-NTA beads (50% slurry) were added and the samples were incubated on a rotating wheel for 3 h at RT. After the incubation, beads were sedimented by centrifugation and washed one time with Ubi-buffer A, two times with Ubi-buffer A/B (mixed 1:4) and one time with Ubi-buffer B. The remaining supernatant was removed and 10 µl 1 M imidazole was added to the beads. The beads were boiled with 100 µl sample buffer at 95°C for 5 min to elute His-tagged proteins. The supernatant and the previously taken input controls were subjected to SDS-PAGE and immunoblot analysis (see 3.3.4 and 3.3.5).

3.3.9 Cycloheximide decay assay

To determine the half-life of a protein, a cycloheximide decay assay was performed. To this end, cells were incubated with 100 µg/ml cycloheximide for a different period of time. Cells were washed with ice-cold PBS and directly lysed on the plate with RIPA lysis buffer and lysates were analyzed by SDS-PAGE and immunoblot (see 3.3.4 and 3.3.5).

3.3.10 Immunoprecipitation (IP)

3.3.10.1 Immunoprecipitation of exogenous proteins

To detect protein-protein interaction, an immunoprecipitation under native conditions was performed. Cells were lysed either in TNT- or 1x HEGN-lysis buffer (supplemented with 150 mM NaCl) containing protease- and phosphatase inhibitors and the lysates were sonified for 20 s (5s pulse, 10 s pause) and 20% amplitude. Lysates were centrifuged for 20 min at 20,000 x g and 4°C to pellet cell debris. The supernatant was transferred into a new reaction tube and the total protein concentration was determined with the Bradford assay (see 3.3.3.2). The same protein amount was used per IP and thy lysates were pre-cleared for 3 h with washed Protein A-Sepharose® 4B (Life Technologies) to remove proteins which bind unspecific to the sepharose. Afterwards, the sepharose was sedimented by centrifugation for 2 min at 2,000 x g and the supernatant was transferred to a new tube. An input sample was taken which was boiled with sample buffer at 95°C for 5 min and stored at -20°C till further use. Per IP 2 µg antibody were used and the samples were incubated over night at 4°C on a rotating wheel. On the next day, 50 µl Protein A-Sepharose® 4B was added to the samples and incubated for additional 3 h on the rotating wheel at 4°C. The sepharose was sedimented by centrifugation and washed with 1 ml lysis buffer. The washing was performed three times and the samples were incubate between the washing steps on the rotating wheel at 4°C. When the HEGN-lysis buffer was used, the NaCl concentration was increased for the last washing step from 150 mM to 200 mM NaCl. After the last washing step, the buffer was removed and the remaining buffer carefully removed with a Hamilton syringe. The beads were boiled in sample buffer for 5 min at 95°C and subjected together with the input samples to SDS-PAGE and immunoblot analysis.

3.3.10.2 Immunoprecipitation of endogenous proteins

For immunoprecipitation of endogenous proteins, nuclear cell extracts were prepared. To this end, cells were incubated in hypotonic sucrose buffer with freshly added 0.1% NP-40 and homogenized with a dounce tissue grinder. All centrifugation steps were performed at 4°C. Nuclei were collected by centrifugation at 800 x g and lysed in high salt lysis buffer (1x HEGN buffer with 300 mM KCl) containing protease and phosphatase inhibitors. Lysates were incubated at 4°C while shaking and centrifuged at 20,000 x g for 30 min. The supernatant was diluted to a salt concentration of 120 mM KCl with 1x HEGN buffer and spun down for 15 min at 20,000 x g. Protein concentration of the nucler extract was determined using the Bradford assay and the same protein amount was used for immunoprecipitation. Nuclear extracts were incubated with antibodies coupled to Dynabeads over night at 4°C on a rotating wheel. Immunoprecipitates were washed four times with 1x HEGN-120 mM KCl, boiled in sample buffer and subjected to immunoblot analysis.

3.3.10.3 Denaturing immunoprecipitation

To immunoprecipitate a protein without interaction partners, the IP was performed under denaturing conditions. To this end, the cell pellet was solubilized in PBS and the same volume denaturing lysis buffer was added. The suspension was boiled for 10 min at 95°C and vortexed in between. The sample was diluted ten fold with TNT-lysis buffer and centrifuged for 30 min at 20,000 x g. The supernatant was subjected to immunoprecipitation.

3.3.11 Peptide-pulldown assay

Peptide-pulldown assays were performed with N-MYC MYC box I peptides and nuclear extracts from HeLa cells. Nuclear extracts were prepared as described for immunoprecipitation of endogenous proteins (see 3.3.10.2). M-280 Streptavidin Dynabeads were washed with TBS and resuspended in peptide binding buffer (2% BSA, 0.05% NP-40 in TBS). 20 µg MYC peptide was added and incubated for 30 min at RT on a rotating wheel. Streptavidin Dynabeads were washed with TBS and resuspended in 1x HEGN lysis buffer (120 mM KCl). Nuclear extracts were added to the beads and incubated at 4°C for 2 h while rotating. The samples were washed four times with 1x HEGN lysis buffer containing 120 mM KCl, resuspended in sample buffer and subjected to immunoblot analysis.

3.3.12 Chromatin immunoprecipitation (ChIP)

Chromatin immunoprecipitation was performed to detect protein-DNA interactions. Therefore, proteins were cross-linked to DNA by formaldehyde, the chromatin isolated and subsequently fragmented. The protein-DNA fragments were precipitated using specific antibodies against the protein and enrichment of the DNA was detected by quantitative real-time PCR using primers for a certain DNA sequence.

Formaldehyde fixation and chromatin isolation

For a ChIP, cells were grown on 15 cm dishes and per IP, approximately $1x10^7$ cells were used. To cross-link proteins to DNA, the cells were fixed with 1% formaldehyde for 15 min at RT while slowly shaking. By addition of glycine to a final concentration of 125 mM the fixation was stopped and the plates were incubated for 5 min at RT on a shaker. To detect indirect chromatin binding, which was mediated by protein-protein interactions, cells were additionally cross-linked with disuccinimidyl glutarate (DSG) for 45 min at RT prior to formaldehyde cross-linking.

The following steps were carried out on ice or at 4°C. Cells were washed twice with ice-cold PBS and scraped off the plates with PBS containing 1 mM PMSF. After centrifugation for 10 min at 1000 x g, the cell pellets were resuspended in 5 ml hypotonic ChIP swelling buffer (the volume was increased depending on the size of the cell pellet) containing proteinase and phosphatase inhibitors and incubated for 10 min on ice. The cell membranes were disrupted by 15 strokes with a dounce homogenizer and nuclei were pelleted by centrifugation for 10 min at 800 x g. Nuclei were resuspended in 1 - 2.5 ml (depending on the size of the nuclear pellet) ChIP sonication buffer containing proteinase- and phosphatase inhibitors and sonified in order to obtain DNA fragments between 200 - 300 bp. Sonication conditions and time was determined empirically for every cell line. Chromatin of IMECs was fragmented for 15 - 20 min at 35% amplitude (10 s pulse, 50 s break). After sonication the size of the fragmented chromatin was determined.

Chromatin size control

For size control, 20 µl chromatin was diluted with 380 µl ChIP elution buffer, 16.8 µl 5 M NaCl was added and the samples were incubated at 65°C for 6 h while shaking. Then, 1 µl RNase A (10 mg/ml stock solution) was added, followed by incubation at 37°C for 1 h. Afterwards, 2 µl proteinase K (1 mg/ml stock solution) was added and the samples incubated at 45 °C for 2 h in a thermo shaker. Chromatin was purified by phenol-chloroform extraction, precipitated with 100% EtOH and 3 M Na-acetate and washed with 80% EtOH. The DNA was air-dried, solubilized in 20 µl ddH_2O and loaded with 6 x DNA-loading buffer on a 2 % agarose gel. After size control, the chromatin was centrifuged for 60 min at 20.000 x g and the supernatant containing the soluble chromatin was transferred into 1.5 ml low binding microtubes.

Coupling of antibodies to protein A or G dynabeads

Per 1 µg antibody, 10 µl protein A or G dynabeads were used for ChIP. The dynabeads were washed three times with ChIP blocking solution. Usually 2 µg antibody was used per IP and incubated with the washed dynabeads in 500 µl ChIP blocking solution over night at 4°C on a rotating wheel. On the following day, the blocking solution was removed and the beads were resuspended in blocking solution (in 1/10 of the chromatin volume used for the ChIP) and added to the chromatin. As a reference, 1% of the chromatin was taken as an input sample.

Immunoprecipitation

The chromatin was incubated with the antibody-coupled dynabeads over night at 4°C on a rotating wheel in low binding tubes. On the next day, the beads were washed two times with ChIP sonication buffer, two times with ChIP high salt buffer and one time with ChIP LiCl buffer. After each washing step, dynabeads were sedimented with a magnetic rack, the buffer removed and fresh buffer added. Each washing step included an incubation for 5 min on the rotating wheel at 4°C.

Elution, decrosslinking and DNA purification

To elute the precipitated DNA from dynabeads, beads were resuspended in 230 µl ChIP elution buffer and incubated for 15 min at 65°C while intensively shaking. The beads were sedimented with a magnetic rack and 200 µl of the eluted DNA was transferred to a fresh reaction tube. 200 µl fresh ChIP elution buffer was added to the beads, the incubation was repeated and again 200 µl were transferred to the tubes. Afterwards, 16.8 µl 5 M NaCl was added to the 400 µl eluate. The input samples were filled up with elution buffer to a volume of 400 µl. To revert the cross-linking, the samples were incubated at 65°C for at least 6 h while shaking. Then, 1 µl RNase A (1 mg/ml stock concentration) was added and the samples incubated for 1 h at 37°C, followed by addition of 2 µl proteinase K (1 mg/ml stock concentration) and incubation at 45°C for 2 h. The DNA was purified by phenol-chloroform extraction. To this end, 420 µl phenol-chloroform-isoamyl alcohol was added, the samples were vortexed and centrifuged for 10 min at 20,000 x g at RT. The upper phase (~390 µl) was transferred to a new 1.5 ml reaction tube, 2.5 sample volumes 100% EtOH, 1/10 sample volume 3 M Na-acetate pH 5.2 and 2 µl glycoblue (Life technologies, 15 mg/ml) were added. The samples were incubated for 30 min at -80°C, centrifuged for 30 min at 20,000 x g and the DNA pellet was washed with 80 % EtOH. After air-drying, the DNA pellet was solubilized in 250 µl ddH_2O. For quantitative real-time PCR, 5 µl of chromatin was used per reaction (see 3.2.12.2).

3.4 Next-generation sequencing

3.4.1 ChIP for deep sequencing

For ChIP-Sequencing the standard ChIP procedure was performed with a few exceptions. The amount of cells, antibody and dynabeads were increased approximately 5 fold. The precipitated and purified DNA was solubilized in 40 µl ddH_2O and quantified using the Quanti-iT™ PicoGreen® dsDNA Assay Kit (Life technologies).

3.4.2 mRNA isolation, fragmentation and cDNA synthesis for RNA-Sequencing

For RNA-Sequencing, total RNA was isolated with RNeasy® Mini Columns (see 3.2.10.2). Quality of the RNA was analyzed using the Experion™ Automated Electrophoresis System (Biorad) with RNA standard sense Chips according to manufacturers' protocol. RNA used for RNA-Sequencing had at least a RNA quality indicator (RQI) of 9. The RQI can range from 10 (intact RNA) to 1 (degraded RNA). After quality analysis, 1 µg total

RNA was used to isolate mRNA with the NEBNext® Poly(A) mRNA Magnetic Isolation Module according to the manufacturer's instructions. Agencourt AMPure XP Beads (Beckman Coulter) were used to purify the double stranded cDNA and used for library preparation starting with the DNA end repair.

3.4.3 Library preparation

3.4.3.1 NEBNext® Ultra™ RNA Library Prep Kit for Illumina®

RNA library preparation was performed according to manufactures' instructions. Libraries were size-selected using Agencourt AMPure XP Beads followed by amplification with 12 PCR cycles. Libraries were quantified and the library size was determined with the Experion Automated Electrophoresis System (Bio-Rad).

3.4.3.2 NEBNext® ChIP-Seq Library Prep Master Mix Set for Illumina®

ChIP-Seq libraries were prepared following the instruction manual. Libraries were size-selected on an agarose gel and purified by gel extraction (Qiagen). Libraries were amplified with 18 PCR cycles. Quantification and size determination was performed with the Experion Automated Electrophoresis System (Bio-Rad).

3.4.4 Sequencing data analysis

For sequencing data analysis, FASTQ-files were generated, aligned to the human genome "hg19" with BOWTIE v.0.12.8 and the resulting .sam files were converted into binary .bam files by Samtools. All further analyses were performed in R v3.1.1.
For RNA-Sequencing, the program edgeR was used to analyze the data sets for differential gene expression.
All bioinformatical analyses of deep-sequencing data were performed by Dr. Björn von Eyß.

4 Results

4.1 MYC is a ubiquitinated protein

MYC is a well-established target of the ubiquitin-proteasome system. Nevertheless, it remained open which lysines in MYC are ubiquitin acceptor sites. To identify ubiquitinated lysine residues in MYC, mass spectrometric analysis of immunoprecipitated MYC was performed in collaboration with the mass spectrometry technology platform of the Max-Delbrück Centre (MDC) in Berlin headed by Dr. Gunnar Dittmar. To analyze samples by mass spectrometry, proteins are fragmented by tryptic digestion. When a lysine is ubiquitinated, the two C-terminal glycine residues of ubiquitin remain attached to the respective target lysine residue after trypsin digestion, resulting in a characteristic shift of the expected molecular weight of the peptide (Peng et al., 2003).

Flag-tagged MYC was immunoprecipitated from HeLa cell lysates and a fraction of the eluate was subjected to SDS-PAGE analysis followed by silver staining. Cells transfected with the corresponding vector served as a control. The silver staining showed a band at the expected molecular weight in the eluate of Flag-tagged MYC-expressing cells, which was absent in the eluate of vector-expressing cells (Fig. 4.1 A). The presence of Flag-MYC in the eluate was confirmed by immunoblot analysis (Fig. 4.1 B). Mass spectrometric analysis identified lysine 148 and lysine 389 as ubiquitin acceptor sites in MYC (Fig. 4.1 C, marked in red).

Kim et al. performed a global mass spectrometric approach to characterize the human ubiquitin-modified proteome and identified seven lysines in endogenous MYC as being ubiquitinated; three lysines in the N-terminal region (K52, K148 and K157) and four lysines in the C-terminal region of MYC (K323, K355, K389, K412) (Kim et al., 2011) (Fig. 4.1 C, marked in black and red). These analyses show that exogenous and endogenous MYC is post-translationally modified with ubiquitin.

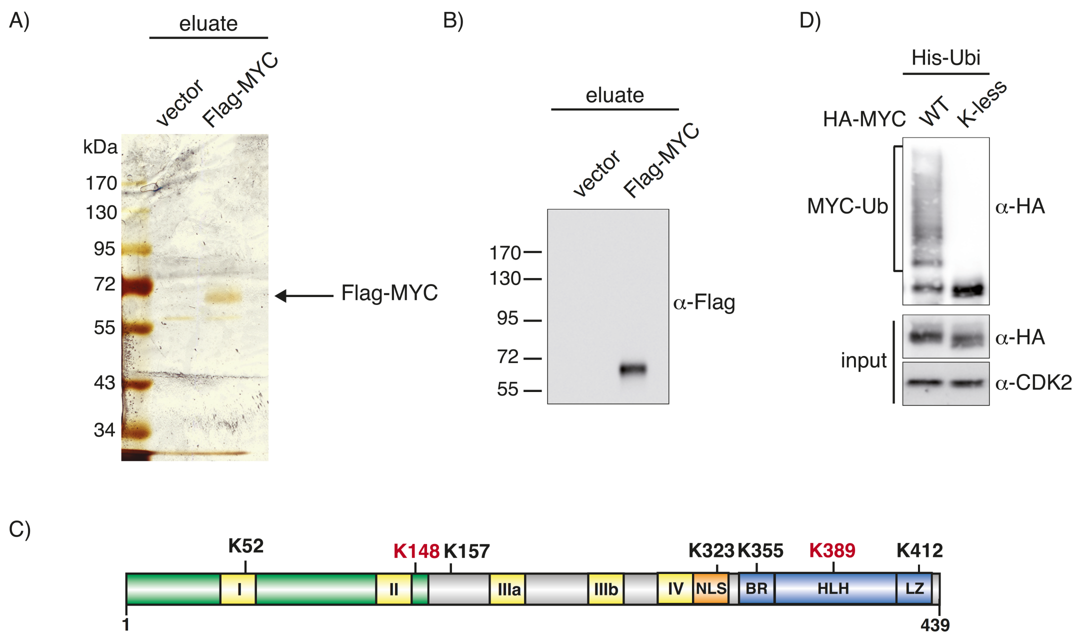

Figure 4.1: Identification of ubiquitin acceptor sites in MYC

A) Silver staining of eluates from vector and Flag-MYC-expressing cells. Flag-MYC was immunoprecipitated under denaturing conditions from transiently transfected HeLa cells and eluted with Flag-peptide.

B) Immunoblot analysis of eluates from vector and Flag-MYC-expressing cells. Presence of Flag-MYC in the eluate was detected with a Flag antibody.

C) Schematic domain structure of MYC. Lysines marked in red were identified as ubiquitin acceptor sites by mass spectrometry. Ubiquitinated lysine residues identified by (Kim et al., 2011) are marked in red or black.

D) *In vivo* ubiquitination assay of wild type (WT) and K-less MYC. HeLa cells were transfected with His-tagged ubiquitin and either N-terminally HA-tagged WT or K-less MYC. 48 h after transfection, His-ubiquitin modified proteins were precipitated under denaturing condition with Ni^{2+}-NTA-agarose and analyzed by immunoblotting. An input sample (10%) was analyzed as a control.

This figure was submitted for publication in similar form in (Jaenicke et al., under review).

4.1.1 K-less MYC is not ubiquitinated *in vivo*

Ubiquitin-modified MYC can be detected by an *in vivo* ubiquitination assay. To compare the ubiquitination status of wild type (WT) and K-less MYC in this assay, HeLa cells were transfected with His-tagged ubiquitin and either HA-tagged WT or K-less MYC. 48 h after transfection all His-ubiquitin modified proteins were precipitated under denaturing conditions with Ni^{2+}-NTA-agarose. Subsequent immunoblot analysis revealed that WT MYC is modified with His-ubiquitin due to characteristic slower migrating ubiquitin-MYC conjugates (Fig. 4.1 D). Consistently, ubiquitin-MYC conjugates are absent in K-less MYC overexpressing cells. In both precipitated samples a band at a molecular weight of about 60 kDa is detected with a HA antibody, representing unmodified WT and K-less MYC that bind unspecifically to the Ni^{2+}-NTA-agarose (Fig. 4.1 D). The ubiquitination assay demonstrates that ubiquitinated WT MYC, but not K-less MYC is ubiquitinated *in vivo*.

4.2 K-less MYC retains significant biological activity

4.2.1 K-less MYC interacts with known MYC interaction partners

Since the mutation of lysine to arginine residues in K-less MYC could influence the structure and thereby the general function of the protein, it was investigated whether the mutations affect binding to known MYC interaction partners.

The interaction of MYC with MAX is crucial for DNA-binding and transcriptional regulation. MYC heterodimerizes via its helix-loop-helix-leucine zipper domain with MAX and several lysine residues are located within this region (Blackwood and Eisenman, 1991). To test whether K-less MYC is able to interact with MAX, a co-immunoprecipitation assay was performed from HeLa cells transiently expressing HA-tagged WT or K-less MYC. Endogenous MAX was precipitated and co-precipitated MYC was detected by immunoblotting with an antibody against the N-terminal HA-tag. Both WT and K-less MYC co-precipitated with MAX revealing that the mutation of lysines to arginines does not interfere with MAX binding (Fig. 4.2 A, lane 1 and 2). The immunoprecipitation was specific since depletion of endogenous MAX by co-transfected shRNAs resulted in decreased co-precipitation of MYC and no protein was precipitated with the unspecific IgG control (Fig. 4.2 A lane 3 and 4).

The helix-loop-helix domain mediates interaction of the MYC/MAX heterodimer with the transcription factor MIZ1, which form a repressive complex (Peukert et al., 1997). To investigate whether mutation of lysine residues in MYC abrogates interaction with MIZ1, co-immunoprecipitation assays of transfected HeLa cells were performed. WT and K-less MYC interacted with MIZ1 with the same efficiency (Fig. 4.2 B, lane 2 and 3). The interaction was specific since MYC was neither detected in the IgG precipitation nor in the samples that did not overexpress MIZ1 (Fig. 4.2 B, lanes 1 and 4 for IgG control and lanes 8 and 9). This result was further verified by MYC immunoprecipitation and detection of co-precipitated MIZ1 (Fig. 4.2 B, lanes 5-7).

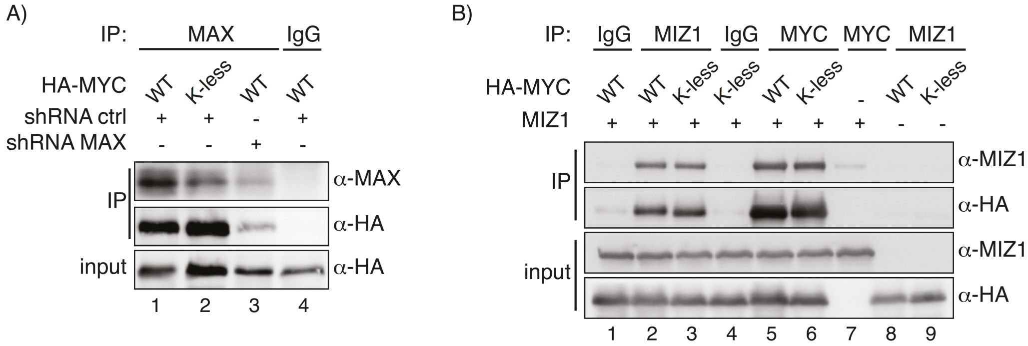

Figure 4.2: K-less MYC interacts with MAX and MIZ1[1]

A) Co-Immunoprecipitation of WT and K-less MYC with endogenous MAX. HeLa cells were transiently transfected with N-terminally HA-tagged WT or K-less MYC and either a control shRNA that does not target any gene or shRNAs targeting MAX. 48 h after transfection cell lysates were prepared and either MAX was immunoprecipitated or an immunoprecipitation with unspecific rabbit anti-IgG was performed. Precipitated proteins were detected by immunoblotting with the indicated antibodies.

B) Exogenous co-immunoprecipitation of WT and K-less MYC with MIZ1. HeLa cells transiently expressing HA-tagged WT or K-less MYC and MIZ1 were harvested 48 h after transfection and subjected to immunoprecipitation using either a MYC or MIZ1 specific antibody or an unspecific rabbit anti-IgG. Immunoprecipitated proteins were detected by immunoblot analysis.

These results illustrate that K-less MYC interacts with known MYC-interaction partners suggesting that the mutation of lysines to arginine residues does not affect basic properties of MYC.

4.2.2 K-less MYC is a nuclear, chromatin-associated protein

Ubiquitination of proteins can influence their cellular localization and chromatin association (see 1.2.4). Therefore, it was important to assess whether both WT and K-less MYC are located in the nucleus and show the same distribution in fractionation assays.

To determine the cellular localization of WT and K-less MYC, immunofluorescence staining of immortalized mammary epithelial cells (IMECs) stably expressing HA-tagged WT or K-less MYC was performed. Both proteins localized to the nucleus as revealed by the co-localization of the HA-signal with Hoechst (Fig. 4.3 A).

[1]This figure was published in similar form in (Popov et al., 2010).

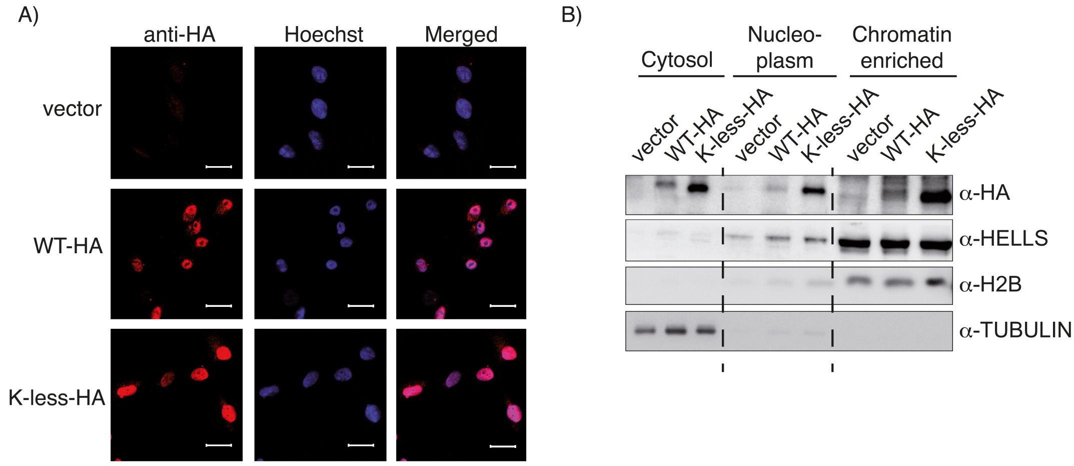

Figure 4.3: K-less MYC localizes to the nucleus and is chromatin-associated[2]

A) Immunofluorescence staining of WT and K-less MYC. Cells stably expressing WT-HA or K-less-HA MYC were seeded on cover slips and their localization was detected with a HA antibody. Vector-infected cells served as a control. Nuclei were stained with Hoechst.
Scale bar = 20 µm

B) Fractionation assay of cells stably expressing vector, WT-HA or K-less-HA. Cell lysates were separated into cytosolic, nucleoplasmic and chromatin-enriched fraction and the presence of WT and K-less MYC was determined with a HA antibody. Tubulin served as a control for cytosolic, H2B and HELLS for the chromatin-enriched fraction.

To test whether WT and K-less MYC bind to chromatin, cell lysates of cells stably expressing vector, WT-HA or K-less-HA were separated by centrifugation and Benzonase digestion into cytosolic, nucleoplasmic and chromatin-enriched fraction. This separation produced pure fractions, since tubulin (a cytoplasmic protein) could only be detected in the cytosolic fraction whereas histone H2B was present in the chromatin-enriched fraction. The DNA helicase HELLS was used as an example of a nuclear protein that is associated with chromatin (Yan et al., 2003). Consistently, HELLS was detected in the chromatin-enriched and nucleoplasmic fraction. MYC is a predominately nuclear protein that shuttles between nucleus and cytosol (Arabi et al., 2003). In agreement, WT MYC was detected in the chromatin-enriched fraction and to some extent in the cytosolic and nucleoplasmic fractions. Importantly, WT and K-less MYC showed a similar distribution in this assay (Fig. 4.3 B). Thus, the absence of lysine residues in K-less MYC does not change its cellular localization or chromatin-association.

[2] This figure was submitted for publication in similar form in (Jaenicke et al., under review) (see also following pages).

4.2.3 K-less MYC activates an E-box luciferase reporter

To assess whether K-less MYC retains basic transactivating functions, a luciferase reporter assay was performed. The prothymosin-α promoter contains a canonical E-box, which was subcloned in front of the firefly luciferase open reading frame (Gaubatz et al., 1995).

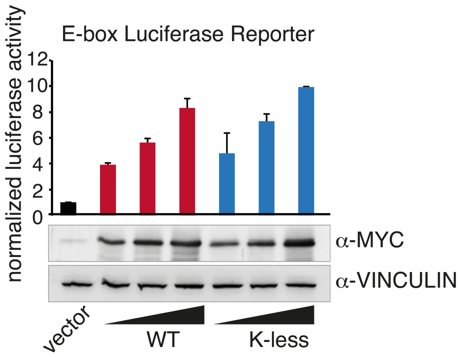

Figure 4.4: WT and K-less MYC activate an E-box luciferase reporter[2]
HeLa cells were transfected with the indicated MYC-expression vectors and a luciferase reporter construct containing the prothymosin-α promoter. An expression vector encoding for β-galactosidase was co-transfected. 48 h after transfection luciferase activity was determined and normalized to β-galactosidase activity. Error bars represent standard deviation of biological triplicates. MYC expression was confirmed by immunoblot analysis. VINCULIN served as a loading control.

Expression of increasing amounts of WT MYC resulted in an increased luciferase activity. Expression of K-less MYC had the same effect and transactivated the luciferase reporter to the same extent as WT MYC (Fig. 4.4). Thus, K-less MYC activated an E-box-luciferase reporter as efficiently as the WT protein.

4.2.4 K-less MYC has an increased half-life

MYC is a short-lived protein that is rapidly turned over by the ubiquitin-proteasome system (Farrell and Sears, 2014) and lysines are the major acceptor site for ubiquitin (Komander and Rape, 2012). Accordingly, mutation of all lysine residues of a short-lived protein to arginine is expected to increase its half-life.

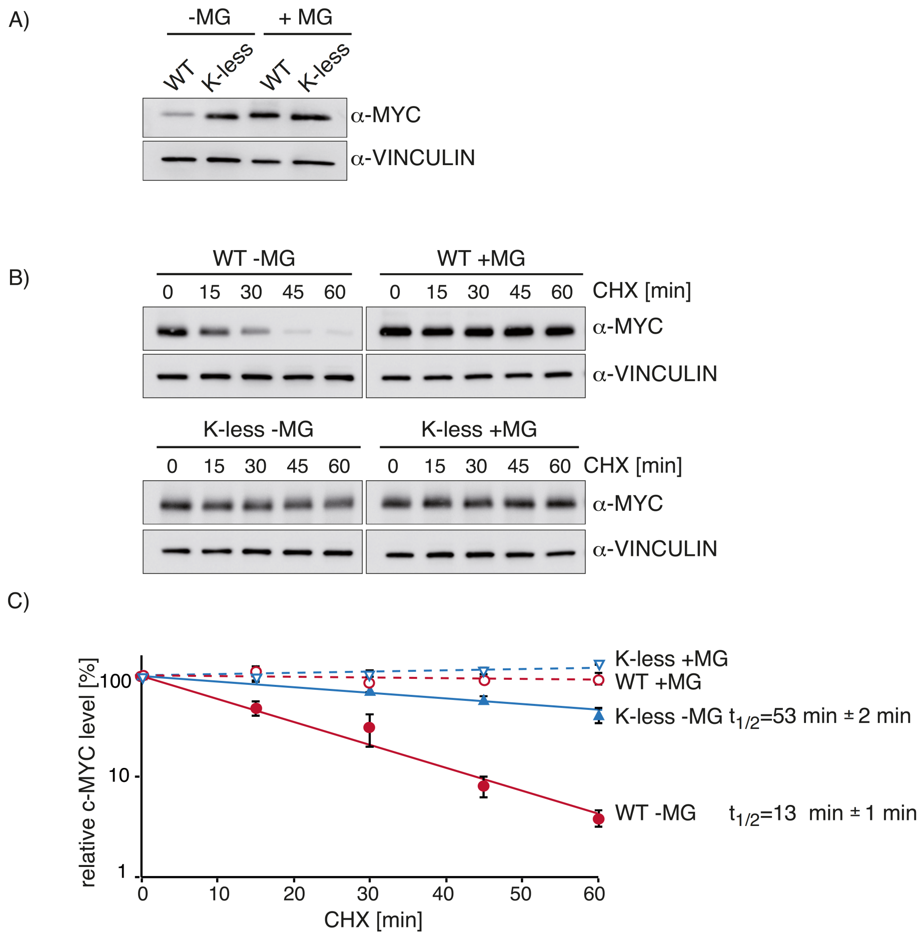

Figure 4.5: K-less MYC has an increased half-life compared to WT MYC[2]

A) Comparison of steady-state MYC protein levels of WT and K-less MYC. Protein lysates of WT and K-less MYC-expressing cells were analyzed by immunoblot analysis. Cells were either treated with EtOH (-MG) or MG132 (+MG) 4 h prior to cell lysis. Cell lysates were analyzed by immunoblotting for the abundance of WT and K-less MYC using a MYC-specific antibody. VINCULIN served as a loading control.

B) Cycloheximide decay assay of WT and K-less MYC-expressing cells. IMECs stably expressing WT or K-less MYC were treated with MG132 (+MG) or EtOH (-MG) 2 h prior to cycloheximide (CHX) addition. Additionally, cells were treated with cycloheximide for the indicated timepoints. Cell lysates were analyzed by immunoblotting with the indicated antibodies. VINCULIN was used as a loading control.

C) Quantification of cycloheximide decay assays. Three biological independent experiments were quantified, MYC level were normalized to VINCULIN and the relative MYC level were averaged. Relative MYC level were plotted over time of cycloheximide treatment. Error bars represent standard error of the mean of three independent biological experiments.

Stable expression of WT and K-less MYC in IMECs revealed a higher steady-state level of K-less MYC compared to WT MYC level (Fig. 4.5 A, -MG). MG132 is a membrane-permeable inhibitor that blocks the proteolytic activity of the proteasome by binding to the active sites of the 20S core particle (Lee and Goldberg, 1996). Consequently, treating cells with MG132 should increase the abundance of short-lived proteins. As expected, WT and K-less MYC steady-state level were equalized by the treatment with the proteasome inhibitor MG132 (Fig. 4.5 A). This result suggests that K-less MYC has an increased protein half-life compared to WT.

To confirm differences in protein half-life of WT and K-less MYC, a cycloheximide decay assay was performed. Protein half-life was determined by addition of the protein translation inhibitor cycloheximide for various time points. Thereby, new protein synthesis is blocked and turnover of a protein can be followed by immunoblot analysis. To assess, whether the protein turnover is mediated by proteasomal degradation, the cycloheximide decay assay was performed in the presence and absence of proteasome inhibition.

WT MYC was rapidly turned over as judged by the decreasing MYC-level over time. This effect was proteasome-dependent since treatment with MG132 abolished MYC turnover and completely stabilized the protein (Fig. 4.5 B, compare WT –MG with WT +MG). Quantification revealed a half-life of WT MYC in IMECs of approximately 13 min. K-less MYC was more stable with a half-life of 53 min. The remaining K-less MYC turnover could be rescued by proteasomal inhibition (Fig. 4.5 B and C). Therefore, mutation of ubiquitin-acceptor-sites in the short-lived protein MYC increases its protein half-life by attenuating proteasome-mediated degradation.

4.3 K-less MYC is unable to induce proliferation and apoptosis in immortalized mammary epithelial cells

K-less MYC retains significant biological activity and acts similar to the WT protein in several functional tests. However, previous reports clearly implicate that ubiquitination has a regulating effect on MYC activity (see 1.3.3.2.4). Thus, the biological effect of mutating ubiquitin acceptor sites in MYC was investigated in mammary epithelial cell lines, which show a strong biological response upon MYC expression and, therefore, are a useful system to study MYC-induced phenotypes.

MCF10A cells are non-transformed human epithelial cells from the mammary gland. They were spontaneously immortalized, harbor a *MYC* amplification and *CDKN2A* deletion (Kadota et al., 2010; Soule et al., 1990; Worsham et al., 2006). Their endogenous MYC level is comparable to the transformed human osteosarcoma cell line U2OS but lower compared to the transformed human cervix adenocarcinoma cell line HeLa (Fig. 4.6).

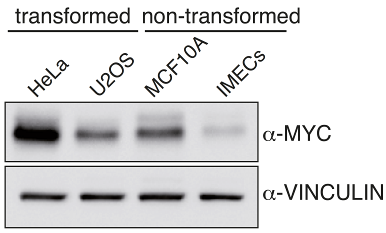

Figure 4.6: Endogenous MYC level in different cell lines
Comparison of endogenous MYC level in different cell lines. Endogenous MYC level of two transformed cell lines were compared to the level of two non-transformed immortalized mammary epithelial cell lines. Cell lysates were analyzed by immunoblotting using a MYC-specific antibody and VINCULIN as a loading control.

The non-transformed human mammary epithelial cell line IMECs (immortalized mammary epithelial cells) was immortalized by stably overexpressing the catalytic subunit of human telomerase (hTERT) (DiRenzo et al., 2002). IMECs express little endogenous MYC on protein level relative to transformed cell lines like HeLa or U2OS or the non-transformed MCF10A cell line (Fig. 4.6).

4.3.1 WT but not K-less MYC induces apoptosis in MCF10A cells

One major phenotype observed in MCF10A cells after MYC overexpression is a strong induction of apoptosis (Wiese et al., 2015). To analyze whether K-less MYC is able to induce apoptosis in these cells, MCF10A cells were transduced with lentiviruses encoding for WT or K-less MYC or an empty vector control. While vector- and K-less MYC-expressing cells showed only minor signs of apoptosis, WT MYC-expressing cells were strongly apoptotic (Fig. 4.7 A).

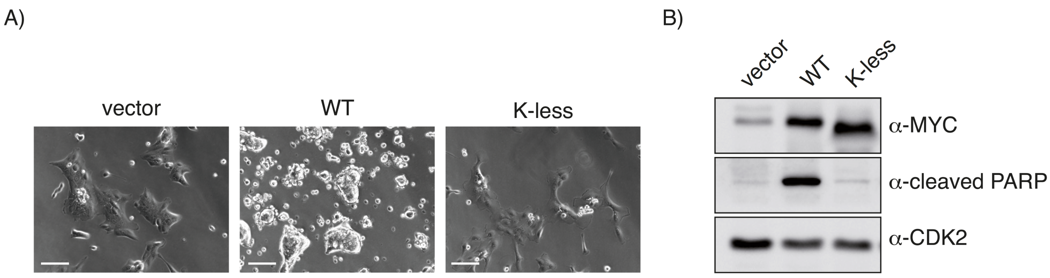

Figure 4.7: K-less MYC is unable to induce apoptosis in MCF10A cells

A) Microscopy pictures of MCF10A cells stably expressing vector, WT or K-less MYC. Scale bar =25 µm
B) Immunoblot analysis of cell lysates from vector, WT and K-less MYC-expressing MCF10A cells. Apoptosis induction was analyzed by detection of cleaved-PARP. CDK2 was used as a loading control.

Apoptosis induction by elevated WT MYC level was confirmed by detection of cleaved poly(ADP-ribose) polymerase (PARP), a marker of apoptosis. Cleaved PARP was detected only in WT MYC-expressing but not in vector or K-less MYC-expressing cells, showing that absence of lysine residues decreased MYC's ability to induce apoptosis in MCF10A cells (Fig. 4.7 B).

4.3.2 WT but not K-less MYC induces proliferation in IMECs

Ectopic expression of MYC induces proliferation of IMECs (Cowling et al., 2007). To assess whether K-less MYC promotes proliferation, IMECs were transduced with lentiviruses encoding for WT or K-less MYC or an empty vector control. As expected, WT MYC induced proliferation compared to vector-expressing cells, as determined by crystal violet staining of the cells. Interestingly, K-less MYC-expressing cells did not show enhanced proliferation (Fig 4.8 A). This result could further be verified by a cumulative growth curve. Expression of WT but not K-less MYC resulted in an increase in cell number compared to vector-infected cells, although K-less MYC was expressed at higher level (Fig. 4.8 B).
To investigate whether the growth advantage of WT MYC-expressing IMECs is cell-autonomous, a single-color competition assay was performed. Expression of vector, WT and K-less MYC was coupled to GFP by an internal ribosomal entry site (IRES). 20 % of infected, GFP-positive cells either expressing vector, WT or K-less MYC were mixed with 80% uninfected GFP-negative cells and the percentage of GFP-positive cells was monitored by FACS over time. The percentage of GFP-positive, WT MYC-expressing cells increased over time whereas the fraction of K-less MYC or vector-expressing cells remained constant (Fig. 4.8 C), demonstrating that vector or K-less MYC cells do not have a growth advantage compared to uninfected IMECs. In contrast, WT MYC induces a growth advantage in IMECs. The absence of lysine residues in K-less MYC, therefore, resulted in an inability to induce proliferation in IMECs.

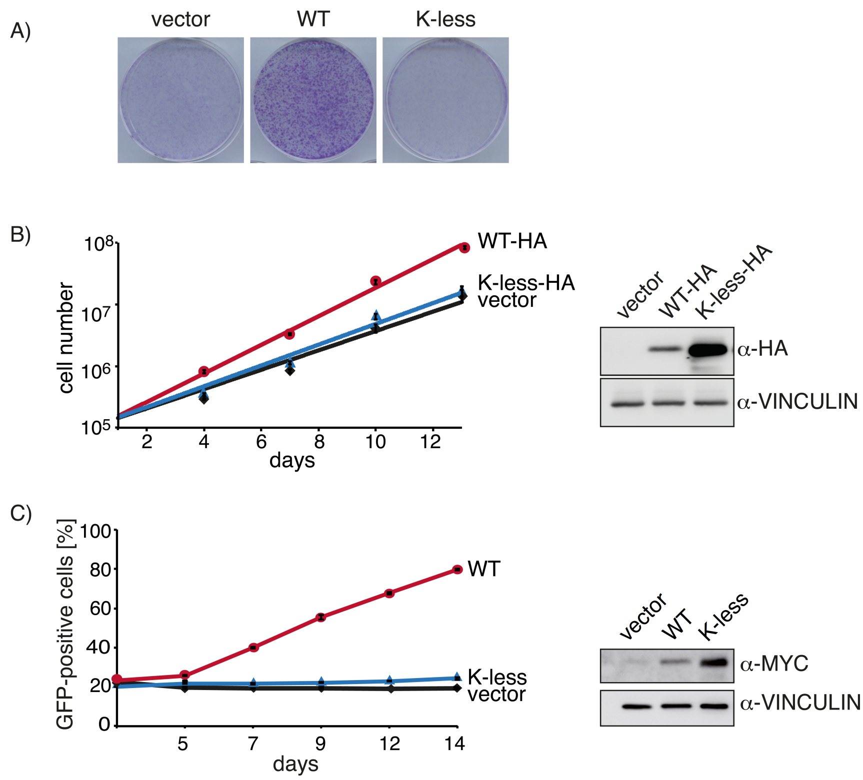

Figure 4.8: Proliferation assays in IMECs expressing WT or K-less MYC[2]

A) Crystal violet staining of IMECs expressing vector, WT or K-less MYC. Equal cell numbers of IMECs stably expressing vector, WT or K-less MYC were seeded. After six days, cells were stained with crystal violet.

B) Cumulative growth curve of IMECs expressing vector, WT-HA or K-less-HA MYC. Results are presented as mean ± SD of triplicates (left panel). MYC expression was confirmed by immunoblot analysis using a HA antibody recognizing the C-terminal HA-tag of MYC. VINCULIN served as a loading control (right panel).

C) Single-color competition experiment of IMECs expressing vector, WT and K-less MYC coupled to GFP expression. Infected GFP-positive cells were mixed with uninfected GFP-negative cells and percentage of GFP-positive population was monitored over time by FACS analysis. Results are presented as mean ±SD of triplicates (left panel). Immunoblot analysis of the corresponding stable cell lines documents MYC expression (right panel).

4.3.3 K-less MYC is impaired in inducing S-phase entry of starved IMECs

Mammary epithelial cells can be arrested in G1-phase by withdrawal of the mitogen EGF (Abukhdeir et al., 2008). To analyze whether MYC expression induces S-phase entry in the absence of growth factors, IMECs expressing doxycycline-inducible WT-HA or K-less-HA MYC were starved of EGF and MYC expression was induced by addition of doxycycline (Dox). MYC-induction was documented by immunoblot analysis (Fig. 4.9 A). Vector-expressing cells were used as a control to exclude effects of Dox alone on S-phase entry. Subsequently, S-phase entry was analyzed by BrdU/PI-FACS.

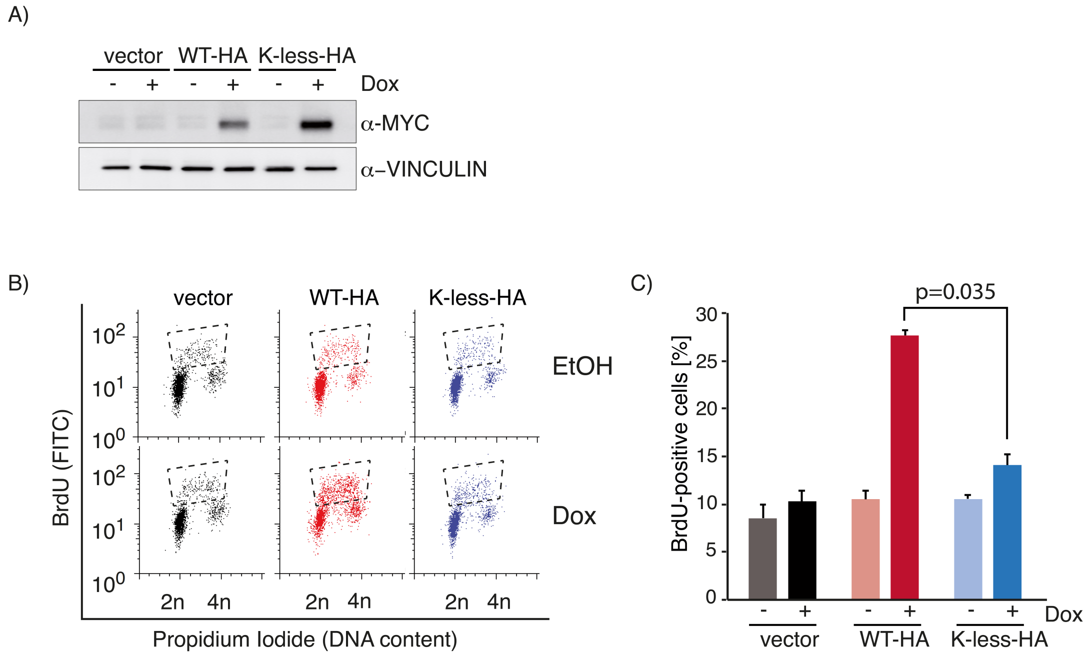

Figure 4.9: WT but not K-less MYC induces S-phase entry of starved IMECs[2]

A) Immunoblot analysis of lysates from starved IMECs expressing Dox-inducible MYC-HA after 18 h Dox (+) treatment or EtOH (-) as a control. Immunoblot documents MYC expression. VINCULIN served as a loading control.

B) BrdU/PI-FACS of IMECs expressing vector or doxycycline-inducible MYC-HA after 24 h starvation and further 18 h of Dox administration. Depicted is a representative example from biological triplicates. Dashed box marks BrdU-positive cells.

C) Quantification of S-phase entry of starved IMECs after 18 h of MYC-HA induction by Dox administration. Treatment with EtOH served as a control. Error bars represent standard deviation of biological triplicates. P-value was calculated with a Student's t-test.

7-10% of the EtOH treated cells were present in S-phase (BrdU-positive, higher population with DNA-content between 2n and 4n). 18 h after Dox-treatment, 10% of vector expressing cells were BrdU-positive (Fig. 4.9 B, C). WT MYC-expression induced S-phase entry and approximately 27% of WT MYC-expressing cells were BrdU-positive. Upon K-less MYC-expression, around 12% of the cells were present in S-phase (Fig. 4.9 B, C). This shows that K-less MYC is significantly less efficient in S-phase induction than WT MYC in EGF-starved IMECs.

4.4 K-less MYC binds to known MYC-regulated promoters

4.4.1 Genome-wide binding profile of WT and K-less MYC

Ubiquitination of a transcription factor can affect recruitment to promoters and thereby influence its activity (see figure 1.3). Differential binding of WT and K-less MYC to MYC-regulated promoters could explain the observed differences in induction of MYC-mediated phenotypes. To analyze whether WT and K-less MYC differ in binding to MYC-regulated promoter, chromatin immunoprecipitation (ChIP) experiments were performed from IMECs stably expressing WT-HA, K-less-HA or vector as a control.

WT-HA MYC was strongly enriched over IgG at the transcriptional start site (TSS) of known MYC-regulated promoters such as *FBXW8* and *NCL*, whereas K-less MYC showed only a weak binding compared to WT MYC. No specific enrichment could be detected in vector-infected cells, demonstrating the specificity of the HA antibody. As a control, MYC binding to an intergenic region on chromosome 11 was analyzed, where no MYC binding was expected. WT MYC was strongly (36-fold) enriched at the *FBXW8* TSS over control region whereas K-less MYC was only enriched threefold (Fig. 4.10 A).

Although K-less MYC is a nuclear and chromatin-associated protein with a higher steady-state level compared to WT MYC (Fig. 4.3 A, B), less K-less MYC could be immuno-precipitated at MYC-regulated promoters. One explanation for this observation is that K-less MYC is recruited to different sites in the genome compared to WT MYC. To analyze this hypothesis, the genome-wide binding profiles of WT and K-less MYC in IMECs were determined by ChIP-Sequencing (ChIP-Seq). To this end, ChIPs with a HA antibody were performed from IMECs stably expressing WT-HA and K-less-HA MYC, followed by deep sequencing. The bioinformatical analyses of these and all following deep-sequencing data were performed by Dr. Björn von Eyss.

For every condition, more than 2.4×10^7 reads were generated and around 98% of the reads could be mapped to the human genome (Fig. 4.10 B). 4118 MYC peaks were identified in WT-HA MYC expressing cells with 1453 bound promoters in a window of 1500 bp around the TSS. For K-less MYC-expressing cells, 568 MYC peaks were identified with 13 bound promoters (Fig. 4.10 B). One of the best-bound genes by WT MYC was *GNL3*. The ChIP-Seq track for WT-HA MYC showed a strong peak at the TSS of *GNL3* whereas no peak was detectable in the input track. K-less MYC also showed a clear peak at the TSS of *GNL3* with fewer tags. Thus, K-less MYC binding to the *GNL3* TSS appeared weaker compared to binding of WT MYC (Fig. 4.10 C).

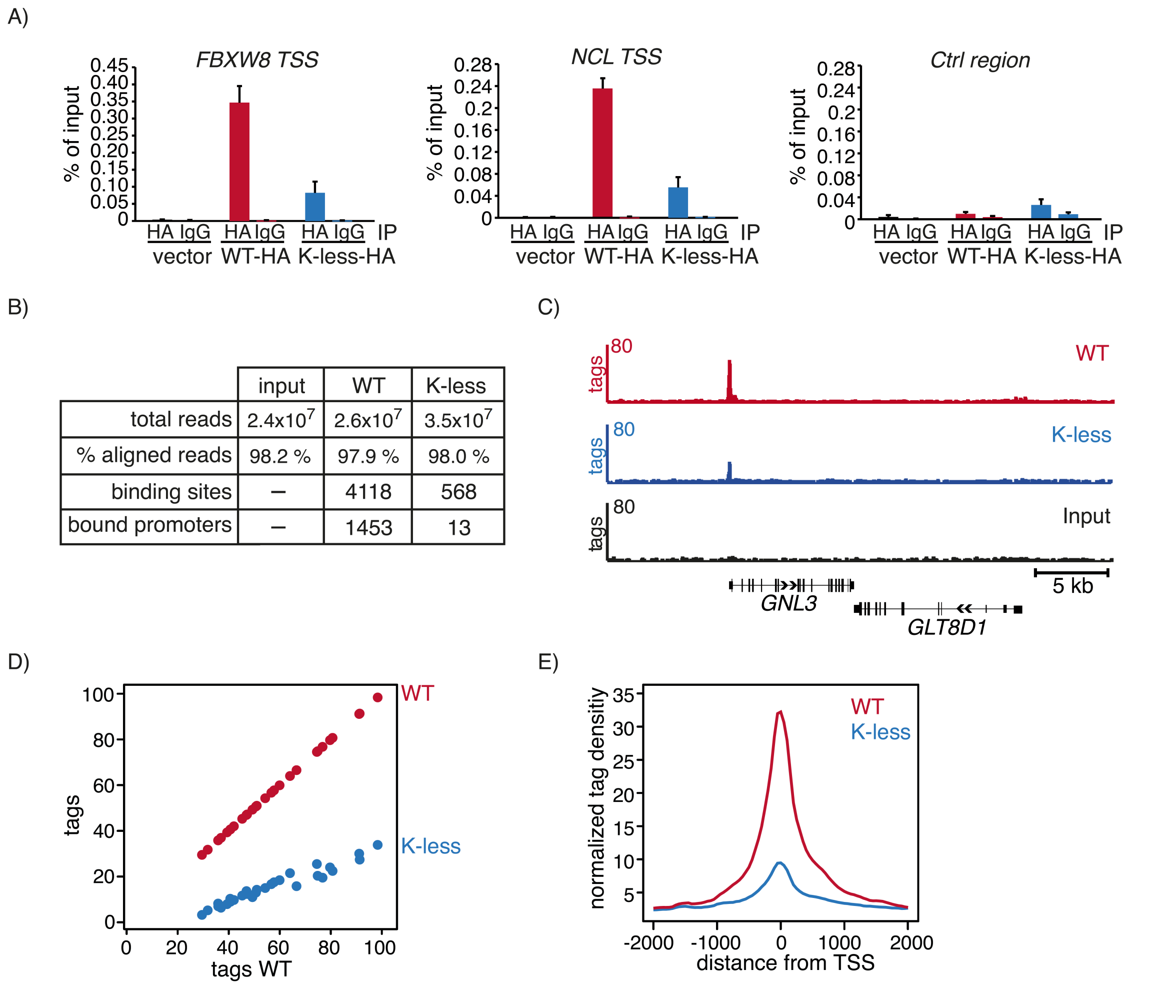

	input	WT	K-less
total reads	$2.4x10^7$	$2.6x10^7$	$3.5x10^7$
% aligned reads	98.2 %	97.9 %	98.0 %
binding sites	–	4118	568
bound promoters	–	1453	13

Figure 4.10: Genome-wide binding profiles of WT and K-less MYC[2]

A) Chromatin-immunoprecipitation of WT-HA and K-less-HA MYC-expressing IMECs. Chromatin of IMECs stably expressing WT-HA, K-less-HA or vector was immunoprecipitated with a HA antibody or an unspecific IgG as a control. Precipitated and purified DNA was analyzed by qPCR with primers amplifying the transcriptional start site (TSS) of the indicated genes or an intergenic control region (Ctrl region). Data are represented as mean ± SD.

B) Summary of the ChIP-Sequencing (ChIP-Seq) results. Comparison of reads, binding sites and bound promoters for the different samples is shown.

C) Genome browser picture displaying ChIP-Seq tracks for WT-HA, K-less-HA and the input sample. Shown is a genomic region on chromosome 3 with the genes *GNL3* and *GLT8D1*.

D) Binned dot plot of peaks, which were detected in the WT-HA sample. Here, the tags were counted in the peaks of the WT-HA sample and the K-less sample, respectively. The windows were derived from the peaks of the WT sample. All peaks were sorted according to their tag counts in the K-less MYC sample and summarized as 30 bins for WT and K-less (92 genes per bin). For each bin, the median was plotted.

E) Histogram of peak distance from TSS. Mean tag density (tags / 50 bp windows) of WT MYC peaks were plotted in a region -/+ 2 kb from the TSS. Tags of K-less MYC peaks within these windows were counted and plotted accordingly.

To compare the genome-wide binding of WT and K-less MYC, a plot for tags within MYC peaks (of WT-HA and K-less-HA MYC) was generated. For WT MYC peaks, a window ±200 bp of the peak summit was defined and tags within these windows were counted for WT and K-less MYC samples. For better illustration, the peaks were grouped into bins. For K-less-HA MYC, each bin includes the same genomic coordinates as WT-HA MYC and the median tag number was plotted against WT tags (Fig 4.10 D). Globally, the binding of K-less MYC appeared weaker.

To determine the relative positioning of the identified peaks to the TSS, tags of peaks identified for WT MYC were counted in 50 bp windows within a distance of 2 kb around the TSS. The mean density was then plotted in a histogram (Fig. 4.10 E). WT MYC peaks had a mean density of around 32 tags and were positioned at the TSS. To compare the positioning to K-less MYC peaks, tags within the same windows were counted and plotted in the same histogram. K-less MYC peaks had less tags compared to WT with a mean density of around 9 tags. Importantly, the distribution of the peaks did not differ and were localized exactly as the WT MYC peaks.

Taken together, the ChIP-Seq data revealed that K-less MYC shows an identical binding profile to WT MYC even though the binding strength appears weaker.

4.4.2 K-less MYC is present at MYC-regulated promoters

The ChIP-Seq results suggested that K-less MYC is less present at MYC-binding sites compared to WT MYC. During the ChIP procedure, formaldehyde is used to cross-link proteins to DNA. Formaldehyde cross-linking occurs between amino and imino groups of DNA bases and different amino acids like lysine, histidine and cysteine or the amino-terminus of a protein (Kuo and Allis, 1999). Here, lysine-residues are preferentially cross-linked, in particular during the short incubation time with formaldehyde used in a ChIP procedure (Lu et al., 2010; Toews et al., 2008). Therefore, the mutation of the most cross-linkable amino acid lysine to an arginine in K-less MYC most likely results in a less efficiently cross-linked protein. This suggests that K-less MYC might bind as efficiently to chromatin as the WT protein but is not as efficiently cross-linked resulting in a poor enrichment in ChIP assays.

To analyze whether K-less MYC binds as efficiently to MYC-regulated promoter as the WT protein, native ChIPs from either vector, WT-HA or K-less-HA MYC infected IMECs were performed. In a native ChIP, no cross-linkers are used but the DNA is fragmented by

MNase digestion and the immunoprecipitation occurs under mild, native conditions (Kasinathan et al., 2014). K-less MYC showed a strong enrichment over vector and control region at the previously identified MYC-binding site in the *GNL3* promoter and the binding seemed even stronger compared to WT MYC (Fig. 4.11 A).

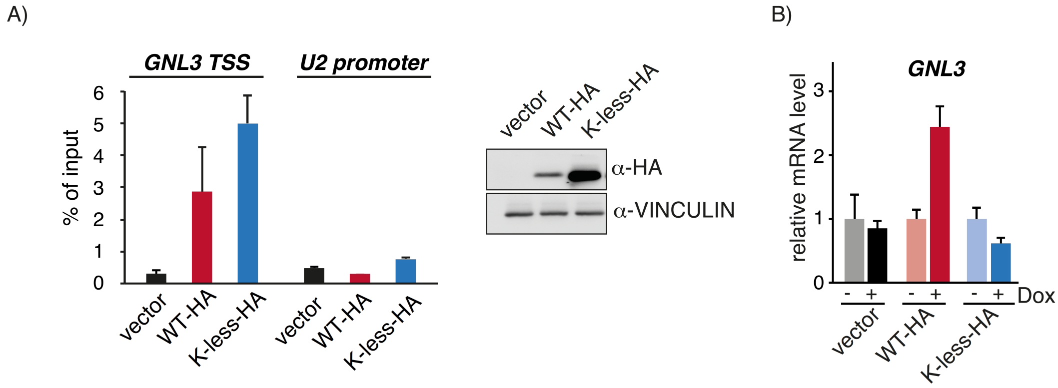

Figure 4.11: K-less MYC binds to MYC-regulated promoters[2]

A) Native ChIP from IMECs stably expressing vector, WT-HA or K-less-HA. The ChIP was performed with a HA antibody under native conditions and binding to the *GNL3* TSS or, as a negative control, to the *U2* promoter was analyzed by qPCR. Results are given as mean ±SD (left panel). The native ChIP was performed by Dr. Björn von Eyß. Immunoblot analysis confirmed expression of WT and K-less MYC. VINCULIN was used as a loading control (right panel).

B) Analysis of *GNL3* mRNA expression by qPCR. Cells stably expressing Dox-inducible WT-HA, K-less-HA or vector were treated either with EtOH (-) or Dox (+) for 4 h. Results are given as mean ±SD.

GNL3 is not only bound but also induced by WT MYC. Interestingly, although K-less MYC bound to the *GNL3* TSS, it was unable to induce *GNL3* mRNA expression, indicating that the defect in induction of *GNL3* mRNA is associated with a post-DNA-binding step (Fig. 4.11 B).

The binding of K-less MYC to MYC-regulated promoters was further confirmed by its ability to replace other BR-HLH/LZ transcription factors from E-boxes. In addition to MYC, MAX heterodimerizes with proteins of the MXD family. These heterodimers bind to E-boxes but repress transcription by recruiting histone deacetylase complexes (Adhikary and Eilers, 2005). MXD6 (MNT) is co-expressed with MYC in proliferating cells (Hurlin et al., 1997). Since MXD6/MAX dimers also bind E-box sequences, MYC expression is expected to displace MXD6 from these sites whereas MAX occupancy should not change.

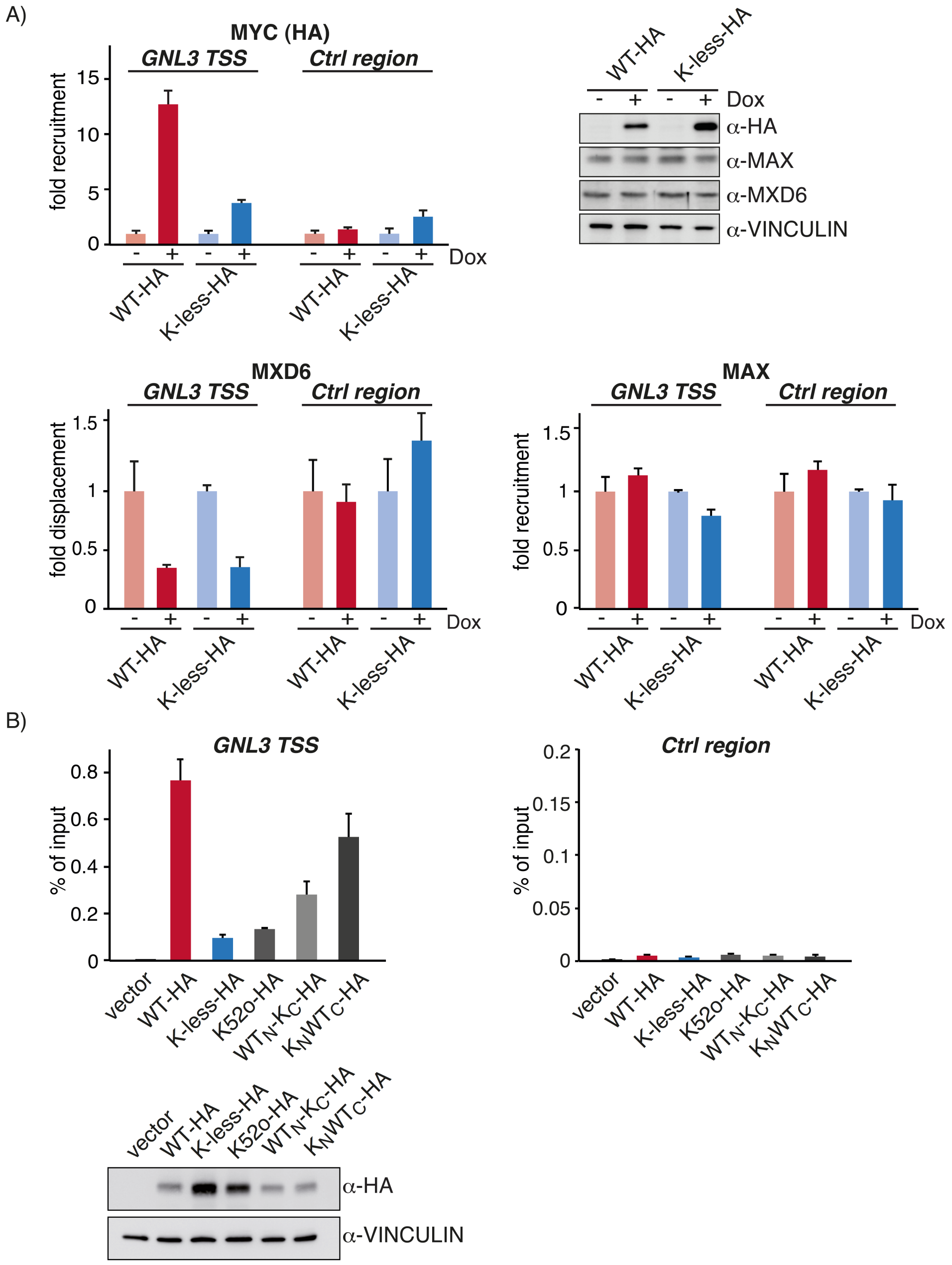

Figure 4.12: K-less MYC binds to MYC-regulated promoters[2]

A) Expression of WT-HA or K-less-HA was induced by addition of Dox for 3 h. ChIP assays were performed with either a HA, MXD6 or MAX antibody. Precipitated and purified DNA was analyzed by qPCR with primers amplifying the TSS of *GNL3* or a control region (*Ctrl region*). Fold displacement and fold recruitment was calculated in reference to the corresponding EtOH treated sample. Results are given as mean ±SD (upper left and lower panels). Immunoblot analysis documents induction of MYC expression 3 h after Dox administration. Lysates were further analyzed for MXD6 and MAX expression (upper right panel).

B) ChIP of MYC-expressing IMECs. Formaldehyde cross-linked chromatin of IMECs stably expressing the indicated MYC-HA alleles or vector was immunoprecipitated with a HA antibody. Precipitated and purified DNA was analyzed by qPCR with primers amplifying the TSS of *GNL3* or a control region (*Ctrl region*). Data are represented as mean ± SD (upper panel). MYC expression was analyzed by immunoblotting with a HA antibody. VINCULIN served as a loading control (lower panel) (see Fig. 4.15 for detailed description of the mutants).

Activation of MYC in IMECs stably expressing Dox-inducible WT or K-less MYC resulted in a strong recruitment of WT MYC to the TSS of *GNL3* whereas recruitment of K-less MYC appeared to be much weaker (Fig. 4.12 A upper panel, left). MAX and MXD6 protein level were not affected by induction of MYC expression (Fig. 4.12 A upper panel, right).

Importantly, recruitment of WT MYC to the *GNL3* TSS displaced MXD6 from this site but had no effect on MAX binding and induction of K-less MYC also resulted in an equivalent displacement of MXD6 (Fig. 4.12 A lower panel, left and right).

In line with these observations, cross-linking efficiency and the resulting ChIP signal increased with number of reconstituted lysine residues in K-less MYC. A MYC mutant harboring one lysine residue at position 52 (K52o) showed similar binding to K-less MYC. When the seven N-terminal lysines were reconstituted (WT_N-K_C) the ChIP signal increased and it further increased with a MYC mutant harboring 18 C-terminal lysine residues (-$K_N WT_C$) (Fig. 4.12 B, for a detailed description of the mutants see Fig. 4.15).

4.5 K-less MYC is a weaker transcriptional regulator

The inability of K-less MYC to induce *GNL3* mRNA expression indicated that K-less MYC is a weak transcriptional activator (see figure 4.11 B). To analyze whether K-less MYC is generally compromised in transcriptional activation, global gene expression profiles of WT and K-less MYC were compared by RNA-Sequencing (RNA-Seq). IMECs were transduced with lentiviruses encoding for Dox-inducible WT-HA or K-less-HA MYC or the empty vector. Vector, WT-HA and K-less-HA MYC-expressing cells were treated for 4 h either with EtOH as a control or with Dox to induce MYC expression. MYC expression was verified by immunoblot analysis (Fig. 4.13 A), RNA was isolated and libraries were prepared from mRNA samples followed by deep sequencing.

The $\log_2$ fold change (FC) (Dox versus EtOH) of the genes was plotted over their abundance (logCPM, counts per million) in a MA-plot. Significantly regulated genes ($\log_2 FC>0$, $padj<0.05$) were colored in red. More genes were significantly up- or downregulated upon WT MYC expression compared to K-less MYC (Fig. 4.13 B).

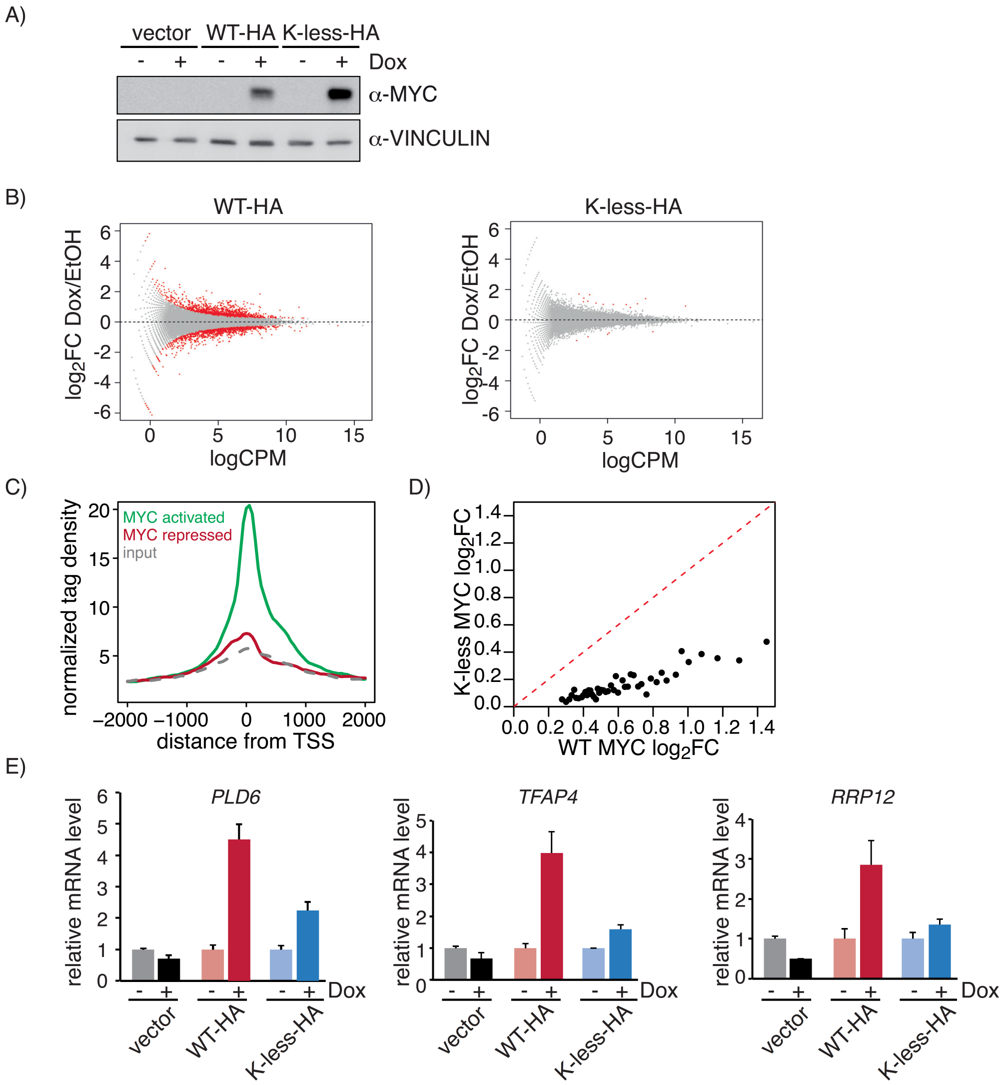

Figure 4.13: K-less MYC is a weaker transcriptional activator[2]

A) Immunoblot analysis of IMECs stably expressing Dox-inducible WT-HA or K-less-HA MYC or empty vector. Cells were treated with EtOH (-) or Dox (+) for 4 h and subjected to immunoblot analysis. VINCULIN was used as a loading control.

B) MA-plot for WT-HA and K-less-HA samples. All detected transcripts were plotted according to their abundance (logCPM) against the $\log_2$ fold change (FC) (Dox/EtOH). Transcripts that were significantly (padj < 0.05) up- or downregulated are colored in red.

C) Histogram of peak distance from TSS for MYC-activated (green) and repressed genes (red). Normalized tags of WT MYC peaks of regulated genes were plotted in a region -/+ 5 kb from the TSS. This plot was submitted for publication in similar form (von Eyss et al., in revision).

D) Binned dot plot of RNA-Seq results from WT and K-less MYC activated genes. Each dot represents the median $\log_2$ fold change of 30 genes ranked by WT $\log_2$ fold change induction. Red dotted line represents the progression if WT and K-less MYC induce the genes in the same manner.

E) Validation of the RNA-Seq results by qPCR. IMECs expressing Dox-inducible WT-HA MYC, K-less-HA MYC or the empty vector were treated for 4 h either with EtOH (-) or Dox (+). RNA was isolated and the mRNA level of the indicated genes were analyzed by qPCR. Expression was normalized to *β2M*. The relative mRNA expression was set in relative to the corresponding EtOH treated sample. Data are represented as mean ±SD of technical triplicates.

To analyze whether the up- and downregulated genes after WT MYC expression are direct MYC targets, genes were grouped into activated and repressed genes and their normalized tag density from the ChIP-Seq result was plotted over distance from the TSS (Fig. 4.13 C). MYC activated genes showed a peak at the TSS whereas hardly any enrichment for MYC binding was detectable at MYC repressed genes. This suggests that downregulated genes are not directly repressed by MYC in IMECs since no MYC binding could be detected at these promoters. Therefore, to study direct MYC effects, only activated genes were taken into consideration in the subsequent analyses.

To globally compare the transcriptional activity of WT and K-less MYC, genes from the RNA-Seq significantly induced by WT MYC compared to vector infected cells ($log_2FC > 0$, padj < 0.05) were sorted according to their log_2 fold change. Genes were then grouped into 45 equally sized bins with 30 genes per bin and the median of the bin was plotted as a dot. For K-less-HA MYC, each bin includes the same genes as WT-HA and the median log_2 fold change was calculated. Bins were plotted in a dot plot with the log_2 fold change of WT MYC regulated genes on the X-axis and the log_2 fold change of these genes in K-less-HA MYC expressing cells on the Y-axis (Fig 4.13 D). The dot plot shows that K-less MYC is globally a weaker transcriptional activator. The bins are shifted below the dotted red line, which represents the position when both WT and K-less MYC would activate the genes to a similar extent.

This global result was validated for individual genes by qPCR. The direct MYC target genes *PLD6*, *TFAP4* and *RRP12* were induced by WT MYC after 4 h Dox treatment. K-less MYC induced these genes to a lesser extent and no induction was detectable in vector expressing cells (Fig. 4.13 E).

RNA-Seq data were further analyzed with Gene Set Enrichment analysis (GSEA) to compare the expression profiles with published gene sets. Comparing the gene expression profiles of WT MYC with the C6 oncogenic signatures from the Molecular Signature Database (MSigDB) (Subramanian et al., 2005), the gene set with the strongest enrichment was the MYC_UP signature (Fig. 4.14, left panel). The enrichment was statistically significant with a nominal p-value < 0.001 (NOM p-value) and a false discovery rate (FDR) or q-value < 0.001. The MYC_UP signature was generated from human mammary epithelial cells overexpressing MYC compared to GFP as a control (Bild et al., 2006). For K-less MYC expression profiles, the MYC_UP signature was also the signature with the strongest statistically significant enrichment (NOM p-value < 0.001; FDR < 0.001) (Fig.

4.14, right panel). Comparison of the normalized enrichment score (NES) showed that the enrichment for the WT MYC profile was better than for the K-less MYC profile (compare WT NES 2.4 to K-less NES 1.98), supporting the notion that K-less MYC is a weaker transcriptional activator.

WT-HA MYC versus vector 4h Dox

Rank	Gene Set	NES	NOM p-val	FDR q-val
#1	MYC_UP.V1_UP	2.4	< 0.001	< 0.001

K-less-HA Myc versus vector 4h Dox

Rank	Gene Set	NES	NOM p-val	FDR q-val
#1	MYC_UP.V1_UP	1.98	< 0.001	< 0.001

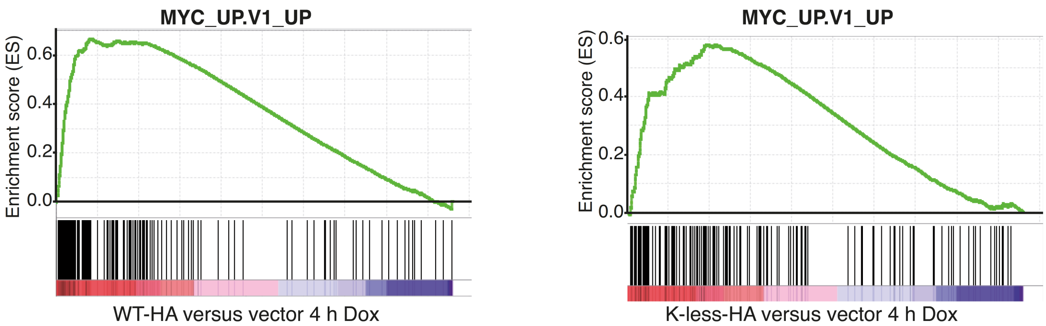

Figure 4.14: Gene Set Enrichment Analysis of WT-HA and K-less-HA expressing IMECs[2]
Gene expression profiles of WT-HA and K-less-HA MYC expressing IMECs were compared to published gene sets from the oncogenic signatures (C6) from the Molecular Signature Database. NES: normalized enrichment score; NOM p-val: nominal p-value; FDR q-val: false discovery rate

4.6 Distinct lysine residues can restore K-less MYC function

The previous results showed that the presence of lysine residues is important for MYC's transcriptional activity and MYC-mediated phenotypes. To investigate whether positioning of lysines in MYC is important, two MYC mutants were generated which either harbored seven N-terminal lysines (WT_N-K_C) or eighteen lysines located in the C-terminal region of MYC (-$K_N WT_C$). WT_N-K_C includes the lysines from MBI (K51 and K52) to K206, which is located shortly after MBIIIa but all other lysines are mutated to arginine. -$K_N WT_C$ possesses eighteen lysines starting from K269 in MBIIIb to K430 located in the LZ but the first seven lysines are mutated to arginine (Fig. 4.15).

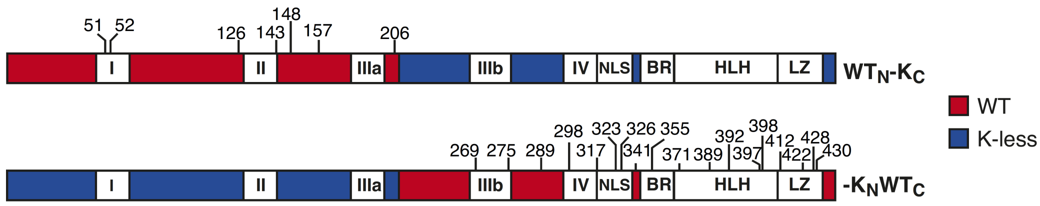

Figure 4.15: Position of lysine residues present in the MYC mutants WT_N-K_C and -$K_N WT_C$[2]
Numbers indicate the amino acid position of the lysine residues present in the respective mutant.

4.6.1 Reconstitution of individual lysine residues in K-less MYC rescues its turnover

As described previously, mass spectrometry analysis revealed that at least three lysine residues within the N-terminal region of MYC and at least four lysine residues in the C-terminal part of MYC can be ubiquitinated (Fig. 4.1 C) (Kim et al., 2011). To analyze whether ubiquitination of WT_N-K_C and –$K_N WT_C$ can be detected in an *in vivo* ubiquitination experiment, HeLa cells were transfected with His-tagged ubiquitin and the indicated HA-MYC alleles. As a control for the specificity of the HA antibody, a vector control was included. Ubiquitinated proteins were precipitated using Ni^{2+}-NTA agarose and HA-MYC was detected with a HA antibody. WT MYC showed a strong ubiquitination signal, which was absent in K-less MYC. For K-less MYC, only a signal of the unmodified protein was detected as shown in Figure 4.1 D. Strinkingly, WT_N-K_C MYC showed a clear ubiquitination pattern demonstrating that N-terminal lysines can function as ubiquitin acceptor sites. The ubiquitination signal of WT MYC was stronger than for WT_N-K_C MYC indicating that additional lysines in the C-terminal region might be ubiquitinated. Accordingly, ubiquitination of -$K_N WT_C$ MYC could also be detected (Fig. 4.16 A).

The absence of ubiquitin acceptor sites in K-less MYC resulted in a more stable protein compared to WT MYC (see Fig. 4.5). Since lysines in the N- and C-terminal region in MYC can serve as ubiquitin-acceptor sites, it was investigated whether these ubiquitination events can increase protein turnover compared to K-less MYC. A cycloheximide decay assay was performed to compare the half-life of WT, K-less, WT_N-K_C and -$K_N WT_C$ MYC in IMECs. While K-less MYC showed the longest half-life of around 49 min, reconstitution of either the N- or C-terminal lysines resulted in similar turnover rates as for WT MYC (Fig. 4.16 B).

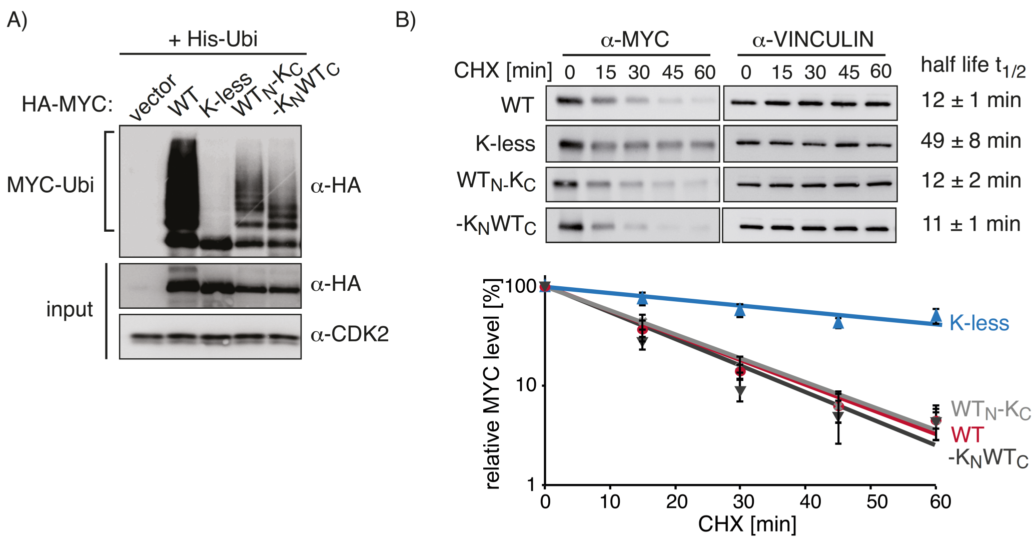

Figure 4.16: Reconstitution of distinct sets of lysine residues rescues protein turnover[2]

A) *In vivo* ubiquitination assay of WT, K-less, WT_N-K_C and -$K_N WT_C$ MYC. HeLa cells were transfected with His-tagged ubiquitin and the corresponding HA-MYC plasmids. Vector transfected cells served as a control. 48 h after transfection, His-ubiquitin modified proteins were pulled down under denaturing condition with Ni^{2+}-NTA-agarose and analyzed by immunoblotting. A 10% input sample was analyzed as a control. CDK2 served as a loading control.

B) Cycloheximide decay assay of WT, K-less, WT_N-K_C and -$K_N WT_C$ MYC-expressing cells. IMECs stably expressing the indicated MYC alleles were treated with cycloheximide (CHX) for the indicated time points. Cell lysates were analyzed by immunoblotting with the indicated antibodies. VINCULIN served as a loading control. The mean calculated half-life of at least three independent experiments is depicted next to representative immunoblots (upper panel). The lower panel illustrates the quantification of the cycloheximide decay assay. Time points were set in reference to time point 0 (100%). Error bars represent standard error of the mean of at least three independent biological replicates.

To analyze whether the presence of lysine residues within the N- or C-terminal part in MYC can rescue K-less MYC's inability to induce proliferation, IMECs were infected with lentiviruses carrying either vector, WT, K-less, WT_N-K_C or -$K_N WT_C$ *MYC* linked to GFP and their expression was confirmed by immunoblot analysis (Fig. 4.17 A, right panel). In a single-color competition assay, WT, WT_N-K_C and -$K_N WT_C$ were all capable to overgrow the uninfected cell population whereas the percentage of K-less and vector expressing cells remained constant (Fig. 4.17 A, left panel).

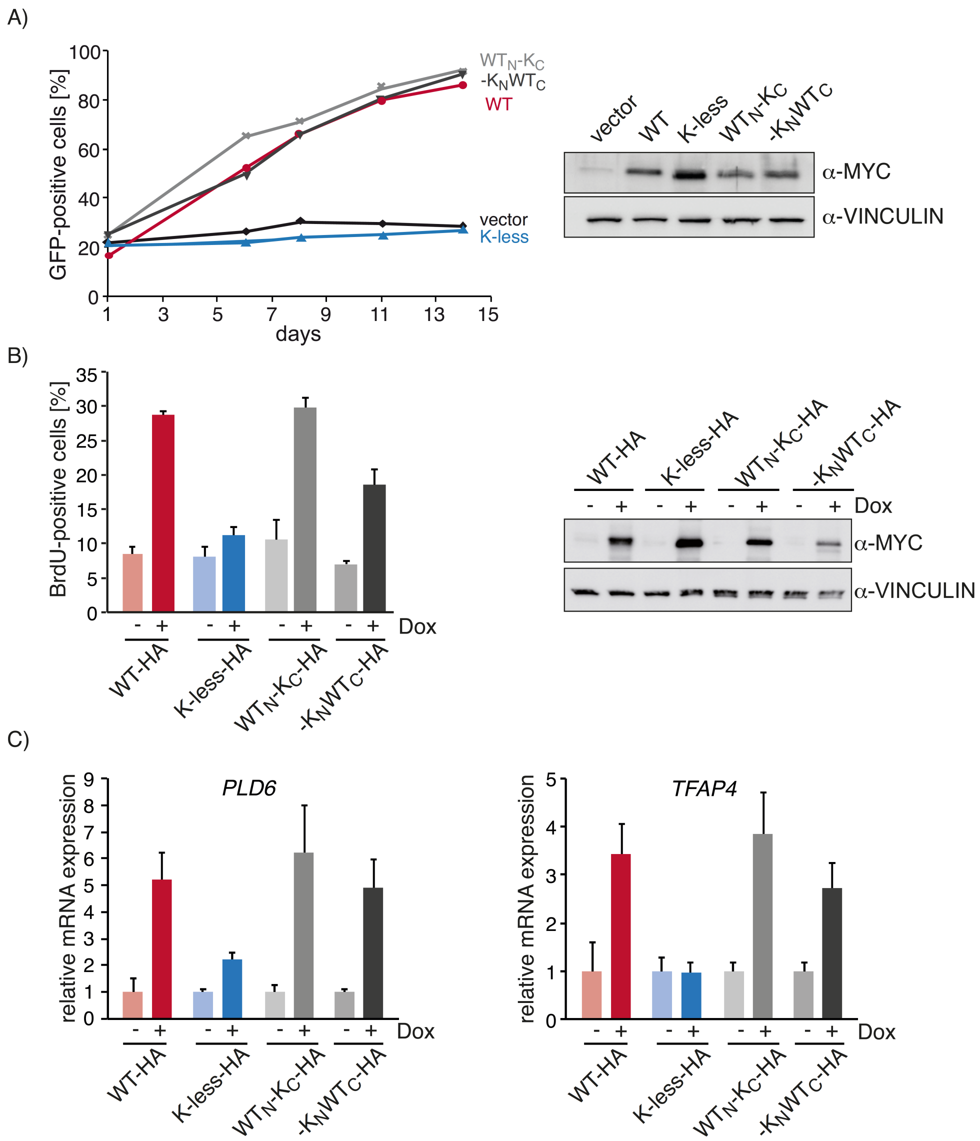

Figure 4.17: Restoration of N- or C-terminal lysines in MYC rescues MYC transcriptional activity and biological phenotypes[2]

A) Single-color competition experiment of IMECs stably expressing vector, WT, K-less, WT$_N$-K$_C$ or -K$_N$WT$_C$ MYC coupled to GFP-expression. Infected GFP-positive cells were mixed with uninfected GFP-negative cells and percentage of GFP-positive population was monitored over time by FACS measurement (left panel). MYC expression was analyzed by immunoblot (right panel).

B) Quantification of BrdU/PI-FACS of IMECs stably expressing Dox-inducible WT, K-less, WT$_N$-K$_C$ or -K$_N$WT$_C$ MYC. Cells were starved for 24 h and MYC expression was induced for 18 h by Dox addition. Error bars indicate standard deviation of the mean of biological triplicates (left panel). Immunoblot analysis of lysates from starved IMECs after 18 h Dox-induction. MYC expression was determined with a MYC-specific antibody. VINCULIN was used as a loading control (right panel).

C) MYC target gene induction by WT, K-less, WT$_N$-K$_C$ and -K$_N$WT$_C$ MYC was analyzed by qPCR. IMECs stably expressing Dox-inducible WT-HA, K-less-HA, WT$_N$-K$_C$ or -K$_N$WT$_C$ MYC were treated for 4 h either with EtOH (-) or Dox (+). RNA was isolated and mRNA expression of the indicated genes was analyzed by qPCR. Expression was normalized to *β2M*. The relative mRNA expression was set in reference to the corresponding EtOH treated sample. Error bars indicate standard deviation of the mean of technical triplicates.

Moreover, WT_N-K_C and -K_NWT_C MYC's ability to induce S-phase entry of EGF-starved IMECs was investigated. IMECs expressing doxycycline-inducible WT-HA, K-less-HA, WT_N-K_C-HA or -K_NWT_C-HA MYC were starved and cells were treated with Dox for 18 h to induce MYC-expression or with EtOH as a control. Expression of MYC was verified by immunoblot analysis (Fig. 4.17 B, right). WT-HA and WT_N-K_C-HA expressing cells were both able to induce S-phase entry to the same extent whereas expression of K-less-HA had a weak effect on S-phase. -K_NWT_C-HA MYC-expressing cells showed an intermediate phenotype and more cells entered S-phase compared to K-less MYC-expressing cells (Fig. 4.17 B, left).

Since the presence of either N- or C-terminal lysine residues was sufficient to induce MYC-mediated proliferation, it was further investigated, whether these MYC mutants are able to induce expression of MYC target genes. Thus, expression of WT, K-less, WT_N-K_C and -K_NWT_C MYC was induced for 4 h by Dox and induction of direct MYC target genes was analyzed by qPCR. Consistent with the effects on proliferation, both, WT_N-K_C and -K_NWT_C MYC were able to induce the expression of *PLD6* and *TFAP4* mRNA similarly to WT MYC. In contrast, K-less MYC induced these genes to a much weaker extent (Fig. 4.17 C). Therefore, restoration of either N- or C-terminal lysines in MYC is sufficient to re-establish MYC's transcriptional activity.

4.6.2 Reconstitution of a known ubiquitin-acceptor site largely rescues MYC-mediated phenotypes

Lysines are not only acceptor sites for ubiquitin but can also be acetylated. In the N-terminal region of MYC, K52 was shown to be ubiquitinated but not reported to be acetylated (see 1.3.3.2.1 and Fig. 4.1 C). To investigate whether ubiquitination is important for the observed phenotype, a MYC mutant was generated harboring only lysine 52 in MBI but all other lysines were mutated to arginine (K52only MYC, K52o) (Fig. 4.18 A). Ubiquitination of K52 could be confirmed by an *in vivo* ubiquitination assay - K52o MYC was efficiently ubiquitinated, albeit weaker when compared to WT MYC (Fig. 4.18 B).

Reconstitution of K52 reduced the half-life of K-less MYC from 49 min to 18 min, which was only 1.5 times longer than the half-life of WT MYC with 12 min (Fig. 4.18 C).

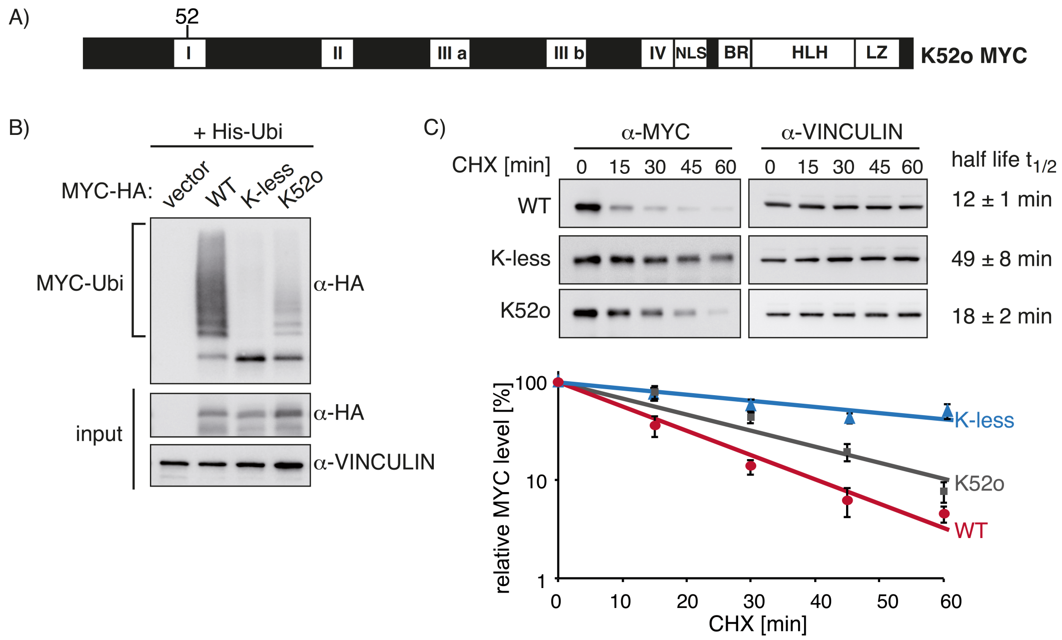

Figure 4.18: Reconstitution of K52 partially rescues MYC-mediated turnover[2]

A) Position of lysine 52 present in the MYC mutant K52o.

B) *In vivo* ubiquitination assay of K52o MYC. HeLa cells were transfected with plasmids encoding His-tagged ubiquitin, WT-HA, K-less-HA, K52o-HA or vector as a control. The assay was performed as described in Fig. 4.16 A. VINCULIN was used as a loading control.

C) Cycloheximide decay assay of WT, K-less and K52o MYC-expressing cells. The assay and quantification was performed as described in Fig. 4.16 B. Note that WT and K-less MYC quantification is the same as shown in Fig. 4.16 B.

To analyze the impact of K52 reconstitution on MYC-mediated phenotypes, a single-color competition assay was performed. K52o MYC-expressing cells were able to overgrow the uninfected cell population in contrast to K-less MYC- and vector-expressing cells. The proliferative capacity, however, was not as high as in WT MYC-expressing cells (Fig. 4.19 A).

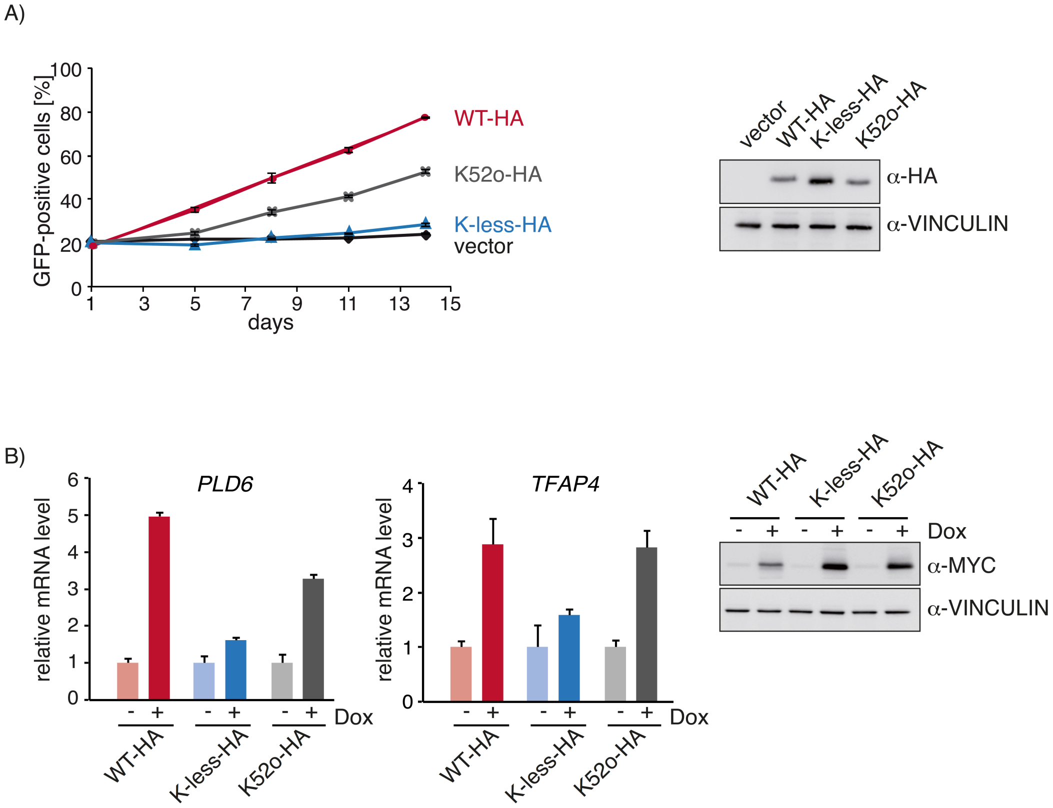

Figure 4.19: K52o MYC largely rescues MYC-mediated phenotypes and target gene expression[2]

A) Single-color competition experiment of IMECs stably expressing vector, WT, K-less or K52o MYC coupled to GFP expression. Infected GFP-positive cells were mixed with uninfected GFP-negative cells and percentage of GFP-positive population was monitored over time by FACS measurement (left panel). MYC expression was confirmed by immunoblot analysis (right panel).

B) Target gene induction by K52o MYC. MYC expression was activated in IMECs stably expressing WT-HA, K-less-HA and K52o-HA by Dox administration for 4 h. The relative mRNA expression is given in reference to the corresponding EtOH treated cells. Data are represented as mean ±SD (left panel). Immunoblot documents MYC expression (right panel).

To analyze how the ability to induce proliferation relates to MYC target gene expression, K52o transcriptional activity was analyzed by qPCR. As previously shown, WT-HA MYC expression in IMECs by addition of Dox for 4 h resulted in an induction of *PLD6* and *TFAP4* expression whereas K-less MYC was impaired in target gene induction. K52o MYC induced *TFAP4* to the same extent as WT MYC and *PLD6* expression was partially rescued (Fig. 4.19 B).

These results suggest that the presence of a single ubiquitin acceptor site in MYC largely rescues transcriptional activity and MYC-induced proliferation.

4.7 Proteasomal activity is required for MYC target gene induction

4.7.1 Depletion of *FBW7* does not influence MYC target gene induction

Several E3 ligases are known to ubiquitinate MYC. Since lysines are important for MYC function and reconstitution of K52, a known ubiquitination site, can largely rescue defects of K-less MYC, the impact of E3 ubiquitin ligases on MYC target gene induction was investigated. The two F-box proteins FBW7 and SKP2 were of particular interest since both were shown to be present at MYC-regulated promoters, suggesting that they could promote promoter-associated turnover of MYC and both ligases bind close to K52 (Farrell et al., 2013; Lehr et al., 2003). Moreover, SCF-SKP2 mediates proteasomal turnover of MYC but is also important for MYC transcriptional activity (Kim et al., 2003; Lehr et al., 2003; Zhang et al., 2013).

If ubiquitination by one of these ubiquitin ligase complexes is the critical modification for MYC activity, depletion of the F-box proteins should result in a reduced transcriptional activity of MYC and mimic K-less MYC.

To analyze the impact of FBW7 and SKP2 on MYC transcriptional activity, cells were transfected with the corresponding siRNAs and MYC's ability to induce gene expression was analyzed by qPCR. *FBW7* was depleted to 30% relative to siCtrl-transfected cells and *SKP2* knockdown efficiency was 90% (Figure 4.20 A, upper panel). While MYC target genes *TFAP4* and *PLD6* were still induced after *FBW7* depletion, the induction of these genes was impaired when *SKP2* was depleted, arguing that SCF-SKP2 might be the critical ubiquitin ligase to stimulate MYC transcriptional activity (Figure 4.20 lower panel). Depletion of *FBW7* or *SKP2* had a subtle effect on MYC protein level when MYC expression was induced for 4 h by Dox administration (Figure 4.20 B).

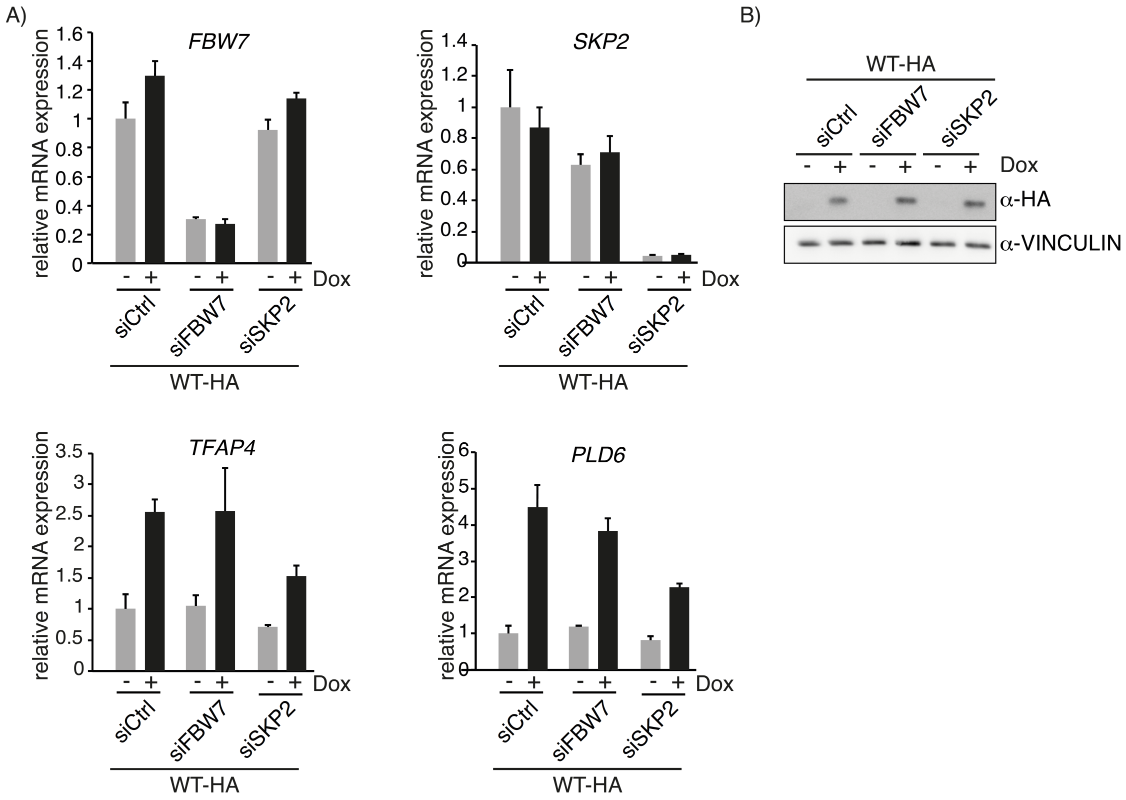

Figure 4.20: Effect of depleting *FBW7* and *SKP2* on MYC target gene induction[2]

A) IMECs stably expressing Dox-inducible WT-HA MYC were transfected with siRNAs targeting FBW7, SKP2 or a non-targeting siRNA as a control. 44 h after siRNA transfection, MYC expression was induced for 4 h with Dox (+). Depletion of FBW7 or SKP2 and MYC target gene induction was analyzed by qPCR. Expression was normalized to *β2M*. The relative mRNA expression was set in reference to the siCtrl EtOH (-) treated sample. Error bars indicate standard deviation of the mean of technical triplicates.

B) Immunoblot analysis documents MYC expression. VINCULIN was used as a loading control.

4.7.2 Depletion of *SKP2* does not globally affect MYC transcriptional activity

Depletion of *SKP2* showed a strong effect on the induction of two direct MYC target genes analyzed by qPCR. Therefore it was investigated whether depletion of *SKP2* has a global effect on WT MYC target gene induction by RNA-Seq.

IMECs stably expressing Dox-inducible WT-HA MYC were transfected with siSKP2 or siCtrl and MYC expression was induced by Dox-treatment for 4 h. Depletion of SKP2 had no effect on MYC protein level as determined by immunoblotting (Fig 4.21 A). RNA was isolated for RNA-Seq and depletion of SKP2 was confirmed by qPCR. Depletion efficiency was 80-90% (Fig. 4.21 B).

To determine whether depletion of *SKP2* had a global effect on MYC target gene induction, density profiles for the $\log_2$FC of the RPKM (reads per kilobase per million mapped reads; to normalize for total read length and the number of sequencing reads) for the control siRNA (siCtrl) and siSKP2 situation were generated. To this end, only genes that were significantly regulated by WT MYC in the previous RNA-Seq experiment were considered (see figure 4.13, $log_2FC>0.5$, padj<0.05; RPKM>1). Depletion of *SKP2* did not generally affect WT MYC target gene induction (Fig. 4.21 C).

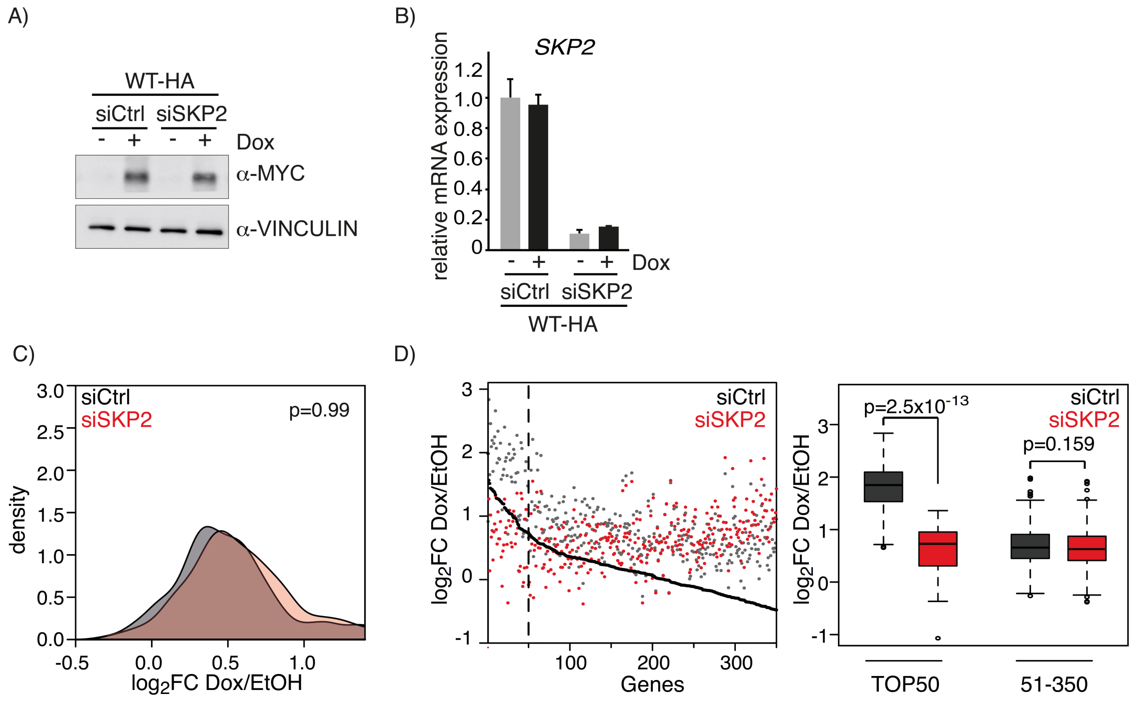

Figure 4.21: Global effects of *SKP2* depletion on MYC transcriptional activity[2]

A) Immunoblot analysis of cell lysates from IMECs stably expressing Dox-inducible WT-HA. Cells were transfected with siRNAs targeting either *SKP2* or a non-targeting siRNA control (siCtrl). 44 h after siRNA transfection, cells were treated for 4 h with Dox (+) to induce WT MYC expression or EtOH (-) as a control. Lysates were blotted for MYC and VINCULIN as a loading control.

B) Depletion of SKP2 was confirmed by qPCR. Cells were treated a described in A. Expression was normalized to *β2M*. The relative *SKP2* mRNA expression was set in reference to the siCtrl EtOH (-) treated sample. Error bars represent standard deviation of the mean of technical triplicates.

C) Density profiles for the log_2FC Dox/EtOH of RPKM values for siCtrl and siSKP2 samples. The p-value was calculated using a one-sided Wilcoxon rank sum test.

D) Dot plot for log_2FC Dox/EtOH of RPKM values. Genes ranked according to the difference log_2FC Dox/EtOH_siCtrl-log_2FC Dox/EtOH_siSKP2. The top 350 genes were plotted. The continuous black line depicts the result for the difference of log_2FC_Dox/EtOH_siCtrl and log_2FC_Dox/EtOH_siSKP2. Genes left of the dashed black line denote the top 50 genes.

To analyze whether a subset of MYC target genes were SKP2-dependent, deregulated genes were ranked according to difference of their log_2FC in the siCtrl and siSKP2 situation and the top 350 genes were plotted (log_2FC_siCtrl-log_2FC_siSKP2) (Fig. 4.21 D, left panel). The top 50 genes were regulated in a SKP2-dependent manner. Comparison of these 50 SKP2-dependent genes with the other 300 genes in a boxplot showed that these 50 genes were indeed significantly regulated in a SKP2-dependent manner, whereas activation of the other 300 genes did not depend on SKP2 (Fig. 4.21 D, right panel).

In summary, a subset of MYC target genes is activated in a SKP2-dependent manner. However, depletion of SKP2 does not globally affect MYC target gene induction.

4.7.3 Proteasomal inhibition results in a decreased in transcriptional activity of MYC

While depletion of *SKP2* did have an effect on some MYC target genes, it did not result in a global loss of transcriptional activity of MYC. This suggests that there are additional ubiquitin ligases, which can regulate MYC in a redundant manner. The majority of ubiquitin ligases targeting MYC promote its proteasome-dependent turnover. Therefore the effect of proteasomal inhibition on MYC transcriptional activity was investigated.

IMECs stably expressing Dox-inducible WT-HA, K-less-HA or WT_N-K_C-HA MYC were treated with the proteasome inhibitor MG132 and either Dox or EtOH for 4 h. Proteasome inhibition increased WT and WT_N-K_C MYC protein level, while K-less MYC level remained unchanged, showing that the treatment with MG132 resulted in proteasome inhibition and the accumulation of short-lived proteins (Fig. 4.22 A).

Effects of proteasome inhibition on MYC transcriptional activity were analyzed by qPCR. MG132 treatment did not influence expression of the MYC transgenes, indicating that transcription *per se* is not influenced (Fig. 4.22 B). However, induction of the target genes *PLD6* and *TFAP4*, which were both induced after expression of WT and WT_N-K_C MYC, was strongly impaired when proteasome activity was blocked (Fig. 4.22 C).

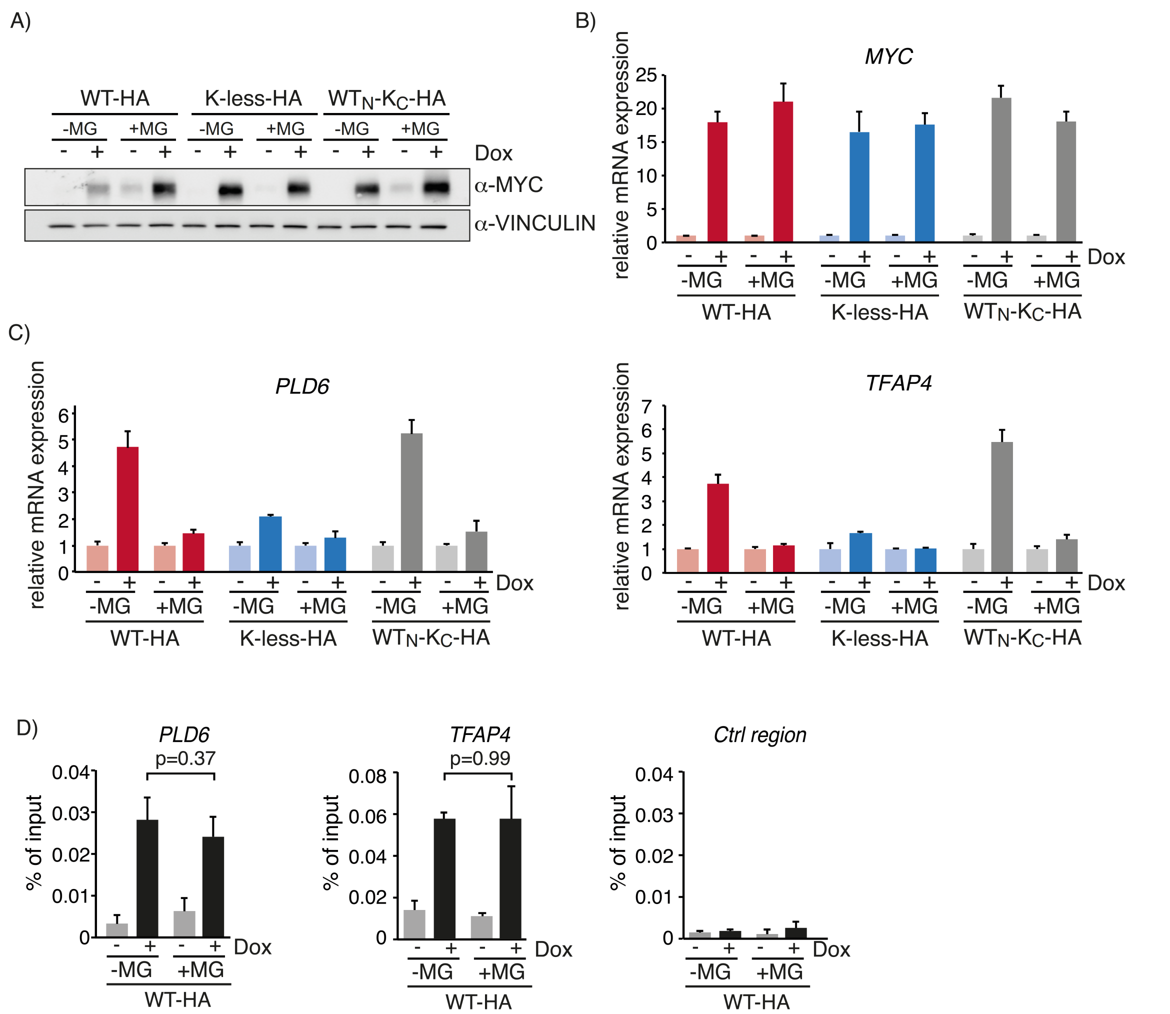

Figure 4.22: Proteasome inhibition blocks MYC transcriptional activity[2]

A) Immunoblot analysis of cell treated with the proteasome inhibitor MG132. IMECs stably expressing Dox-inducible WT-HA, K-less-HA or WT_N-K_C-HA MYC were either treated with MG132 (+MG) or EtOH (-MG) as a control. At the same time, either Dox (+) or EtOH (-) was administered to induce MYC expression. Lysates were analyzed for MYC and VINCULIN expression.

B) Analysis of *MYC* mRNA induction after proteasome inhibition. Cells were treated as described in A and *MYC* mRNA level were analyzed. Expression was normalized to *β2M*. The relative mRNA expression was set in reference to the corresponding EtOH (-) treated sample. Error bars indicate standard deviation of the mean of technical triplicates.

C) Analysis of MYC target gene induction after proteasome inhibition. The qPCR was analyzed as decribed in B.

D) ChIP experiment of IMECs stably expressing Dox-inducible WT-HA MYC in the presence (+MG) and absence (-MG) of the proteasome inhibitor MG132. Cells were treated as described in A. Formaldehyde cross-linked chromatin was immunoprecipitated with a HA antibody. Precipitated and purified DNA was analyzed by qPCR with primers amplifying the MYC-binding site in the *PLD6* and *TFAP4* promoter or an intergenic control region (Ctrl region). Data are represented as mean ±SD. P-values were calculated with a Student's t-test.

To analyze whether MYC is recruited to target gene promoters in the presence of proteasome inhibition, ChIP experiments were performed. To this end, IMECs stably expressing Dox-inducible WT-HA MYC were treated with EtOH (-) or Dox (+) to induce MYC expression in the presence (+MG) or absence (-MG) of proteasome inhibitor and MYC binding to the *TFAP4* and *PLD6* promoter was analyzed. Binding of MYC to the analyzed promoters was not affected after MG132 treatment, indicating that the inability of MYC to induce *TFAP4* or *PLD6* when proteasome activity is inhibited occurs after binding to the promoters (Fig. 4.22 C).

To assess whether proteasome inhibition globally inhibits MYC transcriptional activity, RNA-Seq was performed.

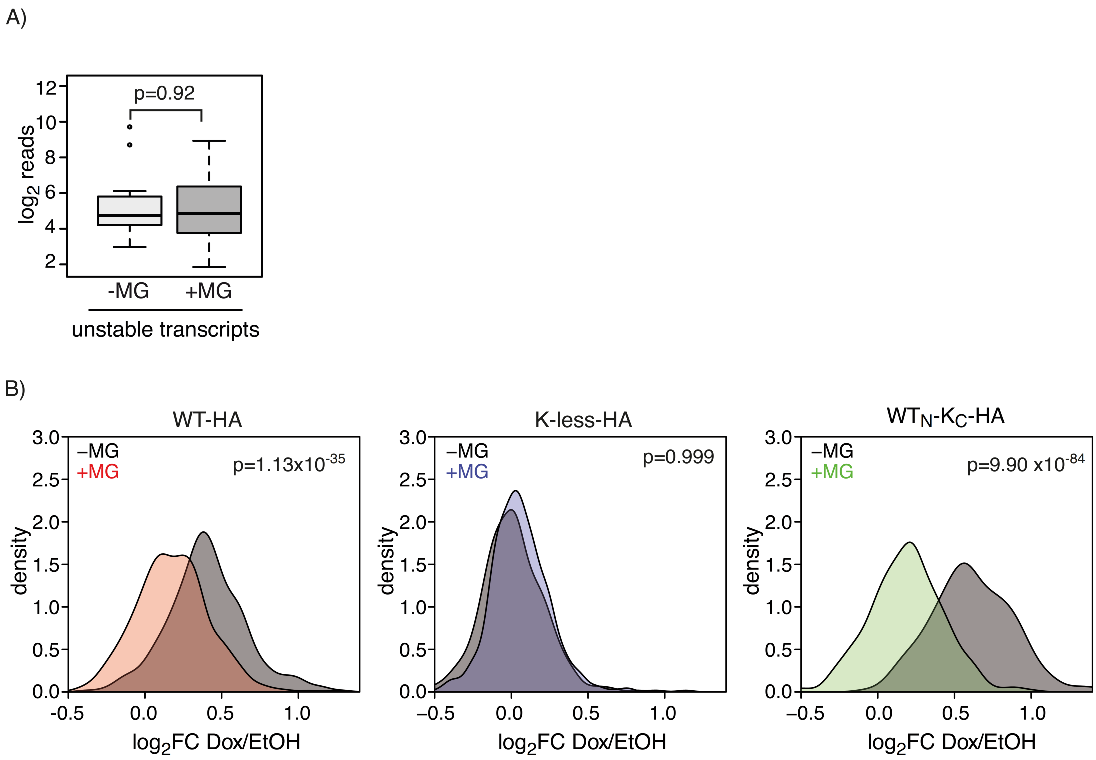

Figure 4.23: Proteasome inhibition globally affects MYC transcriptional activity[2]

A) Effect of MG132 treatment on all unstable transcripts. Unstable transcripts have been described previously (Schwanhäusser et al., 2011). Log_2 reads of all unstable transcripts was plotted after EtOH (-MG) or MG132 (+MG) treatment. The p-value was calculated with a two-sided Wilcoxon rank sum test.

B) Density plot for the log_2FC of RPKM of MYC target genes for WT-HA, K-less-HA or WT_N-K_C-HA in the presence (+MG) or absence (-MG) of proteasome inhibition. P-value was calculated with a two-sided Wilcoxon rank sum test.

Since MG132 treatment could potentially inhibit transcription on a global level independently of MYC activity, expression of unstable transcripts was compared in the presence (+MG) and absence (-MG) of proteasome inhibition. Unstable transcripts were analyzed because cells were treated with MG132 only for a brief time (4 h). If MG132 treatment generally inhibits transcription, this should result in a drop of unstable transcripts. The expression of unstable transcripts did not change upon treatment with MG132, demonstrating that proteasome inhibition does not have a global effect on transcription (Fig. 4.23 A).

To analyze the effect of proteasome inhibition on MYC target gene induction, genes were filtered for being significantly activated by WT MYC in the first RNA-Seq experiment (see Fig. 4.13; $log_2FC>0.5$, padj<0.05, RPKM>1).

WT and WT_N-K_C MYC induced target gene expression in the absence of proteasome inhibition, which was significantly reduced upon MG132 treatment. In contrast, proteasome inhibition had no detectable effect on MYC target genes in K-less MYC-expressing cells (p=0.999) (Fig. 4.23 B).

This shows that inhibition of proteasome activity globally inhibits MYC target gene induction.

4.8 Release of elongating RNAPII is impaired in K-less MYC expressing cells

MYC affects several stages of the transcription cycle: recruitment of RNAPII to promoters, increase of transcription initiation and stimulation of transcriptional elongation (Bouchard et al., 2004; Lin et al., 2012; Nie et al., 2012; Rahl et al., 2010; Walz et al., 2014).

Experimentally, these different steps in transcription can be discriminated by the analysis of the phosphorylation status of RNAPII. The C-terminal repeat domain (CTD) of RNAPII contains multiple consensus heptarepeats with the sequence $_1$YSPTSPS$_7$. RNAPII is recruited to promoters in a hypo-phosphorylated state and becomes phosphorylated at Ser5 of the CTD during transcription initiation, primarily by the CDK7 subunit of the general transcription factor TFIIH (Heidemann et al., 2013). Transcription elongation is regulated by phosphorylation of Ser2 in the CTD, which was shown to be primarily mediated by P-TEFb but other kinases like CDK12 and CDK13 might also be involved in Ser2 phosphorylation (Heidemann et al., 2013).

To analyze if there are differences between WT and K-less MYC in regulating one of these transcriptional steps, ChIP assays were performed using antibodies that recognize the different phosphorylated forms of RNAPII.

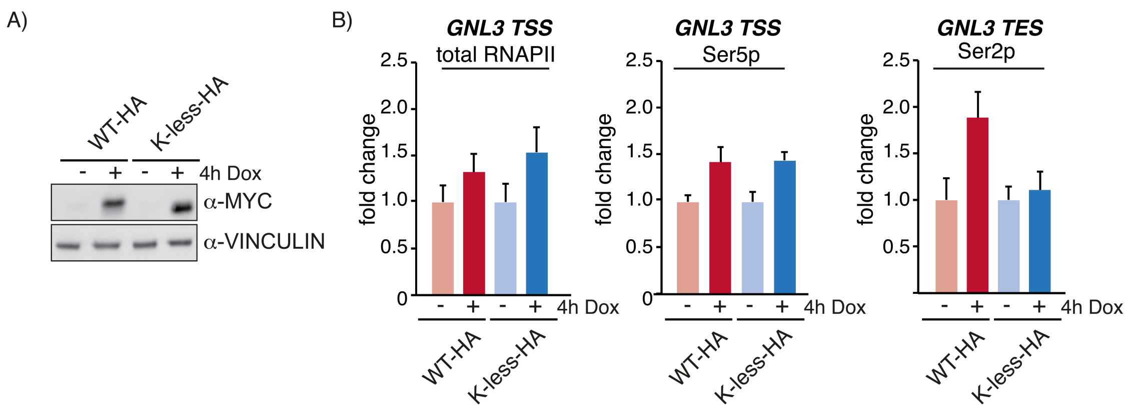

Figure 4.24: WT but not K-less MYC increases Ser2p RNAPII at the TES

A) IMECs stably expressing Dox-inducible WT-HA or K-less-HA MYC were treated with Dox (+) or EtOH as a control (-) for 4 h. MYC expression was confirmed by immunoblot analysis. VINCULIN served as a loading control.

B) ChIP of RNAPII after 4 h MYC induction. Cells were treated as described in A. Formaldehyde cross-linked chromatin was immunoprecipitated with antibodies recognizing total RNAPII, RNAPII phosphorylated at Ser5 (Ser5p) or Ser2 (Ser2p) in its C-terminal domain. Precipitated and purified DNA was analyzed by qPCR with primers spanning the TSS or the transcriptional end site (TES) of the MYC target gene *GNL3*. The fold change was calculated in reference to the corresponding EtOH (-) treated sample. Data are represented as mean ±SD.

Expression of either WT or K-less MYC was induced in IMECs by Dox administration for 4 h and expression was confirmed by immunoblot analysis (Fig. 4.24 A).

ChIP assays were performed with antibodies recognizing either total RNAPII, RNAPII phosphorylated at Ser5 or Ser2 of the CTD. After WT and K-less MYC induction, total RNAPII increased at the transcriptional start site (TSS) of the MYC target gene *GNL3*. Moreover, an increase of Ser5p RNAPII was detected at the *GNL3* TSS indicating that both WT and K-less MYC stimulated transcription initiation. Elongating RNAPII phosphorylated at Ser2 is detectable in the gene body of actively transcribed genes and increases towards the 3'end of the gene (Heidemann et al., 2013). An increase in Ser2p RNAPII at the transcriptional end site (TES) of *GNL3* was detected after WT but not after K-less MYC induction (Fig. 4.24 B), suggesting that K-less MYC is deficient in promoting the transition from transcription initiation to productive elongation.

4.8.1 K-less MYC globally induces RNAPII recruitment and initiation but not elongation at direct MYC target genes

To investigate whether the defect of K-less MYC in gene activation could be due to impaired transcriptional elongation, distribution of total RNAPII, and its Ser5- and Ser2-

phosphorylated forms was analyzed by ChIP-Seq. IMECs stably expressing Dox-inducible WT-HA or K-less-HA MYC were treated with Dox for 4 h to induce MYC expression or EtOH as a control. Total RNAPII was immunoprecipitated with an antibody recognizing an epitope at the N-terminus of RNAPII. Ser5- and Ser2-phosphorylated RNAPII were immunoprecipitated with antibodies recognizing the corresponding phosphorylated form of the CTD of RNAPII.

RNAPII distribution along genes was visualized by generating metagenes. To this end, all genes were divided into 400 windows. The promoter of every gene was divided into 80 windows each consisting of 50 bp covering the region from -2000 to +2000 bp around the TSS. The end of a gene was divided into 120 windows consisting of 50 bp ranging from -2000 to +4000 bp around the TES. The tags within these windows were counted and divided by the number of genes. To normalize for different transcript lengths, the gene body was divided into 200 windows and the tags within the first 50 bp of the respective window were counted. Normalized tag densities of total RNAPII were plotted within this metagene for the EtOH and MYC-activated situation respectively to visualize RNAPII distribution along the genes (Fig. 4.25).

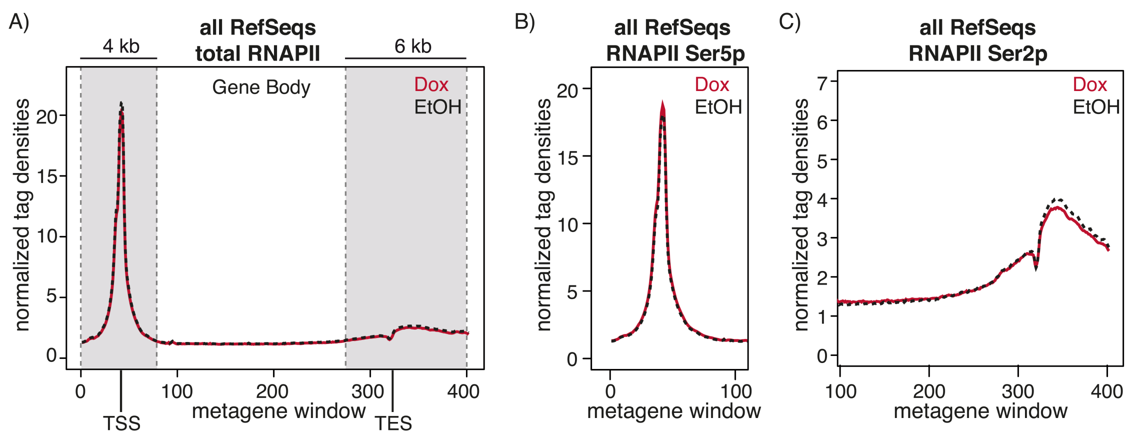

Figure 4.25: Distribution of RNAPII along all genes

A) Metagene plot of total RNAPII at all genes. Position of the TSS and TES is indicated.
B) Ser5-phosphorylated RNAPII at the TSS of all genes.
C) Ser2-phosphorylated RNAPII along the gene body and the TES of all genes.

A sharp RNAPII peak was detected at the TSS of all genes, fewer tags were present in the gene body and tag density slightly increased again at the TES, the side of 3'end processing where RNAPII slows down and accumulates (Fig. 4.25 A).

The initiating Ser5-phosphorylated form of RNAPII is detectable at the TSS of a gene and the signal decreases towards the 3'end of the gene. Accordingly, RNAPII phosphorylated at Ser5 showed a peak at the TSS (Fig. 4.25 B). Ser2-phosphorylated polymerase was detectable within the gene body and the signal increased at the TES of the gene (Fig. 4.25 C). Induction of WT MYC by Dox administration did not increase total RNAPII, Ser5p or Ser2p RNAPII suggesting that in this cellular system, MYC does not induce recruitment and phosphorylation of RNAPII at all genes.

To analyze MYC-dependent effects on RNAPII, only those genes were selected that were bound and activated by MYC according to the first RNA- and ChIP-Seq experiments ($log_2FC > 0.5$, see Fig. 4.10 and Fig. 4.13).

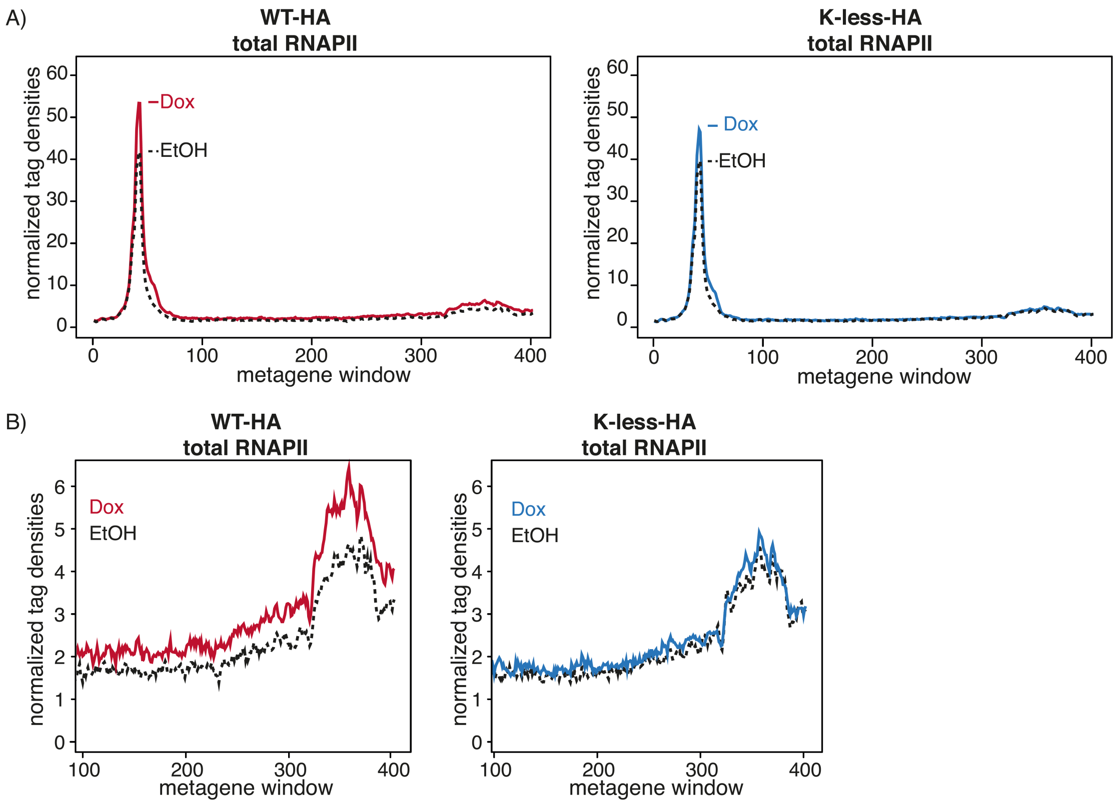

Figure 4.26: Activation of WT MYC increases recruitment and release of RNAPII[2]

A) Distribution of total RNAPII along directly MYC-activated genes after WT MYC (left) or K-less MYC (right) activation.
B) Magnification of the gene body and TES of directly MYC-activated genes with total RNAPII distribution.

The amount of total RNAPII increased at the TSS after WT MYC induction. This was also the case after K-less MYC induction, although to a lesser extent (Fig. 4.26 A). Inspection of the gene body and TES showed an increase of total RNAPII after WT MYC induction. In contrast, induction of K-less MYC did not result in an increase of RNAPII in the gene body or at the TES. In this case, RNAPII distribution after Dox or EtOH treatment was indistinguishable (Fig. 4.26 B).

Activation of both WT and K-less MYC led to an increase of Ser5p RNAPII at the TSS (Fig. 4.27 A).

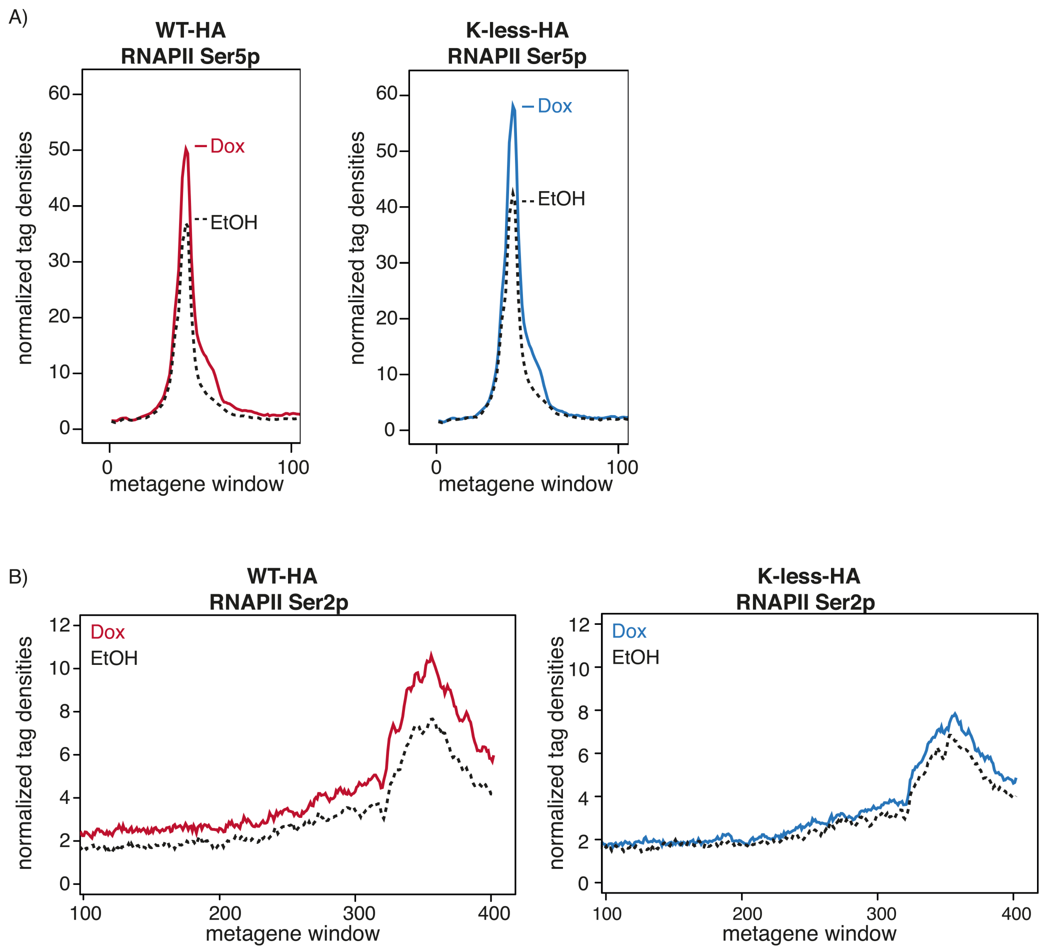

Figure 4.27: Activation of WT and K-less MYC stimulates the initiation of RNAPII[2]

A) Distribution of Ser5-phosphorylated RNAPII at the TSS of directly MYC-activated genes after WT MYC (left) or K-less MYC (right) activation.

B) Distribution of Ser2-phosphorylated RNAPII along the gene body and at the TES of directly MYC-activated genes after WT MYC (left) or K-less MYC (right) activation.

Interestingly, only activation of WT MYC led to an increase of Ser2p RNAPII within the gene body and the TES, highlighting that WT MYC stimulates transcriptional elongation of its target genes. Activation of K-less MYC did not affect the level of Ser2p RNAPII, suggesting that the presence of lysine residues is important for the transition from transcription initiation to efficient elongation (Fig. 4.27 B).

To quantify MYC-mediated effects on initiating and elongating RNAPII, the $\log_2$FC (DOX/EtOH) of Ser5p RNAPII was plotted for the TSS and gene body, respectively.

Induction of WT MYC increased Ser5p RNAPII at the TSS and gene body while K-less MYC only increased Ser5p RNAPII at the TSS (Fig. 4.28 A). While the difference of Ser5p RNAPII at the TSS and gene body is not significant for WT MYC-expressing cells, K-less MYC-expressing cells showed a statistically significant difference of Ser5p RNAPII present at the TSS and gene body. This was further reflected by the change of Ser2p RNAPII in the gene body and TES after MYC expression. As expected from the metagenes, WT MYC induction by Dox increased Ser2p RNAPII in the gene body and at the TES, whereas K-less MYC expression led to a marginal increase of Ser2p RNAPII at these sites (Fig. 4.28 B).

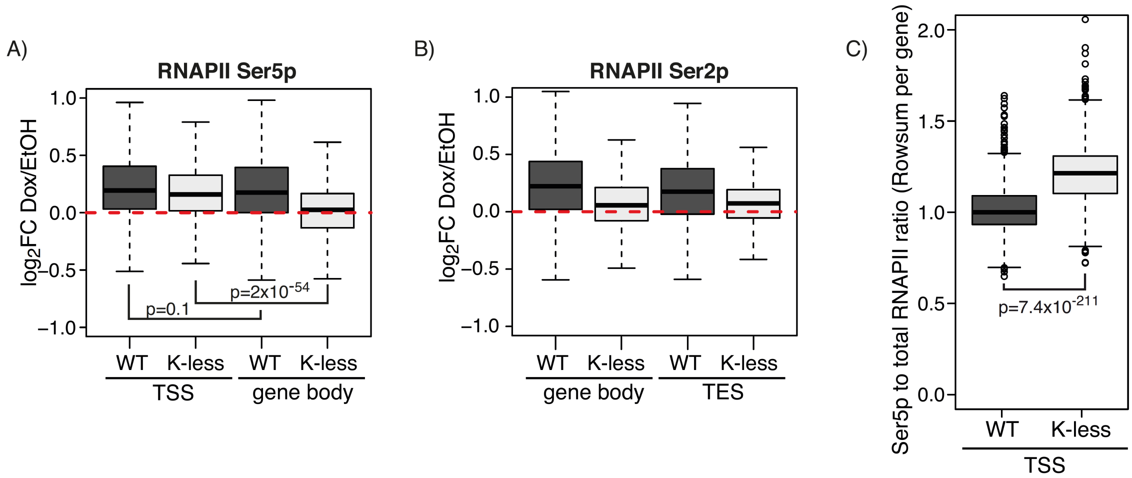

Figure 4.28: K-less MYC is impaired in releasing elongating RNAPII[2]

A) Boxplot of changes in Ser5-phosphorylated RNAPII at the TSS and gene body of MYC-bound genes after MYC induction. Log_2 fold changes of Ser5-phosphorylated RNAPII in Dox versus EtOH treated cells were plotted for WT and K-less at TSS and gene body. P-value was calculated with a two-sided Wilcoxon rank sum test.

B) Boxplot of changes in Ser2-phosphorylated RNAPII at the gene body and TES of MYC-bound genes after MYC induction. Log_2 fold changes of Ser2-phosphorylated RNAPII in Dox versus EtOH treated cells were plotted for WT and K-less at the gene body and TES.

C) Boxplot of Ser5-phosphorylated RNAPII at the TSS normalized to total RNAPII after MYC-induction (Dox). P-value was calculated with a two-sided Wilcoxon rank sum test.

Since WT MYC increased the amount of total RNAPII at the TSS somewhat better than K-less MYC (Fig. 4.26 A), the amount of Ser5p RNAPII at the TSS was normalized to total RNAPII after WT and K-less MYC-induction, respectively. While no change in the Ser5p to total RNAPII ratio was observed in WT MYC-expressing cells, a significant increase of the Ser5p/total RNAPII ratio was detected in K-less MYC-expressing cells, suggesting that Ser5p RNAPII accumulates at the TSS of K-less MYC-expressing cells (Fig. 4.28 C).

Thus, expression of WT MYC increases the amount of total, initiating and elongating RNAPII whereas K-less MYC induces only total and initiating RNAPII at the TSS. These results strongly suggest that in K-less MYC expressing cells the transition from initiation to elongation is blocked, resulting in an accumulation of initiating RNAPII at the TSS.

4.9 K-less MYC is impaired in the recruitment of cofactors to MYC-regulated promoters

4.9.1 K-less MYC is impaired in inducing histone acetylation

MYC has an established role in stimulating transcription by recruiting HATs to promoters, which induce histone acetylation (see 1.3.2.1) (Bouchard et al., 2001; Frank et al., 2003; McMahon et al., 2000). To study whether both WT and K-less MYC induce histone acetylation in this cellular system, changes in histone acetylation at the *GNL3* promoter were analyzed by ChIP assays after MYC induction. IMECs stably expressing Dox-inducible WT-HA or K-less-HA MYC were treated with Dox for 3 h. Total H3, H3Ac and H4Ac were immunoprecipitated and changes in histone acetylation were normalized to total H3.

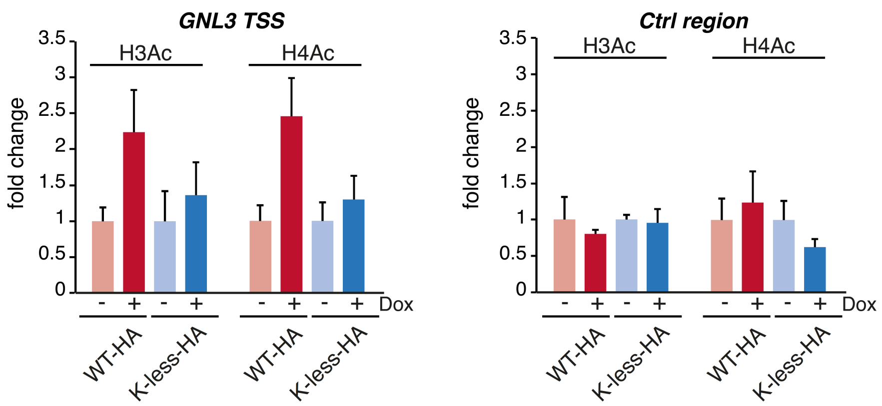

Figure 4.29: Expression WT but not K-less MYC induces histone acetylation[2]
IMECs stably expressing Dox-inducible WT-HA or K-less-HA MYC were treated with Dox (+) or EtOH as a control (-) for 3 h. Formaldehyde cross-linked chromatin was immunoprecipitated with antibodies recognizing total H3, acetylated H3 (H3Ac) and acetylated H4 (H4Ac). Precipitated and purified DNA was analyzed by qPCR with primers amplifying the TSS of the MYC target gene *GNL3* or a Ctrl region. Histone acetylation was normalized to total H3 and the fold change was calculated in reference to the corresponding EtOH (-) treated sample. Data are represented as mean ±SD.

Induction of WT MYC increased H3 and H4 acetylation more than twofold. This effect was specific for MYC-regulated promoters since no increase in histone acetylation could be observed in an intergenic control region. In contrast to WT MYC, K-less MYC expression did not result in increased histone acetylation (Fig. 4.29), indicating that K-less

MYC is impaired in recruiting HATs to target gene promoters or that the activity of HATs at the promoters is decreased.

4.9.2 Recruitment of BRD4 and CDK9 is impaired in K-less MYC expressing cells

The absence of elongation competent Ser2-phosphorylated RNAPII in K-less MYC-expressing cells could be due to an inability to resolve the promoter-proximal pausing state of RNAPII. As mentioned previously, RNAPII pauses transcription after promoter escape in a promoter proximal position and is bound by the pausing factors DSIF and NELF. For efficient transcriptional elongation, the pausing state needs to be resolved. A critical protein to release elongating polymerase from the paused state is P-TEFb. P-TEFb phosphorylates DSIF and NELF, leading to dissociation of NELF from the RNAPII and turning DSIF from a negative into a positive elongation factor (Adelman and Lis, 2012). Moreover, productive elongation requires Ser2 phosphorylation of RNAPII, which serves as a binding platform for several RNA-processing factors. Different kinases have been shown to phosphorylate Ser2 with P-TEFb being the best characterized (Eick and Geyer, 2013; Saunders et al., 2006). Recruitment of P-TEFb to promoters can be facilitated by transcription factors like MYC or by interaction with BRD4, a bromodomain protein which binds acetylated H3 and H4 (Bisgrove et al., 2007; Dey et al., 2003; Eberhardy and Farnham, 2002; Yang et al., 2005).

Therefore, binding of BRD4 and CDK9, the kinase subunit of P-TEFb, to the MYC-regulated *GNL3* promoter was analyzed by ChIP.

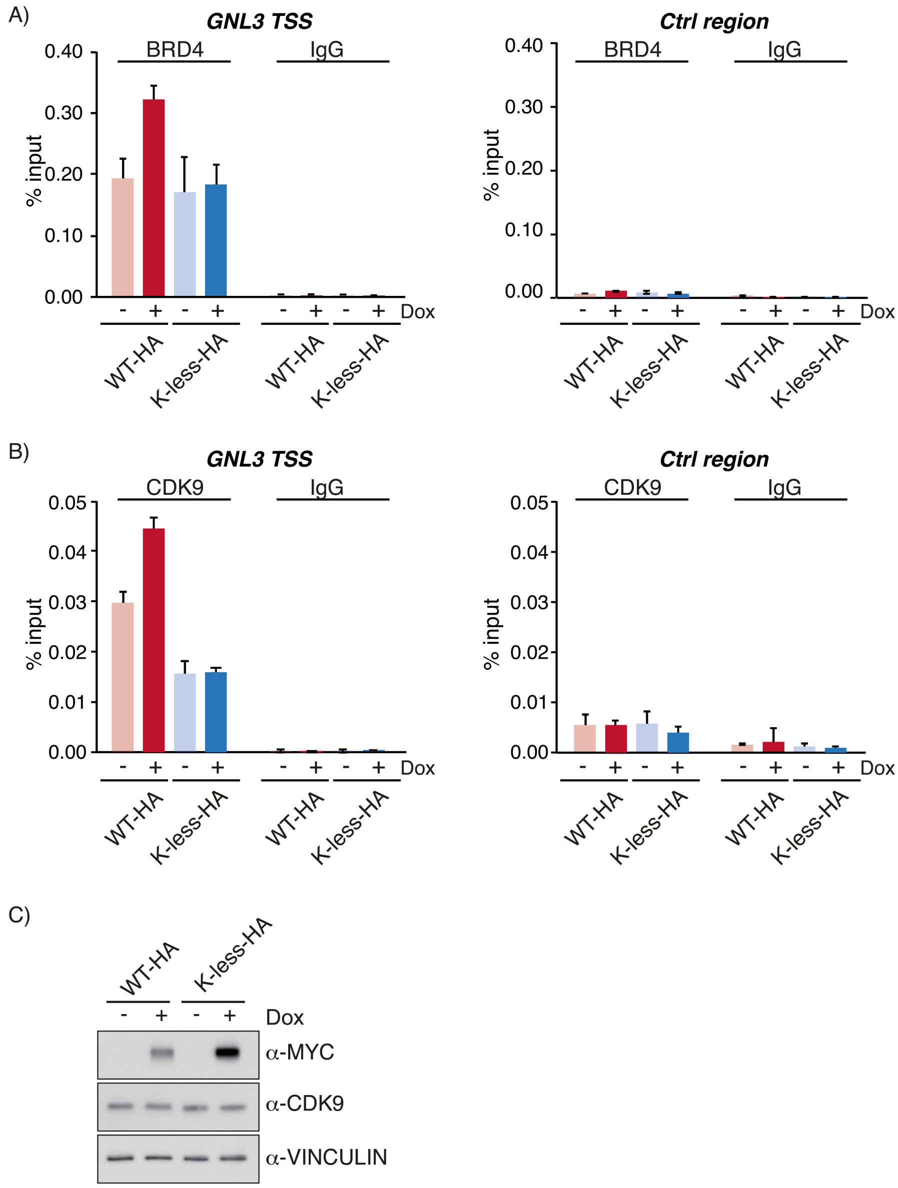

Figure 4.30: Expression of WT but not K-less MYC leads to recruitment of BRD4 and CDK9[2]

A) IMECs stably expressing Dox-inducible WT-HA or K-less-HA MYC were treated with Dox (+) or EtOH (-) for 4 h. Formaldehyde- and DSG-cross-linked chromatin was immunoprecipitated with an antibody recognizing BRD4 or IgG as a control. Precipitated and purified DNA was analyzed by qPCR with primers amplifying TSS of *GNL3* or a negative control region (*Ctrl region*). Data are represented as mean ±SD.

B) Cells were treated as described in A). Chromatin was immunoprecipitated with a CDK9 antibody or IgG as a control.

C) Immunoblot analysis of IMECs stably Dox-inducible WT-HA or K-less-HA MYC. Cells were treated with Dox (+) or EtOH as a control (-) for 4 h. MYC and CDK9 expression was analyzed. VINCULIN served as a loading control.

Upon WT MYC induction by Dox treatment, more BRD4 was detected at the GNL3 promoter whereas activation of K-less MYC did not increase BRD4 binding (Fig. 4.30 A). Concomitantly, expression of WT MYC resulted in an increase of CDK9 binding at the

GNL3 promoter whereas total CDK9 protein level remained unaffected. Expression of K-less MYC neither affected CDK9 binding at the *GNL3* promoter nor total CDK9 protein level in the cell (Fig 4.30 B and C).
Thus, induction of histone acetylation as well as BRD4 and CDK9 recruitment to the *GNL3* promoter was impaired in K-less MYC-expressing cells. This could result in an inability to release paused RNAPII and consequently to unproductive elongation.

4.10 Identification of a MYC-PAF-complex as an intermediate in transcriptional activation

4.10.1 K-less MYC interacts with the PAF complex, a positive elongation factor, at MYC-regulated genes

Besides the requirement of P-TEFb for the release of elongating RNAPII, several positive elongation factors are important for productive elongation. The PAF complex (RNA polymerase II-associated factor) is a multiprotein complex, which plays an important role in transcription elongation, RNA processing and histone modification (Sims et al., 2004).
CTR9, a subunit of the PAF complex, was identified as an interaction partner of the MYC-related protein N-MYC by mass spectrometry (Anne Carstensen, personal communication).
CTR9 associates with elongating RNAPII and can be detected within the coding region of actively transcribed genes. Its occupancy peaks at the 3'end of genes similar to the occupancy of Ser2-phosphorylated RNAPII (Rahl et al., 2010). To investigate whether CTR9 travels with RNAPII at MYC-regulated genes, CTR9 occupancy at the TES of *GNL3* was analyzed. WT or K-less MYC expression was induced for 4 h by Dox treatment and CTR9 was immunoprecipitated. A robust CTR9 signal could be detected at the TES of *GNL3.* CTR9 occupancy increased upon WT MYC expression demonstrating that also at MYC-regulated genes CTR9 travels with RNAPII. K-less MYC expression did not increase CTR9 occupancy at the *GNL3* TES (Fig. 4.31 A).
Further, it was analyzed, whether physical association between CTR9 and MYC is regulated by ubiquitination and/or protein turnover. MYC was immunoprecipitated from IMECs stably expressing WT or K-less MYC alleles using a MYC-specific antibody and

the precipitate was analyzed for CTR9. Vector infected cells were used as control.

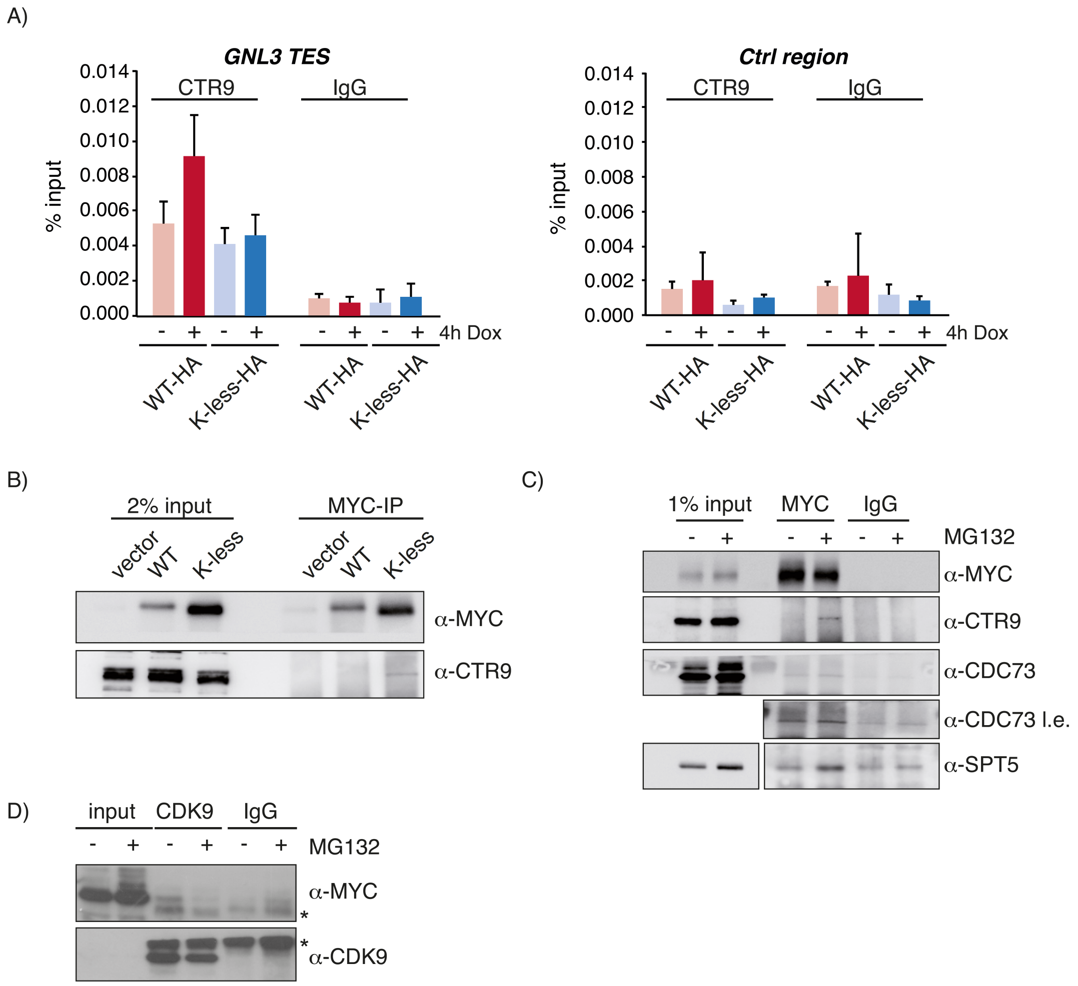

Figure 4.31: The PAF complex is a positive elongation factor at MYC-regulated genes and interacts with stabilized MYC[2]

A) Cells were treated as described in Fig. 4.29 A. Formaldehyde- and DSG-cross-linked chromatin was immunoprecipitated with an antibody recognizing CTR9 or IgG as a control. Precipitated and purified DNA was analyzed by qPCR with primers amplifying the TES of *GNL3* or a control region (*Ctrl region*). Data are represented as mean ±SD.

B) MYC was immunoprecipitated from IMECs stably expressing vector, WT or K-less MYC. 2% input sample, precipitated MYC and co-precipitated endogenous CTR9 were analyzed by immunoblotting.

C) HeLa cells were treated with EtOH (-) or MG132 (+) for 4 h. Endogenous MYC was immunoprecipitated from nuclear extracts. As a control, an immunoprecipitation with the unspecific rabbit IgG was performed. 1% input and the immunoprecipitated samples were analyzed by immunoblotting. l.e. longer exposure

D) HeLa cells were treated as indicated in C. Endogenous CDK9 was immunoprecipitated and the precipitation with the unspecific rabbit IgG served as a control. 1% input and the immunoprecipitated samples were analyzed by immunoblotting. *depicts the heavy chain of the antibody. This experiment was performed by Dr. Nikita Popov.

Strikingly, an interaction between K-less MYC and CTR9 could be detected whereas no binding between WT MYC and CTR9 could be observed (Fig. 4.31 B). This suggests that the MYC-CTR9 interaction is very transient and that the interaction is enhanced by an attenuated MYC turnover, as it is the case for K-less MYC.

In line with the observation that a more stable MYC protein interacts stronger with CTR9, an interaction between MYC and CTR9 could only be detected upon proteasome inhibition in HeLa cells (Fig. 4.31 C).

This shows that either a stable version of MYC or proteasome inhibition stabilizes the interaction between MYC and the elongation factor CTR9. A similar effect, albeit not as pronounced, was found with another PAF component, CDC73, and the DSIF component SPT5, which were also previously identified as N-MYC interacting proteins (Fig. 4.31 C; Anne Carstensen, personal communication). Proteasomal inhibition led to an enhanced interaction between MYC and CDC73 or SPT5 (Fig. 4.31 C). Interestingly, the opposite was observed for the interaction of CDK9 with MYC. In this case, the interaction was strongly reduced when cells were treated with MG132 (Fig. 4.31 D).

The stronger interactions of PAF components with K-less or MG132-stabilized MYC indicate that the association of MYC with PAF is very transient. This complex may represent an intermediate step in MYC-mediated transcriptional activation, which is stabilized in the absence of P-TEFb at the promoters.

4.10.2 Phosphorylation of MBI enhances the interaction with the PAF complex

Interestingly, the PAF complex components CTR9 and CDC73 were identified by mass spectrometry to interact with WT N-MYC but not with a N-MYC mutant, which could not be phosphorylated at T58 and S62 (N-MYC T58A/S62A) (Anne Carstensen, personal communication). Moreover, it was reported that CDC73 and CTR9 interact with RNAPII phosphorylated at Ser5 and Ser2 (Qiu et al., 2012). Therefore it was investigated whether CTR9 and CDC73 interact with MYC in a phosphorylation-dependent manner.

T58 and S62 lie within MBI, which is highly conserved region between MYC and N-MYC (Fig. 4.32 A). Binding of CDC73 and CTR9 to MBI was analyzed with a peptide pulldown assay. Biotinylated N-MYC MBI peptides spanning residues 28-89 with unmodified T58 and S62, phosphorylated T58 or S62 or doubly phosphorylated T58 and S62 were incubated with HeLa nuclear extracts. A robust binding of CDC73 to the MBI peptide could be detected, which was enhanced when the peptide was phosphorylated at one or both phosphorylation sites. CTR9 showed a modest binding to doubly phosphorylated MBI (Fig. 4.32 B).

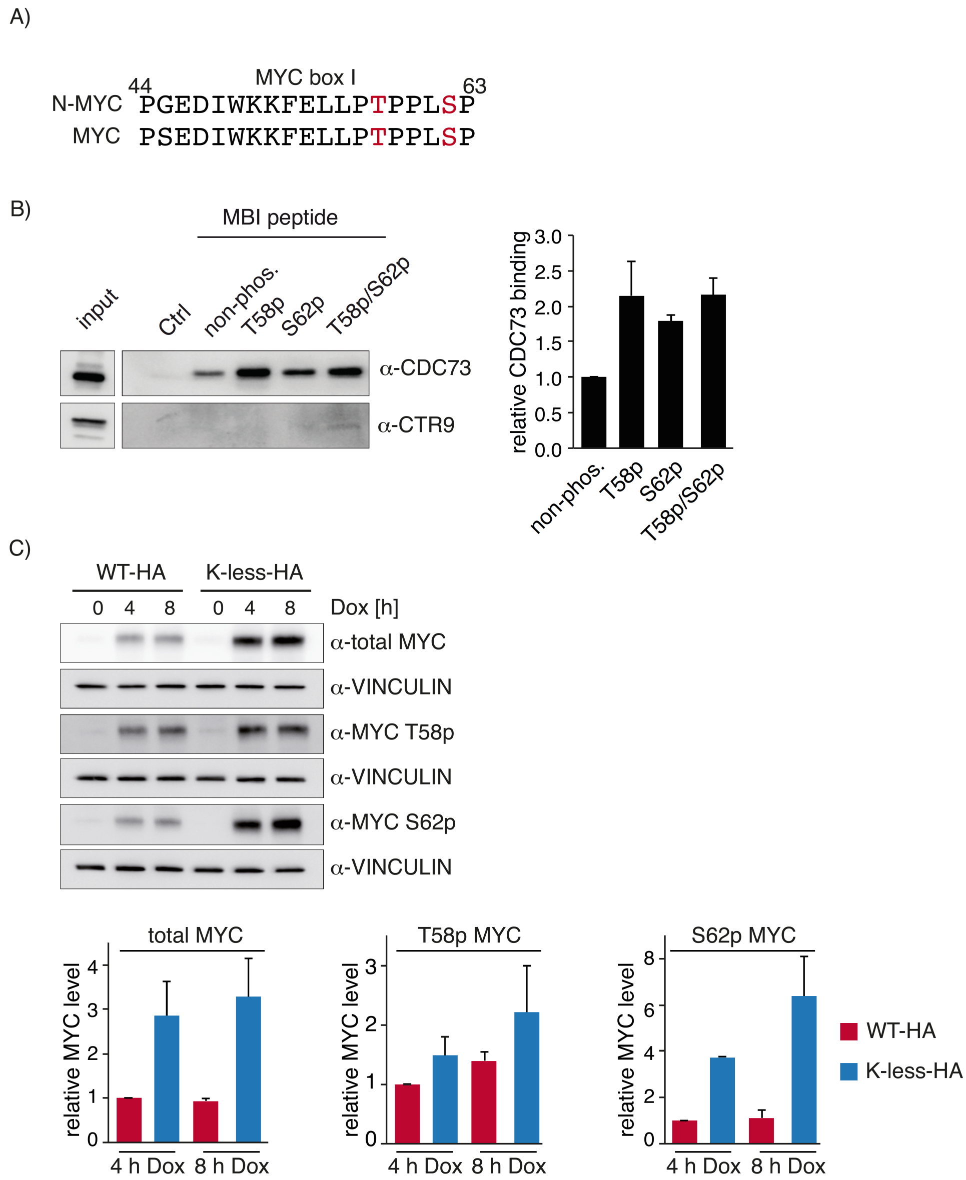

Figure 4.32: The PAF complex interacts with phosphorylated MYC box I[2]

A) Alignment of MYC and N-MYC MYC box I sequence. The residues T58 and S62 are marked in red.

B) Pulldown of CDC73 and CTR9 with N-MYC MYC box I (MBI) peptides. MBI petides were coupled to streptavidin magnetic beads and incubated with nuclear extracts from HeLa cells. Beads without MBI peptide were used as a negative control (Ctrl). Eluates from the pull down were analyzed by immunoblotting with the indicated antibodies (left panel). Binding of CDC73 to the indicated MYC box I peptides was quantified and is given relative to the binding to non-phosphorylated MBI peptide. Data are represented as mean ± SEM from three independent experiments (right panel).

C) Lysates from IMECs expressing Dox-inducible WT-HA and K-less-HA MYC were analyzed by immunoblotting for total, T58-phosphorylated (T58p) and S62-phosphorylated (S62p) MYC after 4 h and 8 h Dox administration or EtOH (0 h) as a control (upper panel). Lower panels document the quantification of three independent experiments. Data were normalized to VINCULIN and error bars represent SEM.

Since the PAF-MYC complex is stabilized with K-less MYC, the phosphorylation status of K-less MYC was investigated with phospho-specific antibodies. In line with the result that CDC73 interacts stronger with phosphorylated MBI, K-less MYC accumulated in a form that is phosphorylated at S62p whereas T58p increased to a weaker extent (Fig. 4.32 C).

Together, these data suggest that the PAF complex is recruited by phosphorylated MYC and is transferred on RNAPII upon CTD phosphorylation by P-TEFb.

5 Discussion

The transcription factor MYC is a short-lived protein rapidly turned over by the ubiquitin-proteasome system. Many ligases have been shown to ubiquitinate MYC and these ubiquitination events can have a negative or a positive effect on MYC transcriptional activity and MYC-mediated phenotypes. Despite the fact that many ubiquitin ligases for MYC have been identified, the contribution of MYC ubiquitination to its function remained unresolved. Therefore the objective of this thesis was to elucidate the direct effect of MYC ubiquitination on its transcriptional activity.

5.1 MYC ubiquitination occurs on multiple lysines

To identify ubiquitination sites in MYC, a mass spectrometric approach was used. Two lysines in MYC (K148, K389) could be identified as ubiquitin acceptor sites. Besides the identification of ubiquitinated MYC peptides, peptides of ubiquitin itself were detected with a di-glycin at lysine 48, showing that ubiquitin chains with the linkage K48 were present in the sample. This suggests that K148 and K389 could be ubiquitinated with a K48-linked ubiquitin chain.

The identified ubiquitinated lysine K148 is located next to MBII, an important domain in MYC that mediates the interaction with several co-activators and is therefore crucial for MYC transcriptional activity (Conacci-Sorrell et al., 2014). Ubiquitination at this lysine could interfere with the binding of cofactors and thereby inhibit MYC transcriptional activity. On the other hand, degradation via this lysine could mark transcriptionally inactive MYC since it is devoid of cofactors and would consequently be removed from the cellular MYC pool.

The second identified ubiquitin acceptor site in MYC, K389, is located in the helix-loop-helix domain, which is important for interaction with MAX and MIZ1. Ubiquitination of this lysine could interfere with the binding of these interaction partners. MYC forms a repressive complex with MIZ1. At promoters with a high MYC/MIZ1 ratio MYC acts as a transcriptional activator, while a lower MYC/MIZ ratio is observed at repressed genes. Ubiquitination at K389 could antagonize MYC/MIZ1 complex formation, shifting the balance to a high MYC/MIZ1 ratio. This could stimulate MYC-mediated transcriptional activation in a manner that has been demonstrated for HUWE1 (Peter et al., 2014). HUWE1 degrades MIZ1 and thereby prevents the assembly of MYC/MIZ1 repressive complexes at MYC-responsive genes. Since HUWE1 also acts as a ubiquitin ligase for MYC, ubiquitination at K389 could further prevent the formation of a repressive complex (Adhikary et al., 2005).

In parallel to the study at hand, a manuscript by the Gygi and Harper laboratories published the human ubiquitin-modified proteome. In contrast to our approach, they performed tryptic digestion of whole cell lysates and enriched for ubiquitinated proteins by precipitating modified-proteins with an antibody recognizing the di-glycine at the modified lysine (Kim et al., 2011). Moreover, the mass spectrometric approach was different since Kim et al. performed SILAC (stable isotope labeling with amino acids in cell culture) to monitor changes in di-glycine site abundance for example upon proteasome inhibition. In total, Kim et al. identified seven lysines in MYC with a di-glycine (K52, K148, K157, K323, K355, K389, K412), including the two identified lysines from our study. This confirms that K148 and K389 are indeed *bona fide* ubiquitination sites in MYC. The enrichment for ubiquitinated proteins with an antibody recognizing the di-glycin isopeptide is a more sensitive approach than the identification of ubiquitination sites of ectopically expressed and purified MYC since one enriches for ubiquitinated peptides. Moreover, Kim et al. treated the cells with the proteasomal inhibitor bortezomib leading to accumulation of ubiquitinated proteins. This could explain why we identified only two out of seven ubiquitinated lysines.

K148 and K389 might be accessible for ubiquitination when MYC is not sequestered in a protein complex with interaction partners. Upon MYC overexpression, binding partners might be limiting and the respective lysines might become accessible for ubiquitination. Therefore, under this situation, ubiquitination of K148 and K389 might be the most abundant sites of modification.

Besides ubiquitin, the active forms of the two ubiquitin-like modifiers NEDD8 and ISG15 contain two C-terminal glycines. Like ubiquitin, NEDD8 and ISG15 are attached to a lysine of the substrate protein via the C-terminal glycine. Thus, in case of a NEDD8- or ISG15-modified lysines, tryptic digestion also generates a di-glycine, which remains attached to the substrate protein. Therefore, it cannot be ruled out that K148 or K389 could also be modified by NEDD8 or ISG15. ISG15 expression is induced upon viral infection and it is undetectable in unstimulated cells (Kim et al., 2011). Thus, modification with ISG15 in unstimulated cells is rather unlikely. Neddylation is an important post-translational modification of cullin-RING ligases and has an activating effect on their E3

ligase activity (Deshaies et al., 2010). Kim et al. showed that only a maximum of 6% of the di-glycine-modified sites in the human proteome were due to neddylation indicating that neddylation, compared to ubiquitination, is a rather rare event (Kim et al., 2011).
Moreover, the identification of di-glycine-modified peptides of ubiquitin itself points to the possibility that K148 and K389 were indeed modified with a ubiquitin chain.
Therefore it can be concluded that MYC becomes ubiquitinated at multiple lysine residues, which are distributed all over the protein.

5.2 K-less MYC, a tool to study effects of MYC ubiquitination

The impact of MYC ubiquitination on its activity is complex. Most of the ubiquitin ligases target MYC for proteasomal degradation leading to a global reduction of MYC protein in the cell and thus a reduction of MYC activity (see 1.3.3.2.4). However, three ubiquitin ligases, HUWE1, SCF-SKP2 and SCF-FBXO28, were reported to stimulate MYC transcriptional activity. While SKP2-mediated ubiquitination also leads to proteasomal turnover of MYC, ubiquitination by SCF-FBXO28 and HUWE1 was shown to stimulate MYC transcriptional activity by recruitment of cofactors (Adhikary et al., 2005; Cepeda et al., 2013; Kim et al., 2003; Lehr et al., 2003). Additionally, as discussed previously, HUWE1 stimulates MYC transcriptional activity by degrading MIZ1 and thereby counteracting the formation of repressive MYC/MIZ1 complexes at MYC-activated target gene promoters (Peter et al., 2014).
Since many different ligases ubiquitinate MYC leading to diverse effects on MYC function, it is difficult to elucidate the mechanisms how MYC ubiquitination stimulates its activity by depleting individual ubiquitin ligases. Furthermore, it is conceivable that certain ubiquitin ligases act in a redundant manner making it impossible to pinpoint the relative contribution of a specific ligase to MYC's transcriptional output.
When this project was initiated, the ubiquitin acceptor sites in MYC were not yet identified. Moreover, for other substrates it has been shown that multiple lysine residues can act as redundant ubiquitin acceptor sites (Hou et al., 1994; King et al., 1996).
To this end, a non-ubiquitinatable MYC mutant was generated (K-less MYC), in which all lysine residues are mutated to arginine residues, which maintain the positive charge but do not provide a free amino group for ubiquitin conjugation.
K-less MYC was used as a tool to investigate the direct impact of ubiquitination on the function and activity of MYC. Nevertheless, it is important to note that lysine residues do

not solely serve as acceptor sites for ubiquitin but also for other posttranslational modifications including acetylation and sumoylation. Therefore, analyzing K-less MYC might produce a mixed picture of effects generated by the absence of ubiquitination but also by the absence of other posttranslational modifications. Consequently, it is important to validate potential results for K-less MYC with methods that specifically probe ubiquitination such as proteasomal inhibition or depletion of ubiquitin ligases.

The replacement of ubiquitin-acceptor sides in K-less abolished basal ubiquitination of MYC as shown in an *in vivo* ubiquitination assay (Fig. 4.1 D).

Previously, it has been shown that K-less MYC can be ubiquitinated at its amino-terminus when ubiquitin ligases are ectopically expressed (Popov et al., 2010). Under physiological conditions, the native amino-terminus of MYC starts with a methionine followed by a proline. The methionine is most likely removed by aminopeptidases, leaving the proline as the amino-terminal amino acid being suboptimal for N-terminal ubiquitination (Meinnel et al., 2005). Therefore, no ubiquitin chain could be detected by *in vivo* ubiquitination assays in the absence of ectopic ubiquitin ligases.

5.2.1 K-less MYC retains basic functionality

MYC contains 25 lysines, which have been replaced by arginine residues in K-less MYC. To rule out adverse effects of these mutations, biochemical properties of K-less MYC were compared to WT MYC. Co-immunoprecipitation experiments showed that neither MYC's ability to bind to its interaction partner MAX nor its interaction with MIZ1 was affected (Fig. 4.2). Moreover, K-less MYC showed a subcellular localization and chromatin binding that resembled the WT protein (Fig. 4.3).

Importantly, K-less MYC was able to activate a synthetic canonical E-box reporter as efficiently as WT MYC (Fig. 4.4).

These results demonstrate that mutation of lysine to arginine residues do not affect basic structural and biochemical properties of MYC. Additionally it shows that K-less MYC does bind to DNA and is able to activate transcription, at least from episomal DNA templates.

5.2.2 K-less MYC is a stable protein

Since MYC is a short-lived protein that is rapidly turned over by the ubiquitin-proteasome system, mutation of the ubiquitin-acceptor sites should result in a more stable protein.

Indeed, steady-state level of WT and K-less MYC proteins substantially differed when they were stably expressed in immortalized breast epithelial cells (IMECs). Treatment with the proteasome inhibitor MG132 equalized WT and K-less MYC protein level, indicating that K-less MYC is impaired in proteasomal degradation. Consistently, K-less MYC had a 4-fold longer protein half-life compared to WT MYC as determined by cycloheximide decay assays, showing that turnover of MYC is primarily mediated by lysine ubiquitination. Notably, K-less MYC was still detectably turned over and treatment with MG132 completely stabilized the protein (Fig. 4.5). Several pathways could account for the residual proteasomal degradation of K-less MYC.

First, MYC harbors a central PEST sequence and a D-element. Both elements enhance MYC turnover without affecting its ubiquitination status (Gregory and Hann, 2000; Herbst et al., 2004). This suggests that the remaining proteasomal turnover of K-less MYC occurs via these domains and is mediated independently of ubiquitination. Indeed, several proteins are known to be degraded by the proteasome in a ubiquitin-independent manner. For example, ornithine carboxylase (ODC) is degraded by the proteasome without being ubiquitinated (Murakami et al., 1992; Rosenberg-Hasson et al., 1989). The cell-cycle inhibitor $p21^{Cip1}$ can be degraded in a ubiquitin-dependent and -independent manner, showing that a single protein may be targeted by different degrading pathways (Lu and Hunter, 2010; Sheaff et al., 2000).

Second, in some cases, atypical ubiquitination can occur when ubiquitin is conjugated to cysteine residues via a thioester bond or to serine and threonine residues via an ester bond. For example, the N-terminal fragment of the cleaved pro-apoptotic protein BID (BH3 interacting-domain death agonist) is ubiquitinated on cysteine, serine and threonine residues (Tait et al., 2007). While ubiquitination at serine or threonine residues of K-less MYC should be detected in the *in vivo* ubiquitination assay, ubiquitination at cysteine residues cannot be ruled out. The thioester bond is sensitive to DTT, which is included in the sample buffer for SDS-PAGE.

Additionally, if the N-terminal methionine is not cleaved off by aminopeptidases, ubiquitination of the α-amino group of the methionine in K-less MYC could occur. N-terminal ubiquitination of K-less MYC was observed upon overexpression of E3 ubiquitin ligases and therefore may be relevant in some *in vivo* contexts (Popov et al., 2010). The absence of a detectable ubiquitin chain in the *in vivo* ubiquitination assay might be due to limitations in detection sensitivity.

Thus, with the absence of detectable ubiquitination, an increased stability but correct localization and association with crucial interaction partners, K-less MYC is a useful tool to study the impact of lysine modifications on MYC function.

5.2.3 K-less MYC fails to promote proliferation and apoptosis

To investigate the biological importance of lysine residues on MYC function, cell lines were generated that stably express WT or K-less MYC. In the immortalized mammary epithelial cell line MCF10A, ectopic expression of MYC induced apoptosis (Fig. 4.7) (Wiese et al., 2015). MCF10A cells harbor a MYC amplification and therefore express endogenous MYC at levels comparable to the transformed cell line U2OS (Fig. 4.6). Additional expression of WT MYC resulted in an apoptotic phenotype documented by changes in cell morphology and detection of cleaved PARP. Expression of K-less MYC in MCF10A cells did not result in induction of apoptosis and the cells (Fig. 4.7). Since MYC-mediated apoptosis induction in MCF10A cells is dependent on repression by MYC/MIZ1 (Wiese et al., 2015), this points to an additional role of MYC ubiquitination in repression. As direct repression by MYC was not observed in IMECs (Fig. 4.13 C), this work focused on the connection between MYC's transactivating functions and MYC ubiquitination.

Ectopic expression of MYC induces proliferation in the immortalized mammary epithelial cell line IMECs, in which the endogenous MYC level is very low (Cowling et al., 2007). Interestingly, K-less MYC did not stimulate proliferation although it was expressed at higher levels than WT MYC. This effect was documented by several assays, all yielding the same result (Fig. 4.8).

Since proliferation defects documented by a cumulative growth curve or crystal violet staining could be influenced by induction of apoptosis, the ability to stimulate proliferation was analyzed in a more direct way by measuring BrdU incorporation. While induction of WT MYC stimulated S-phase entry in the absence of growth factors in IMECs, K-less MYC was clearly impaired in promoting the entry into S-phase (Fig. 4.9).

Therefore, lysine residues in MYC are important for MYC-induced phenotypes in mammary epithelial cells.

5.2.4 K-less MYC binds to MYC-regulated promoters but poorly regulates transcription

Ubiquitination of a transcription factor can affect its functionality in multiple ways. As mentioned previously, ubiquitination can help to recruit activators to specific promoters or it can mediate the opposite effect and help to extract activators from chromatin (see 1.2.4). To this end, it was investigated whether K-less MYC is present at known MYC-regulated promoters.

In ChIP experiments, K-less MYC was detectable at known MYC binding sites but with a lower enrichment compared to WT MYC. Global analysis by ChIP-Seq confirmed this observation. However, K-less MYC could not be detected at promoters where WT MYC did not bind. Instead, K-less MYC was present at the same sites as WT MYC but with a decreased binding intensity (Fig. 4.10).

A likely explanation for the apparent weaker binding of K-less MYC is a lower cross-linking efficiency of K-less MYC to DNA. During the ChIP procedure, proteins are cross-linked to DNA by formaldehyde. Cells are incubated with formaldehyde for 15 min, a short time when preferentially free amino groups of lysine residues are used for the cross-linking reaction (Toews et al., 2008). Therefore, the mutations from lysine to arginine residues in K-less MYC do not only abolish a potential ubiquitination site but also impair the ability to cross-link MYC to DNA. This suggests that K-less MYC is actually present at known MYC-binding sites but cannot be cross-linked as efficiently to DNA as WT MYC. During the ChIP procedure, nuclei are lysed with a SDS-containing lysis buffer and the chromatin is intensively sonified. Under these conditions, protein-DNA interactions, which are not fixed by formaldehyde, are lost, and consequently, this would result in a weak ChIP efficiency as observed for K-less MYC.

The ChIP-Seq results alone cannot rule out that ubiquitination of MYC is involved in defining a binding site specificity of MYC. If ubiquitination helps to recruit MYC to promoters, K-less MYC could be unspecifically distributed along the chromatin and this would not result in a significant enrichment of K-less MYC at these sites.

Therefore, it was investigated whether K-less MYC is present at MYC-regulated promoters but not efficiently cross-linked. To this end, a native ChIP was performed, where the proteins are not cross-linked to DNA by formaldehyde and the DNA is fragmented by MNase treatment instead of sonication. Indeed, under these native conditions, K-less MYC bound to the *GNL3* promoter equally well as WT MYC (Fig. 4.11). In agreement with the native ChIP, K-less displaced the E-box binding protein MXD6 from the *GNL3* promoter as efficiently as WT MYC (Fig. 4.12). Although K-less MYC was present at the *GNL3* promoter, it was incapable of inducing *GNL3* mRNA expression, suggesting that K-less MYC fails to promote a step in transcriptional activation subsequent to chromatin recruitment.

In line with these experiments, reconstitution of lysine residues increased the ability to detect MYC binding at promoters and the detected binding increased with the number of reconstituted lysines (Fig. 4.12). Importantly, this was not correlated with the ability to induce gene expression since both mutants, either containing the seven N-terminal or the 18 C-terminal lysines, were able to induce MYC target gene expression (Fig. 4.17).

These experiments support the hypothesis that K-less MYC is present at known MYC-bound promoters and that lysine modifications are dispensable for MYC binding to its target sites.

MYC is a transcriptional regulator that mediates biological processes by modulating expression of multiple target genes. It was previously shown that ubiquitination of MYC by specific E3 ligases stimulates its transcriptional activity (Adhikary et al., 2005; Kim et al., 2003; Lehr et al., 2003). Therefore, it was likely that the inability of K-less MYC to stimulate MYC-mediated phenotypes was due to a weaker transcriptional regulation of MYC target genes. This was already indicated by its inability to induce *GNL3* mRNA expression (Fig. 4.11).

Global gene expression profiles of WT and K-less MYC were compared in IMECs stably expressing Dox-inducible MYC and vector-expressing cells as a control.

The gene expression profiles revealed that K-less is a weaker transcriptional activator. Dox alone did not influence gene activation since no induction was observed in vector-expressing cells (Fig. 4.13). Gene set enrichment analysis showed that a MYC-specific signature was the best enriched signature for both WT and K-less MYC, demonstrating that K-less MYC regulates the same set of genes as WT MYC, albeit to a lesser extent, as shown by the lower normalized enrichment score (NES) (Fig. 4.14).

These data confirm the importance of lysine residues on MYC transcriptional activity at a post-DNA binding step.

5.3 MYC function can be mediated by diverse ubiquitin acceptor sites

The previous results indicate that lysine residues in MYC are important for its transcriptional activity. To investigate whether lysines need to be present at a certain position in MYC, two MYC mutants were generated either harboring the seven N-terminal lysines (WT_N-K_C) or the eighteen C-terminal lysines (-$K_N WT_C$). Importantly, these two MYC mutants do not have any common lysines (Fig. 4.15). Both mutants are efficiently ubiquitinated, confirming that several lysines in MYC can function as ubiquitin acceptor sites. Accordingly, restoration of these lysine resulted in the same turnover rate as observed for WT MYC (Fig. 4.16).

WT_N-K_C MYC was similar to WT MYC in terms of transcriptional activity and downstream cellular phenotypes suggesting that the seven N-terminal lysines are sufficient for MYC activity. Reconstitution of the eighteen C-terminal lysines could also rescue the proliferation phenotype and transcriptional activity of MYC (Fig. 4.17), indicating that ubiquitin acceptor sites in MYC are redundant. This goes in line with the observation that several ubiquitin ligases targeting MYC have binding sites in the N- and C-terminal part of the protein, suggesting that they can target lysines in different positions (see Fig. 1.4).

Zhang *et al.* reported that ubiquitination of MYC within the TRD by the ubiquitin ligase SCF-SKP2 is critical for canonical target gene induction and transformation. Blockage of this ubiquitination via binding of the tumor suppressor protein ARF to the TRD resulted in induction of apoptosis (Zhang et al., 2013). Zhang *et al.* used a MYC mutant, in which the six N-terminal lysines were mutated to arginine (MYC^{N6KR}), generating a protein that is similar to -$K_N WT_C$ MYC. In contrast to our study, the Zhang mutant was substantially more stable than WT MYC and unable to induce E-box containing canonical target genes. To determine protein stability, Zhang *et al*. performed cycloheximide assays with transfected Cos7 cells (Zhang et al., 2013). Already WT MYC, with a half-life of 63 min, was more stable compared to the assessed WT MYC protein half-life in this study. By transient overexpression, it is conceivable that the E3 ligases degrading MYC become limiting. Moreover, in Cos7 cells, the expression of MYC-targeting E3 ligases might be different to IMECs, which would also result in a different turnover. A differential expression of C-terminal targeting ligases could explain why the Zhang mutant MYC^{N6KR} is more stable than WT MYC but -$K_N WT_C$ MYC in IMECs has the same half-life.

Three of the seven N-terminal lysines of WT_N-K_C MYC (K52, K148, K157) were identified as ubiquitin acceptors (Fig. 1 C) (Kim et al., 2011). K148 and K157 were also reported to be acetylated (Zhang et al., 2005). It is a common observation that ubiquitination and acetylation sites overlap and that there is a cross-talk between ubiquitination and other posttranslational modifications (Danielsen et al., 2011). In several cases, acetylation of a known ubiquitination site stabilizes the target protein (Caron et al., 2005; Grönroos et al., 2002). However, the exact opposite effect was also described and acetylation accelerated protein turnover (Caron et al., 2005). As mentioned previously, MYC acetylation can have opposite effects on its stability (see 1.3.3.2.1), highlighting the complexity of lysine modifications.

To preferably study effects of lysine ubiquitination on MYC-mediated phenotypes and transcriptional activity, the role of K52, one of the identified ubiquitination sites that is not acetylated, was investigated. *In vivo* ubiquitination assays confirmed that K52 is efficiently ubiquitinated and the reconstitution of K52 as a single ubiquitin acceptor site substantially rescued MYC turnover. This suggests that ubiquitination at K52 can mediate efficient proteasomal turnover of the protein (Fig. 4.18). Furthermore, reconstituting K52 largely rescued induction of proliferation and target genes in IMECs, highlighting that a single ubiquitin acceptor site of MYC can mediate MYC function (Fig 4.19). Importantly, in agreement with the published observation that K52 was not identified as an acetylation site, there was no evidence that K52o MYC is acetylated (Wenshan Xu, personal communication). This suggests that K52o is an efficient ubiquitin acceptor but not an acetylation site. Thus, the rescue effects by the single K52o MYC are most likely not due to acetylation of this mutant.

To further strengthen this point and to support the idea that the rescue effect of K52o MYC is independent of acetylation, an acetylation-mimicking mutant could be investigated. To mimic acetylation, lysine residues are often mutated to glutamine (Wang and Hayes, 2008). Thus, if the mutant does not rescue it would suggest that acetylation at this specific site is not important for MYC’s function.

In contrast to the ubiquitin-conjugation cascade with around 40 E2 conjugating enzymes, the SUMO conjugation cascade relies on a single E2 conjugating enzyme, UBC9 (Gareau and Lima, 2010). Consequently, depletion of UBC9 by siRNA blocks sumoylation. Although the biological effect is unclear, MYC was reported to be sumoylated (see 1.3.3.2.2). Importantly, depletion of UBC9 did not inhibit MYC target gene induction arguing that the absence of sumoylation in K-less MYC is not responsible for its inability to induce target gene expression (data not shown).

Collectively, these data demonstrate a close correlation between proteasomal turnover and transcriptional activity of MYC, suggesting that the absence of ubiquitination sites in K-less MYC is responsible for its inability to induce target gene expression.

5.4 Proteasomal activity is required for MYC target gene induction

5.4.1 MYC targeting ubiquitin ligases might have redundant roles

In line with previous publications, the results presented here suggest that ubiquitination of MYC is crucial for its function.

To further support this hypothesis, the effect of depleting MYC-targeting ubiquitin ligases was analyzed. The ubiquitin ligase SCF-SKP2 was previously reported to promote MYC turnover and to stimulate MYC transcriptional activity (Kim et al., 2003; Lehr et al., 2003; Zhang et al., 2013). FBW7 binds to a phosphodegron in MBI of MYC and is one of best-studied ubiquitin ligases targeting MYC for proteasomal degradation (Welcker et al., 2004b). Both ligases were previously detected at MYC regulated promoters, suggesting that chromatin-bound MYC can be ubiquitinated by these ligases (Farrell et al., 2013; Lehr et al., 2003).

Thus, the effects of these two ubiquitin ligases on MYC's activity were analyzed. Depletion of FBW7 had only very mild effects, whereas depletion of SKP2 led to a reduced activation of several tested MYC target genes (Fig. 4.20). This confirms the previously published results that SKP2 stimulates MYC transcriptional activity. However, depletion of *SKP2* did not globally influence MYC target gene induction (Fig. 4.21), suggesting that the effect of SKP2 is specific for a subset of MYC target genes and different ubiquitin ligases may have redundant roles in controlling MYC ubiquitination at target gene promoters.

Neither the depletion of FBW7 nor SKP2 depletion affected MYC protein level (Fig. 4.20). This further supports the hypothesis that different MYC-targeting ubiquitin ligases can redundantly control MYC turnover and activity.

Several previous reports further support the idea that SKP2 is not the only ubiquitin ligase required for MYC activity. First, while a *Myc* knockout is embryonically lethal, *Skp2* knockout mice are viable. *Skp2*$^{-/-}$ mice are smaller than their WT littermates and contain cells with enlarged nuclei and multiple centrosomes (Nakayama et al., 2000). Importantly, a critical substrate of SKP2 is p27^{Kip1}, a negative cell cycle regulator, which is upregulated in *Skp2*$^{-/-}$ mice. *Skp2*$^{-/-}$ phenotypes are not manifested in the *Skp2*/*p27*^{Kip1} double knockout mice suggesting that p27^{Kip1} is the critical target of SKP2 (Nakayama et al., 2004; Zhu, 2010). Consindering the very different phenotypes of *Myc* and *Skp2* knockout mice, it is unlikely that MYC activity is solely dependent on the presence of SKP2 (Jin and Harper, 2003). Furthermore, loss of *Skp2* had only modest effects on MYC-induced proliferation and tumorigenesis in a Eμ-*MYC* transgenic mouse model (Old et al., 2010). Thus, additional ubiquitin ligases could compensate for the loss of SKP2 in stimulating MYC activity.

5.4.2 Proteasomal inhibition abolishes MYC transcriptional activity

For several transcription factors it has been shown that ubiquitination is required for their transcriptional activity. While the ubiquitination itself is sufficient for some transcription factors to enhance their activity, others require proteasomal turnover for full transcriptional activity (see 1.2.3).

Salghetti *et al*. investigated how ubiquitination within the transactivation domain (TAD) of VP16 affects its activity. The VP16 TAD requires ubiquitination by the E3 ligase Met30 for its function. The requirement for ubiquitination by Met30 could be circumvented by a fusion of ubiquitin to the amino terminus of VP16. The Ub-VP16 fusion protein was fully active even in a Met30 knockout background but was not degraded by the proteasome. This suggests that under these circumstances ubiquitination has a function independent of proteasomal degradation (Salghetti et al., 2001).

On the other hand, other transcription factors do not only require ubiquitination but also proteasomal degradation for their function. The E3 ligase complex SCF-CDC4 ubiquitinates the yeast transcription factor Gcn4 leading to its proteasomal degradation. Lipford et al. showed that proteasomal turnover is required for Gcn4 activity. Treatment of cells with the proteasome inhibitor MG132 or mutation in ubiquitin (K48R) that prevented formation of K48-linked degrading ubiquitin chains reduced Gcn4 transcriptional activity. Moreover, mutations of the kinases that generate the phosphodegron recognized by SCF-CDC4 or deletion of the E3 ligase itself compromised Gcn4 activity (Lipford et al., 2005).

To investigate whether ubiquitination *per se* or proteasomal turnover is required for MYC transcriptional activity, linear fusions of non-removable ubiquitin to the amino-terminus of K-less MYC were generated. However, the fusion of WT ubiquitin to K-less MYC was unstable and could not be expressed. When ubiquitin in which all lysines were mutated to arginine residues (K0) was fused to K-less MYC, the fusion protein was expressed but did not to rescue the proliferation defect of K-less MYC (data not shown), and did not allow straightforward interpretation of the data. It may suggest that MYC needs to be modified with a ubiquitin chain and monoubiquitination is not sufficient for MYC function. Alternatively, ubiquitination at a specific acceptor site may be required, although the fact that reconstitution of lysines in completely different regions in MYC (see 4.6.1) could rescue the proliferation defect would argue against this possibility. Fusion of ubiquitin bearing a K48R mutation could potentially address this question but the use of ubiquitin mutants in the mammalian system is difficult since the abundant endogenous ubiquitin may promote the assembly of different (undesired) ubiquitin chains. Furthermore, ubiquitin chains linked via lysines other than K48 promote proteasomal degradation, which would confound the interpretation (Kirkpatrick et al., 2006).

Consequently, the effect of proteasomal inhibition on MYC activity was investigated. While proteasomal inhibition did not influence binding of MYC to target gene promoters, target gene induction was strongly impaired (Fig. 4.22 and 4.23). Global analysis by RNA-Seq confirmed that proteasomal activity is required for induction of MYC target genes.

It would be interesting to analyze, whether ubiquitinated MYC accumulates at MYC-regulated promoters after proteasomal inhibition. This would suggest that ubiquitination *per se* is not required for MYC activity but the turnover at the promoter is the important mechanism. No accumulation of MYC after MG132 treatment could be detected, which raises the question whether turnover of MYC actually occurs at promoters. Notwithstanding, it cannot be excluded that the analyzed sites are already saturated and therefore no additional MYC-binding could be observed after proteasomal inhibition.

Ubiquitin ligases targeting MYC as well as proteasomal subunits were detected at MYC-regulated promoters in a MYC-dependent manner, indicating that turnover of MYC can indeed take place at promoters (Farrell et al., 2013; Lehr et al., 2003).

To experimentally investigate whether ubiquitinated MYC is present at promoters, sequential ChIP experiment could be performed. To this end, cells would be treated with MG132 and the lysis buffer would be supplemented with the alkylating reagent N-ethylmaleimide (NEM) to inhibit activity of deubiquitinating enzymes. MYC would be immunoprecipitated according to the standard ChIP protocol with an antibody recognizing the C-terminal HA-tag followed by an elution step with a peptide. This eluate would be used for a second IP to precipitate specifically ubiquitinated proteins using for instance MultiDsk, a ubiquitin-specific affinity resin, or TUBE (tandem-repeated ubiquitin-binding entities) (Hjerpe et al., 2009; Wilson et al., 2012). However, in a ChIP experiment, DNA fragments, where the protein of interest binds to, are precipitated and analyzed. This implies that as soon as other ubiquitinated proteins are bound to the same DNA-fragment as MYC, ubiquitinated histones for example, they would be immunoprecipitated and could result in a misleading interpretation of the experiment. Generating an antibody specifically recognizing ubiquitinated MYC could circumvent this problem. To this end, a MYC peptide would be synthesized and used as an immunogen that is branched with the last ubiquitin amino acids at the site where MYC is ubiquitinated, for example at K52. This approach was used for the generation of antibodies specific for ubiquitinated H2B (Minsky et al., 2008).

Since proteasome inhibition abrogated MYC target gene induction, it is likely that turnover of MYC at its promoters is needed for its transcriptional activity. To experimentally support this suggestion, a K-less MYC version was generated, whose proteasomal degradation can be induced with the auxin-inducible degradation (AID) system. In this system, degradation of an AID-tagged protein can be induced by administration of the plant hormone auxin (Holland et al., 2012; Nishimura et al., 2009).

To this end, a stable IMEC cell line was generated expressing the plant F-box protein TIR1, which can be incorporated into the human SCF complex, and MYC with an AID at its C-terminus. Administration of auxin to the cell culture medium enables the recognition of the AID by TIR1, leads to polyubiquitination of the degron and subsequent proteasomal degradation (Nishimura et al., 2009). If the inducible degradation of K-less MYC rescues target gene induction, it would demonstrate that proteasomal turnover of MYC is required for its activity. Unfortunately, even in the absence of auxin the K-less-AID fusion protein was unstable and it was not possible to express the fusion protein to the same level as WT MYC. The AID-tag contains several lysine residues thus it is likely that these introduced lysines lead to turnover of K-less MYC even in the absence of auxin.

5.5 K-less MYC is impaired in promoting efficient elongation

The previous results show that K-less MYC is impaired in transcriptional activation and suggest that MYC-mediated transcription requires proteasomal activity. Therefore we aimed to pinpoint the step in MYC-mediated transcription, which requires turnover.

As mentioned previously, MYC stimulates transcription by the recruitment of RNAPII to promoters but also by increasing the rate of transcription initiation and elongation (see. 1.3.2.1). To understand whether WT and K-less MYC act differently at one of these steps, ChIP-Seq experiments were performed for total RNAPII, the initiating Ser5p RNAPII and elongating Ser2p RNAPII after 4 h of WT or K-less MYC induction.

Analyzing the effects of MYC activation at the promoters of all genes, no change in total, initiating or elongating polymerase could be observed, indicating that MYC does not globally lead to enhanced stimulation of initiation or elongation in this cellular system (Fig. 4.25).

Filtering the genes for MYC bound and activated genes, WT and K-less MYC stimulated the recruitment of RNAPII to MYC-regulated promoters (Fig. 4.26). Since no difference was observed at all genes, the changes at MYC-regulated promoters are indeed due to direct effects by MYC. Strikingly, while activation of WT MYC also led to an increase of total RNAPII within the gene body and at the end of the gene, activation of K-less MYC resulted solely in an increase of RNAPII at the TSS, suggesting that the release of elongating RNAPII is impaired. This is further supported by the effect of MYC activation on Ser5p and Ser2p RNAPII. WT and K-less MYC both stimulated transcription initiation but only WT MYC expression increased the density of elongating polymerase in the gene body and TES (Fig. 4.27 and 4.28). The fact that Ser5p RNAPII was increased at the TSS by both WT and K-less MYC expression but only WT MYC increased Ser5p RNAPII in the gene body is a good internal quantitative control of the experiment. It demonstrates that the differences observed in the gene body are not due to ChIP-to-ChIP variations since this would lead to a global difference of the signal. Thus, the results suggest that RNAPII is not released from the promoter in K-less MYC expressing cells.

It can be concluded that recruitment of RNAPII and transcription initiation do not depend on ubiquitination of MYC. In contrast, the transition to efficient elongation requires the presence of lysine residues and most likely the turnover of MYC. Thus, the defect of K-

less MYC to activate gene expression is due to a block in transcriptional elongation, resulting in an accumulation of Ser5p RNAPII at the TSS (Fig. 4.28 C).
Several connections between the ubiquitin-proteasome system and transcription elongation have been described (see 1.2.2). In particular, the 19S particle of the proteasome stimulates elongation for example by reducing the nucleosome density. However, since 19S does not possess the catalytic activity of the proteasome, these effects were independent of proteasomal activity (Chaves et al., 2010; Ferdous et al., 2001; 2002). In contrast to these studies, MYC transcriptional activity was abrogated upon proteasome inhibition (Fig. 4.23). Thus, it is unlikely that the absence of the 19S proteasome subunit accounts for the defect in transcriptional elongation in K-less MYC-expressing cells. Observations that the recruitment of proteasome subunits can be mediated by H2B ubiquitination or by interaction with the H4 tail argues against a scenario in which K-less MYC is defective in recruiting the proteasome to promoters (Chaves et al., 2010; Ezhkova and Tansey, 2004; Geng and Tansey, 2012).
Interestingly, in 2005 a study from the Tansey lab described a connection between ubiquitination-dependent turnover of the inducible yeast transcription factor Gal4 and the transcription cycle. Degradation of the transcriptionally active Gal4 is mediated by F-box protein Dsg1 and this turnover is required for productive transcription. More precisely, the Gal4 ubiquitination was specifically required for the phosphorylation of RNAPII at Ser5, which was reduced in Δ*dsg1* strains due to a defect in recruitment of the corresponding kinase (Bur1) to the promoter. The authors concluded that RNAPII recruitment occurs independently of Gal4 ubiquitination and Gal4 turnover is required to disassemble the initiation-competent RNAPII complexes to allow kinases and the RNA processing machinery to associate with the transcribing RNAPII (Muratani et al., 2005). This was one of the first studies to identify the step in the transcription cycle that requires turnover of an activator. This study shows some parallels but also several differences with the effects observed with K-less MYC. While in both studies recruitment of the RNAPII is unaffected or only marginally reduced, K-less MYC is proficient in mediating Ser5 phosphorylation while a Δ*dsg1* strains is impaired in this transcriptional step. Moreover, in K-less MYC-expressing cells RNAPII is poorly released from the promoter and consequently no increase of total RNAPII or Ser5- and Ser2-phosphorylated RNAPII could be detected within the gene body and TES after K-less MYC induction. In a Δ*dsg1* strains, the

polymerase continues transcribing the transcript, generating a full-length RNA, which is not translated due to impaired Ser5 phosphorylation of RNAPII (Muratani et al., 2005).
In contrast, K-less MYC is clearly impaired in induction of mRNAs transcription (see 4.5). The ability of K-less MYC to promote Ser5 phosphorylation, a modification that stimulates the recruitment of the 5'end capping machinery, suggests that the nascent transcripts are capped. Since defects in Ser2 phosphorylation of RNAPII were observed after K-less MYC induction, it is possible that polyadenylation of the transcript is affected. Since K-less MYC cells are impaired in releasing RNAPII, it is likely that short, capped nascent transcripts are synthesized but no further transcription is taking place. It would be interesting to analyze, whether these transcripts are detectable in K-less MYC expressing cells.
Considering both studies it shows that ubiquitination of a transcriptional activator can affect different steps in the transcription cycle.
An increase of total and Ser2p RNAPII in the gene body and TES after WT MYC induction can be interpreted in two different ways. First, the released polymerases are transcribing slower through the gene resulting in an accumulation within the gene body and TES. Second, the higher RNAPII density is due to an enhanced release of RNAPII from the TSS, which would be in line with the observed induction of gene expression. With the static ChIP-Seq data presented in this study, it is not possible to draw any conclusion about the speed of the polymerase. Moreover, it is still under debate what is the rate-limiting step in the transcription cycle and whether gene expression can be regulated at the level of pause release (Ehrensberger et al., 2013). Thus, from the RNAPII sequencing data it cannot be concluded, which MYC-dependent step of the transcription cycle is rate limiting.
To this end, it would be necessary to investigate whether and how MYC activation influences the speed of elongating polymerase. This could be performed with a DRB/GRO-Seq experiment. Here, cells are treated with 5,6-dichloro-1-β-D-ribofuranosylbenzimidazole (DRB), a reversible inhibitor of P-TEFb activity. Treatment with DRB results in a loss of SPT5 and RNAPII Ser2 phosphorylation and thus inhibits the progression of the initiated RNAPII to productive elongation, leading to a synchronization of the transcription cycle (Saponaro et al., 2014). After inhibitor removal, RNAPII is released and can resume elongation. By using DRB-treatment in combination with global run-on sequencing (GRO-Seq), a method that labels newly synthesized RNAs with

bromouridine-triphosphate (BrUTP), the position of RNAPII in the gene body can be analyzed. Labeling of nascent transcripts at different time points after DRB release allows assessing the speed of the elongating RNAPII (Saponaro et al., 2014).

Nevertheless, the increased RNAPII density after WT MYC induction in the gene body was observed at activated MYC target genes. Thus, the RNAPII sequencing data in combination with the results from the RNA-Seq suggest that WT but not K-less MYC expression stimulates efficient elongation.

5.6 Ubiquitination of MYC is required for cofactor recruitment

In order to further characterize the steps in MYC-dependent transcriptional activation, which depend on ubiquitination, MYC-induced histone acetylation was investigated. While WT MYC induced acetylation of histone H3 and H4 at the *GNL3* promoter, K-less MYC was impaired in this process (Fig. 4.29). One explanation of the inability to induce histone acetylation could be an impaired recruitment of HATs to MYC-regulated promoters.

Several histone acetyltransferases are known to interact with MYC; one of them is GCN5, a component of the STAGA complex (SPT3/TAF9/GCN5 acetyltransferase complex) (Liu et al., 2003; McMahon et al., 2000). If the recruitment of this HAT is dependent on ubiquitinated MYC, it is likely that a component of the STAGA complex possesses an ubiquitin-binding domain. Interestingly, the STAGA complex contains a so-called deubiquitinating module (DUB module) consisting of several proteins including the deubiquitinating enzyme USP22 (Zhao et al., 2008b). USP22 deubiquitinates histone H2A and H2B and is required for MYC transactivation activity (Zhang et al., 2008; Zhao et al., 2008b). Moreover, in yeast it has been reported that Ubp8 (the USP22 orthologue) mediated deubiquitination of H2B is required for Ser2 phosphorylation of RNAPII (Wyce et al., 2007). Thus, the STAGA complex was an interesting candidate to study. However, in IMECs, USP22 was not detected at MYC-regulated promoters; neither did USP22 depletion have a consistent effect on MYC target gene induction (data not shown). Moreover, depletion of GCN5 had only subtle effects on MYC target gene induction, suggesting that HATs might act redundantly during transactivation by MYC (data not shown).

It was previously described that the recruitment of p300 to MYC target gene promoters is stimulated by ubiquitinated MYC (Adhikary et al., 2005; Cepeda et al., 2013). Therefore, p300 recruitment by K-less MYC might be impaired. Another possibility is that turnover of MYC might help to displace histone deacetylases from promoters. In line with this idea, MYC was shown to bind several HDACs (Kurland and Tansey, 2008). On the other hand, MYC might recruit HUWE1 to promoters, which degrades HDAC2 (Zhang et al., 2011).

Alternatively, turnover of MYC might be required for the efficient recruitment of HATs to target gene promoters. This mechanism has been previously described for the estrogen receptor (ER). ER-mediated transactivation requires continuous cycling of the ER on the promoter to recruit cofactors including HATs and the cycling is mediated by proteasomal turnover of the ER (Métivier et al., 2003; Reid et al., 2003). This would indicate that continuous turnover of MYC on the promoter maintains the cycling and enables productive recruitment of HATs. It is also possible that ubiquitin-dependent recruitment and degradation are interdependent. In this scenario, ubiquitination would first help to recruit HATs to promoters and then subsequently lead to proteasomal degradation to maintain the cycling.

In line with this model, a previous study reported that MYC cycles at promoters in a proteasome- and PIN1-dependent manner (Farrell et al., 2013). MYC phosphorylated at Ser62 is isomerized by PIN1, facilitating FBW7-mediated degradation. Farrell *et al.* demonstrated that PIN1 enhances recruitment of Ser62-phosphorylated MYC to target gene promoters, which is associated with its subsequent degradation. They suggested that the dynamic MYC binding to promoters is associated with enhanced recruitment of cofactors including HATs and thus contributing to MYC target gene induction (Farrell et al., 2013).

To experimentally test whether proteasomal turnover of MYC is required for induction of histone acetylation, ChIP experiments after proteasomal inhibition with MG132 could be performed. Under MG132 treatment, WT MYC should be impaired in inducing histone acetylation and mimic the K-less situation, where no induction of histone acetylation could be detected. Concomitantly, recruitment of BRD4 by K-less MYC induction was also impaired (Fig. 4.20).

BRD4 is important to regulate the activity of P-TEFb, which is kept in an inactive complex containing the kinase inhibitor HEXIM, the 7SK small nuclear RNA and two auxiliary proteins LARP7 and MePCE (Chen et al., 2014). BRD4 releases P-TEFb from the repressive complex and recruits it to promoters (Jang et al., 2005; Yang et al., 2005; Zhou and Yik, 2006). Thus, the inability of K-less MYC to induce histone acetylation might block this whole cascade, resulting in an impaired recruitment of P-TEFb (with its kinase subunit CDK9) to promoters and compromising the release of paused polymerase (Fig. 4.20 and 5.1). Consequently, proteasome inhibition would lead to decreased histone acetylation, preventing BRD4 and CDK9 recruitment to MYC-regulated promoters. This would give one explanation why the MYC-CDK9 interaction was strongly reduced upon proteasome inhibition (Fig. 4.31 D).

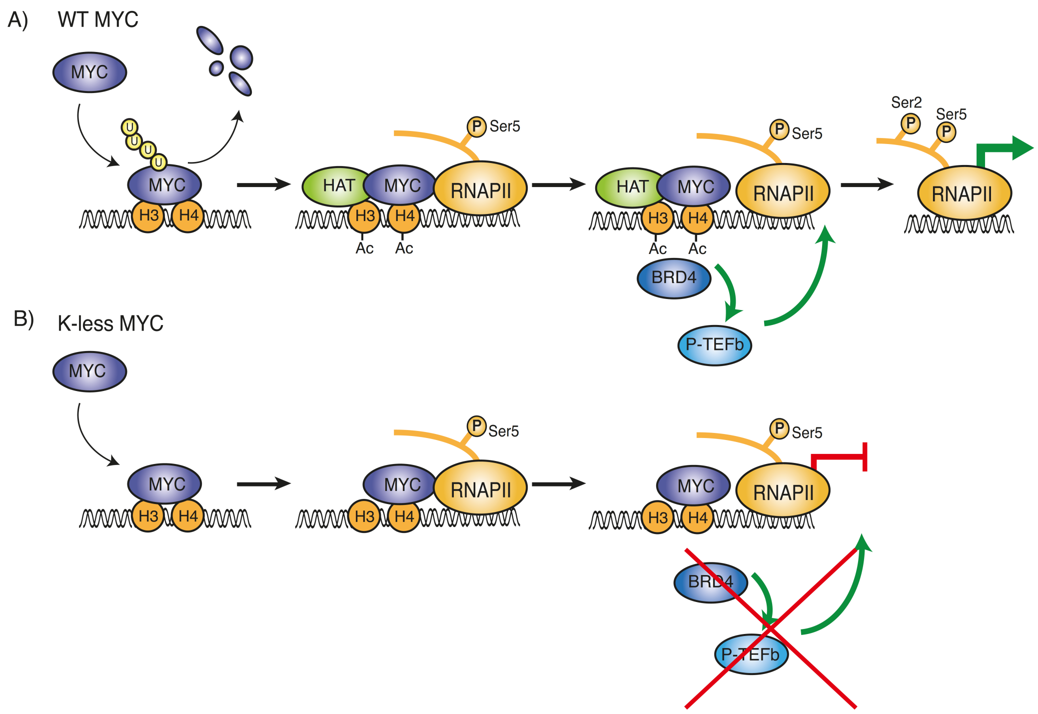

Figure 5.1: Proposed model for turnover-dependent histone acetylation and cofactor recruitment

A) Proteasome-mediated cycling of MYC at promoters might enable efficient recruitment of histone acetyltransferases (HAT) leading to increased histone acetylation and subsequent BRD4 and P-TEFb recruitment. P-TEFb phosphorylates RNAPII at Ser2, releasing elongating RNAPII.

B) K-less MYC is impaired in HAT recruitment, preventing induction of histone acetylation, BRD4 and CDK9 recruitment. Consequently, RNAPII is not released from the promoter and accumulates in a Ser5-phosphorylated state.

MYC was also suggested to directly recruit P-TEFb to promoters (Rahl et al., 2010) even though structure-function analyses using CDK9-binding deficient MYC mutants are missing.

The impaired recruitment of CDK9 to MYC-regulated promoters after K-less MYC expression can explain the effects observed on RNAPII phosphorylation and release. Interestingly, induction of K-less MYC mimics the situation when P-TEFb activity is inhibited with flavopiridol. Upon CDK9 inhibition, RNAPII is depleted from the gene body and remains associated with the promoter-proximal site (Rahl et al., 2010).

5.7 Impaired MYC turnover enables the identification of an intermediate step in MYC-dependent transcription

WT MYC induction led to a significant increase of the total and Ser2p RNAPII density in the gene body (Fig. 4.28). However, as MYC associates with positive elongation factors, which enhance the processivity and speed of RNAPII, this may lead to an underestimation of MYC-mediated effects on RNAP Ser2p density.

MYC was shown to associate with positive elongation factors like CTR9 or CDC73, which are components of the PAF complex (Anne Carstensen, personal communication) (Dingar et al., 2015). The PAF complex is a multiprotein complex involved in transcription-coupled histone modifications and mRNA processing (Krogan et al., 2003; Zhu et al., 2005). In yeast it has been demonstrated that the PAF complex promotes H2B monoubiquitination by recruiting E2 and E3 enzymes to chromatin. H2B monoubiquitination in turn is important for recruitment of the histone chaperone FACT, which mediates efficient elongation through nucleosomes (Formosa, 2012; Tomson and Arndt, 2013).

Upon induction of WT but not K-less MYC, CTR9 accumulated at the 3'end of the MYC target gene *GNL3*, indicating that it travels with the elongating polymerase supporting efficient elongation at MYC-regulated genes (Fig. 4.31). Surprisingly, immunoprecipitation experiments did not detect an interaction between WT MYC and CTR9, whereas K-less MYC robustly bound CTR9 (Fig. 4.31 B). This result suggested that the interaction between MYC and CTR9 is very transient and is stabilized by attenuated turnover of K-less MYC. Similarly, interaction of WT MYC with CTR9 was enhanced upon proteasome inhibition. Supporting this idea, interaction with the other PAF component CDC73 and the DSIF protein SPT5 was also enhanced after proteasome inhibition (Fig 4.31). It can be speculated that MYC acts as an assembly factor; first promoting loading of RNAPII and stimulating initiation independently of proteasomal turnover, which is followed by turnover-dependent induction of histone acetylation, CDK9 recruitment and transfer of positive elongation factors onto RNAPII. Inhibition of the turnover decelerates the conveyance and enables the detection of a MYC-PAF complex most likely as an intermediate step in MYC-mediated transcription.

The PAF complex binds Ser5- and Ser2-phosphorylated RNAP CTD (Qiu et al., 2012). Notably, CDC73 and CTR9 were both identified per mass spectrometry to interact with

WT N-MYC but not with the phosphorylation mutant N-MYC T58A/S62A (Anne Carstensen, personal communication). These phosphorylation sites are located within the highly conserved MBI. Consistently, CDC73 interacted with N-MYC MBI peptide and binding was enhanced when one or both residues were phosphorylated (Fig. 4.32). Only a faint signal for CTR9 was detectable for doubly phosphorylated MBI, suggesting that other regions in MYC might be important for CTR9 binding.

```
               2   5   2   5
RNAPII CTD  YSPTSPS YSPTSPS
      MYC     LPTPPLSP
                58   62

                2   5
RNAPII CTD    YSPTSPS
      MYC    LPTPPLSP
               58   62
```

Figure 5.2: Alignment of MYC phosphorylation sites in MBI and RNAPII CTD
Upper panel shows alignment of the sequence surrounding MYC phosphorylation sites in MBI with two repeats of RNAPII CTD. Lower panel shows alignment of the sequence surrounding MYC phosphorylation sites in MBI with one repeats of RNAPII CTD. Numbers indicate amino acid position within one RNAPII CTD repeat or within MYC respectively Amino acids marked in red indicate the respective phosphorylation sites.

Interestingly, the phosphorylation sites in MBI show some homology to the RNAPII CTD spanning Ser5 and Ser2 on two adjacent heptad repeats (Fig. 5.2, upper panel) and less homology the RNAPII CTD spanning Ser5 and Ser2 on one repeat (Fig. 5.2, lower panel). It is possible that phosphorylated MBI acts as a platform to transiently recruit the PAF complex. In this model, RNAPII becomes the preferred binding partner for the PAF complex when its CTD is phosphorylated at Ser2 by P-TEFb (Figure 5.3).

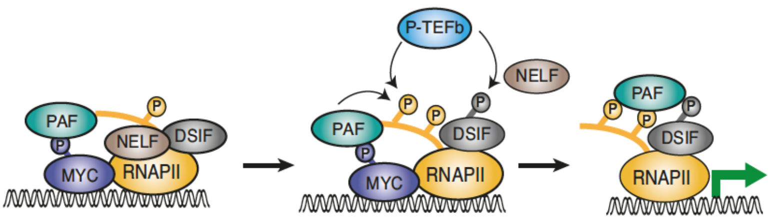

Figure 5.3: Proposed model for the transfer of the PAF complex from MYC onto RNAPII
The PAF complex binds to phosphorylated MYC. DSIF and NELF keep RNAPII in a paused state. Upon P-TEFb recruitment and phosphorylation of DISF and RNAPII, NELF dissociates, DSIF is turned into a positive elongation factor and the PAF complex is transferred onto RNAPII.

In line with this idea, K-less MYC is present in an S62-phosphorylated state, which was reported to be the active form of MYC (Fig. 4.32 C) (Farrell et al., 2013). The impaired recruitment of CDK9 in K-less expressing cells leads to a decreased phosphorylation status of RNAPII CTD, preventing the transfer of the PAF complex onto RNAPII CTD and enabling the detection of the MYC/PAF complex. DSIF acts initially as a negative elongation factor stimulating transcriptional pausing that is turned into a positive elongation factor upon phosphorylation by P-TEFb (Kwak and Lis, 2013; Yamada et al., 2006). Despite its positive role on elongation, the PAF complex was also described to block elongation at promoters of erythroid genes (Bai et al., 2010). Bai et al. suggested that PAF serves a dual function similar to DSIF, first inhibiting elongation but is converted into a positive elongation factor at later stages. Also at MYC regulated promoters the PAF complex may first support the pausing state but act as a positive elongation factor upon RNAPII Ser2 phosphorylation and transfer onto RNAPII.

One interesting question remains: Why is K-less MYC able to activate an E-box luciferase reporter but is impaired in activating endogenous MYC target genes? The firefly luciferase gene of the reporter construct is a short intronless gene. Previously, it has been reported that Ser2 phosphorylation of RNAPII by P-TEFb is not required for efficient transcription of some short intronless genes, suggesting that the impaired recruitment of CDK9 by K-less MYC might be irrelevant for reporter gene activation (Medlin et al., 2005). Moreover, since the reporter construct is not an integrated reporter and thus not properly chromatinized, transactivation could occur independently of positive elongation factors such as FACT and the PAF complex. It can be speculated that K-less MYC is able to activate the reporter construct because CDK9 recruitment and the conveyance of positive elongation factors onto RNAPII is not required.

5.8 Cancer-associated mutations stabilize MYC – how does that fit to the model?

Tumor-associated mutations in the *MYC* gene are relatively rare events. However, in Burkitt's lymphoma, point mutations in *MYC* cluster in MBI and have a stabilizing effect on the MYC protein. For example, the mutation of Thr58 to an alanine disrupts the phosphodegron recognized by FBW7, stabilizes MYC and increases its ability to drive lymphomagenesis (Hemann et al., 2005). How do tumor-associated stabilizing mutations of MYC fit to the model that proteasomal turnover of MYC is required for its transcriptional activity?

Cycloheximide decay assays used to determine MYC protein stability cannot discriminate between the turnover of MYC on target gene promoters and in different subcellular compartments. It is possible, that different pools of MYC exist, whose turnover is differentially regulated. A cancer-associated mutation, such as T58A, could inhibit FBW7-mediated degradation of MYC in the nucleolus but not the turnover at promoters mediated by different ubiquitin ligases.

Muratani et al. suggested that proteasomal turnover of different pools of the yeast transcription factor Gal4 has different outcomes. Turnover of the chromatin-associated, transcriptionally active Gal4 is required for its activity. In contrast, stabilization of the "inactive" pool has a stimulating effect by increasing the total amount of Gal4, which is available for gene activation (Muratani et al., 2005). Thus, these cancer-associated mutations in MYC could increase the overall pool of MYC available for transcription thereby enhancing its activity. In line with this hypothesis, it was shown that chromatin-associated MYC has a different half-life than the soluble MYC pool (Tworkowski et al., 2002).

Farrell *et al.* noted that, similar to non-transformed cells, MYC also dissociates from active promoters in cancer cells. However, the promoters were rapidly re-occupied by MYC, suggesting that this binding might result from the increased soluble pool of MYC, which is present in the cell (Farrell and Sears, 2014; Farrell et al., 2013).

It is tempting to speculate that MYC turnover at promoters is initially required for target gene activation but at the same time shuts off the signal preventing a continued activation of transcription. Thus, turnover might ensure that only a persistent signal, e.g. due to an increased total pool of MYC molecules, leads to a continuous gene activation.

Interestingly, the increased oncogenicity of MYC T58A in mouse models has been linked to an impaired induction of the direct MYC target gene *Bim* and compromised proapoptotic activity (Hemann et al., 2005; Muthalagu et al., 2014; Wang et al., 2011). This implies that transcriptional activity of the stabilized MYC is actually compromised. It would be interesting to analyze, whether MYC dynamics differ at distinct promoters with some requiring rapid turnover of MYC and others being not sensitive to changes in the turnover rate. Tumor cells might maintain a balance between enhanced MYC stability and an optimal rate of degradation. MYC stabilizing mutations might be compromised to an extent, which would block proapoptotic signaling, but would still allow efficient turnover at the promoter and expression of other genes required to maintain the malignant state. Here, it would be further beneficial that a T58A MYC mutant shows constitutive high S62 phosphorylation, which is the active form of MYC (Farrell et al., 2013; Sears et al., 2000).

S62-phosphorylated MYC would enhance recruitment of positive elongation factors to stimulate transcription of these genes.

Moreover, MYC degradation might be dispensable for transcriptional activation once histone acetylation has occurred and P-TEFb is recruited to promoters, implying that not each cycle of RNAPII release has to depend on MYC turnover.

5.9 Cooperation of MBI and MBII in transcriptional activation

The best-characterized function of MBII is the recruitment of HATs to MYC-regulated promoters, leading to increased histone acetylation (Bouchard et al., 2001; Frank et al., 2003; McMahon et al., 2000). This recruitment seems to require ubiquitin-dependent turnover of MYC. BRD4 binds to acetylated histones, and in turn recruits P-TEFb to promoters. The PAF complex binds to phosphorylated MBI and is transferred onto the RNAPII CTD once P-TEFb phosphorylates it at Ser2. Therefore, it can be proposed that MBI and MBII cooperate to activate expression of MYC target genes (Figure 5.4).

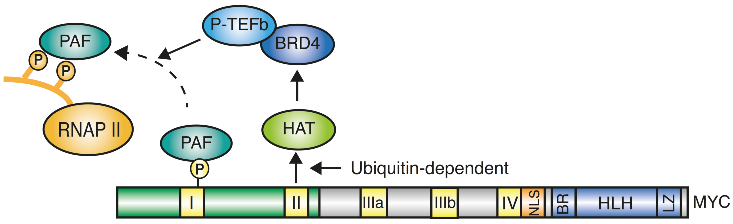

Figure 5.4: Proposed cooperation of MBI and MBII in transcriptional activation

Collectively, the data suggest that turnover of MYC coordinates histone acetylation with recruitment and transfer of elongation factors on RNAPII involving the cooperation of MBI and MBII.

During the last years, MYC was described to act as a transcriptional amplifier that globally enhances transcription (Lin et al., 2012; Nie et al., 2012; Wolf et al., 2015). However, so far there was no mechanism explaining this observation. The ability of MYC to stimulate multiple steps during transcriptional activation, including the transfer of elongation factors onto RNAPII, in combination with the observation that MYC binds to virtually all open promoters, may provide a mechanistic model for MYC's ability to globally enhance transcription.

6 Bibliography

Abukhdeir, A.M., Vitolo, M.I., Argani, P., De Marzo, A.M., Karakas, B., Konishi, H., Gustin, J.P., Lauring, J., Garay, J.P., Pendleton, C., et al. (2008). Tamoxifen-stimulated growth of breast cancer due to p21 loss. Proc. Natl. Acad. Sci. U.S.a. *105*, 288–293.

Adelman, K., and Lis, J.T. (2012). Promoter-proximal pausing of RNA polymerase II: emerging roles in metazoans. Nat. Rev. Genet. *13*, 720–731.

Adhikary, S., and Eilers, M. (2005). Transcriptional regulation and transformation by Myc proteins. Nat. Rev. Mol. Cell Biol. *6*, 635–645.

Adhikary, S., Marinoni, F., Hock, A., Hulleman, E., Popov, N., Beier, R., Bernard, S., Quarto, M., Capra, M., Goettig, S., et al. (2005). The ubiquitin ligase HectH9 regulates transcriptional activation by Myc and is essential for tumor cell proliferation. Cell *123*, 409–421.

Alvarez, E., Northwood, I.C., Gonzalez, F.A., Latour, D.A., Seth, A., Abate, C., Curran, T., and Davis, R.J. (1991). Pro-Leu-Ser/Thr-Pro is a consensus primary sequence for substrate protein phosphorylation. Characterization of the phosphorylation of c-myc and c-jun proteins by an epidermal growth factor receptor threonine 669 protein kinase. J. Biol. Chem. *266*, 15277–15285.

Arabi, A., Rustum, C., Hallberg, E., and Wright, A.P.H. (2003). Accumulation of c-Myc and proteasomes at the nucleoli of cells containing elevated c-Myc protein levels. J. Cell. Sci. *116*, 1707–1717.

Arabi, A., Wu, S., Ridderstråle, K., Bierhoff, H., Shiue, C., Fatyol, K., Fahlén, S., Hydbring, P., Söderberg, O., Grummt, I., et al. (2005). c-Myc associates with ribosomal DNA and activates RNA polymerase I transcription. Nat. Cell Biol. *7*, 303–310.

Archer, C.T., Delahodde, A., Gonzalez, F., Johnston, S.A., and Kodadek, T. (2008). Activation domain-dependent monoubiquitylation of Gal4 protein is essential for promoter binding in vivo. J. Biol. Chem. *283*, 12614–12623.

Auld, K.L., Brown, C.R., Casolari, J.M., Komili, S., and Silver, P.A. (2006). Genomic association of the proteasome demonstrates overlapping gene regulatory activity with transcription factor substrates. Mol. Cell *21*, 861–871.

Bahram, F., Lehr, von der, N., Cetinkaya, C., and Larsson, L.G. (2000). c-Myc hot spot mutations in lymphomas result in inefficient ubiquitination and decreased proteasome-mediated turnover. Blood *95*, 2104–2110.

Bai, X., Kim, J., Yang, Z., Jurynec, M.J., Akie, T.E., Lee, J., LeBlanc, J., Sessa, A., Jiang, H., DiBiase, A., et al. (2010). TIF1gamma controls erythroid cell fate by regulating transcription elongation. Cell *142*, 133–143.

Bild, A.H., Yao, G., Chang, J.T., Wang, Q., Potti, A., Chasse, D., Joshi, M.-B., Harpole, D., Lancaster, J.M., Berchuck, A., et al. (2006). Oncogenic pathway signatures in human cancers as a guide to targeted therapies. Nature *439*, 353–357.

Bisgrove, D.A., Mahmoudi, T., Henklein, P., and Verdin, E. (2007). Conserved P-TEFb-interacting domain of BRD4 inhibits HIV transcription. Proc. Natl. Acad. Sci. U.S.a. *104*, 13690–13695.

Blackwell, T.K., Huang, J., Ma, A., Kretzner, L., Alt, F.W., Eisenman, R.N., and Weintraub, H. (1993). Binding of myc proteins to canonical and noncanonical DNA sequences. Mol. Cell. Biol. *13*, 5216–5224.

Blackwood, E.M., and Eisenman, R.N. (1991). Max: a helix-loop-helix zipper protein that forms a sequence-specific DNA-binding complex with Myc. Science *251*, 1211–1217.

Blackwood, E.M., Lugo, T.G., Kretzner, L., King, M.W., Street, A.J., Witte, O.N., and Eisenman, R.N. (1994). Functional analysis of the AUG- and CUG-initiated forms of the c-Myc protein. Mol. Biol. Cell *5*, 597–609.

Bouchard, C., Dittrich, O., Kiermaier, A., Dohmann, K., Menkel, A., Eilers, M., and Lüscher, B. (2001). Regulation of cyclin D2 gene expression by the Myc/Max/Mad network: Myc-dependent TRRAP recruitment and histone acetylation at the cyclin D2 promoter. Genes Dev. *15*, 2042–2047.

Bouchard, C., Marquardt, J., Brás, A., Medema, R.H., and Eilers, M. (2004). Myc-induced proliferation and transformation require Akt-mediated phosphorylation of FoxO proteins. Embo J. *23*, 2830–2840.

Bradford, M.M. (1976). A rapid and sensitive method for the quantitation of microgram quantities of protein utilizing the principle of protein-dye binding. Anal. Biochem. *72*, 248–254.

Breitschopf, K., Bengal, E., Ziv, T., Admon, A., and Ciechanover, A. (1998). A novel site for ubiquitination: the N-terminal residue, and not internal lysines of MyoD, is essential for conjugation and degradation of the protein. Embo J. *17*, 5964–5973.

Brenner, C., Deplus, R., Didelot, C., Loriot, A., Viré, E., De Smet, C., Gutierrez, A., Danovi, D., Bernard, D., Boon, T., et al. (2005). Myc represses transcription through recruitment of DNA methyltransferase corepressor. Embo J. *24*, 336–346.

Brès, V., Kiernan, R.E., Linares, L.K., Chable-Bessia, C., Plechakova, O., Tréand, C., Emiliani, S., Peloponese, J.-M., Jeang, K.-T., Coux, O., et al. (2003). A non-proteolytic role for ubiquitin in Tat-mediated transactivation of the HIV-1 promoter. Nat. Cell Biol. *5*, 754–761.

Brummelkamp, T.R., Bernards, R., and Agami, R. (2002). A system for stable expression of short interfering RNAs in mammalian cells. Science *296*, 550–553.

Caron, C., Boyault, C., and Khochbin, S. (2005). Regulatory cross-talk between lysine acetylation and ubiquitination: role in the control of protein stability. Bioessays *27*, 408–415.

Carstensen, A. (2014). Personal Communiation.

Carter, P.S., Jarquin-Pardo, M., and De Benedetti, A. (1999). Differential expression of Myc1 and Myc2 isoforms in cells transformed by eIF4E: evidence for internal ribosome repositioning in the human c-myc 5'UTR. Oncogene *18*, 4326–4335.

Cepeda, D., Ng, H.-F., Sharifi, H.R., Mahmoudi, S., Cerrato, V.S., Fredlund, E., Magnusson, K., Nilsson, H., Malyukova, A., Rantala, J., et al. (2013). CDK-mediated activation of the SCF(FBXO) (28) ubiquitin ligase promotes MYC-driven transcription and tumourigenesis and predicts poor survival in breast cancer. EMBO Mol Med *5*, 999–1018.

Chandrasekharan, M.B., Huang, F., and Sun, Z.-W. (2010). Histone H2B ubiquitination and beyond: Regulation of nucleosome stability, chromatin dynamics and the trans-histone H3 methylation. Epigenetics *5*, 460–468.

Channavajhala, P., and Seldin, D.C. (2002). Functional interaction of protein kinase CK2 and c-Myc in lymphomagenesis. Oncogene *21*, 5280–5288.

Chaves, S., Baskerville, C., Yu, V., and Reed, S.I. (2010). Cks1, Cdk1, and the 19S proteasome collaborate to regulate gene induction-dependent nucleosome eviction in yeast. Mol. Cell. Biol. *30*, 5284–5294.

Chen, R., Yik, J.H.N., Lew, Q.J., and Chao, S.-H. (2014). Brd4 and HEXIM1: multiple roles in P-TEFb regulation and cancer. Biomed Res Int *2014*, 232870.

Choi, S.H., Wright, J.B., Gerber, S.A., and Cole, M.D. (2010). Myc protein is stabilized by suppression of a novel E3 ligase complex in cancer cells. Genes Dev. *24*, 1236–1241.

Chymkowitch, P., Le May, N., Charneau, P., Compe, E., and Egly, J.-M. (2011). The phosphorylation of the androgen receptor by TFIIH directs the ubiquitin/proteasome process. Embo J. *30*, 468–479.

Ciechanover, A., and Ben-Saadon, R. (2004). N-terminal ubiquitination: more protein substrates join in. Trends Cell Biol. *14*, 103–106.

Conacci-Sorrell, M., McFerrin, L., and Eisenman, R.N. (2014). An overview of MYC and its interactome. Cold Spring Harb Perspect Med *4*, a014357.

Cowling, V.H., Chandriani, S., Whitfield, M.L., and Cole, M.D. (2006). A conserved Myc protein domain, MBIV, regulates DNA binding, apoptosis, transformation, and G2 arrest. Mol. Cell. Biol. *26*, 4226–4239.

Cowling, V.H., D'Cruz, C.M., Chodosh, L.A., and Cole, M.D. (2007). c-Myc transforms human mammary epithelial cells through repression of the Wnt inhibitors DKK1 and SFRP1. Mol. Cell. Biol. *27*, 5135–5146.

Dang, C.V., and Lee, W.M. (1988). Identification of the human c-myc protein nuclear translocation signal. Mol. Cell. Biol. *8*, 4048–4054.

Dani, C., Blanchard, J.M., Piechaczyk, M., Sabouty, El, S., Marty, L., and Jeanteur, P. (1984). Extreme instability of myc mRNA in normal and transformed human cells. Proc. Natl. Acad. Sci. U.S.a. *81*, 7046–7050.

Danielsen, J.M.R., Sylvestersen, K.B., Bekker-Jensen, S., Szklarczyk, D., Poulsen, J.W., Horn, H., Jensen, L.J., Mailand, N., and Nielsen, M.L. (2011). Mass spectrometric analysis of lysine ubiquitylation reveals promiscuity at site level. Mol. Cell Proteomics *10*, M110.003590.

Dantuma, N.P., and Hoppe, T. (2012). Growing sphere of influence: Cdc48/p97 orchestrates ubiquitin-dependent extraction from chromatin. Trends Cell Biol. *22*, 483–491.

Davis, A.C., Wims, M., Spotts, G.D., Hann, S.R., and Bradley, A. (1993). A null c-myc mutation causes lethality before 10.5 days of gestation in homozygotes and reduced fertility in heterozygous female mice. Genes Dev. *7*, 671–682.

Delmore, J.E., Issa, G.C., Lemieux, M.E., Rahl, P.B., Shi, J., Jacobs, H.M., Kastritis, E., Gilpatrick, T., Paranal, R.M., Qi, J., et al. (2011). BET bromodomain inhibition as a therapeutic strategy to target c-Myc. Cell *146*, 904–917.

Dembla-Rajpal, N., Seipelt, R., Wang, Q., and Rymond, B.C. (2004). Proteasome inhibition alters the transcription of multiple yeast genes. Biochim. Biophys. Acta *1680*, 34–45.

Deshaies, R.J., Emberley, E.D., and Saha, A. (2010). Control of cullin-ring ubiquitin ligase activity by nedd8. Subcell. Biochem. *54*, 41–56.

Dey, A., Chitsaz, F., Abbasi, A., Misteli, T., and Ozato, K. (2003). The double bromodomain protein Brd4 binds to acetylated chromatin during interphase and mitosis. Proc. Natl. Acad. Sci. U.S.a. *100*, 8758–8763.

Dias, D.C., Dolios, G., Wang, R., and Pan, Z.-Q. (2002). CUL7: A DOC domain-containing cullin selectively binds Skp1.Fbx29 to form an SCF-like complex. Proc. Natl. Acad. Sci. U.S.a. *99*, 16601–16606.

Diefenbacher, M.E., Popov, N., Blake, S.M., Schülein-Völk, C., Nye, E., Spencer-Dene, B., Jaenicke, L.A., Eilers, M., and Behrens, A. (2014). The deubiquitinase USP28 controls intestinal homeostasis and promotes colorectal cancer. J. Clin. Invest. *124*, 3407–3418.

Dingar, D., Kalkat, M., Chan, P.-K., Srikumar, T., Bailey, S.D., Tu, W.B., Coyaud, E., Ponzielli, R., Kolyar, M., Jurisica, I., et al. (2015). BioID identifies novel c-MYC interacting partners in cultured cells and xenograft tumors. J Proteomics *118*, 95–111.

DiRenzo, J., Signoretti, S., Nakamura, N., Rivera-Gonzalez, R., Sellers, W., Loda, M., and Brown, M. (2002). Growth factor requirements and basal phenotype of an immortalized mammary epithelial cell line. Cancer Res. *62*, 89–98.

Dubois, N.C., Adolphe, C., Ehninger, A., Wang, R.A., Robertson, E.J., and Trumpp, A. (2008). Placental rescue reveals a sole requirement for c-Myc in embryonic erythroblast survival and hematopoietic stem cell function. Development *135*, 2455–2465.

Eberhardy, S.R., and Farnham, P.J. (2002). Myc recruits P-TEFb to mediate the final step in the transcriptional activation of the cad promoter. J. Biol. Chem. *277*, 40156–40162.

Ehrensberger, A.H., Kelly, G.P., and Svejstrup, J.Q. (2013). Mechanistic interpretation of promoter-proximal peaks and RNAPII density maps. Cell *154*, 713–715.

Eick, D., and Geyer, M. (2013). The RNA polymerase II carboxy-terminal domain (CTD) code. Chem. Rev. *113*, 8456–8490.

Eilers, M., and Eisenman, R.N. (2008). Myc's broad reach. Genes Dev. *22*, 2755–2766.

Escot, C., Theillet, C., Lidereau, R., Spyratos, F., Champeme, M.H., Gest, J., and Callahan, R. (1986). Genetic alteration of the c-myc protooncogene (MYC) in human primary breast carcinomas. Proc. Natl. Acad. Sci. U.S.a. *83*, 4834–4838.

Ezhkova, E., and Tansey, W.P. (2004). Proteasomal ATPases link ubiquitylation of histone H2B to methylation of histone H3. Mol. Cell *13*, 435–442.

Faiola, F., Liu, X., Lo, S., Pan, S., Zhang, K., Lymar, E., Farina, A., and Martinez, E. (2005). Dual regulation of c-Myc by p300 via acetylation-dependent control of Myc protein turnover and coactivation of Myc-induced transcription. Mol. Cell. Biol. *25*, 10220–10234.

Farrell, A.S., and Sears, R.C. (2014). MYC degradation. Cold Spring Harb Perspect Med *4*.

Farrell, A.S., Pelz, C., Wang, X., Daniel, C.J., Wang, Z., Su, Y., Janghorban, M., Zhang, X., Morgan, C., Impey, S., et al. (2013). Pin1 regulates the dynamics of c-Myc DNA binding to facilitate target gene regulation and oncogenesis. Mol. Cell. Biol. *33*, 2930–2949.

Ferdous, A., Gonzalez, F., Sun, L., Kodadek, T., and Johnston, S.A. (2001). The 19S regulatory particle of the proteasome is required for efficient transcription elongation by RNA polymerase II. Mol. Cell *7*, 981–991.

Ferdous, A., Kodadek, T., and Johnston, S.A. (2002). A nonproteolytic function of the 19S regulatory subunit of the 26S proteasome is required for efficient activated transcription by human RNA polymerase II. Biochemistry *41*, 12798–12805.

Filippakopoulos, P., Qi, J., Picaud, S., Shen, Y., Smith, W.B., Fedorov, O., Morse, E.M., Keates, T., Hickman, T.T., Felletar, I., et al. (2010). Selective inhibition of BET bromodomains. Nature *468*, 1067–1073.

Fleming, J.A., Lightcap, E.S., Sadis, S., Thoroddsen, V., Bulawa, C.E., and Blackman, R.K. (2002). Complementary whole-genome technologies reveal the cellular response to proteasome inhibition by PS-341. Proc. Natl. Acad. Sci. U.S.a. *99*, 1461–1466.

Flick, K., Ouni, I., Wohlschlegel, J.A., Capati, C., McDonald, W.H., Yates, J.R., and Kaiser, P. (2004). Proteolysis-independent regulation of the transcription factor Met4 by a single Lys 48-linked ubiquitin chain. Nat. Cell Biol. *6*, 634–641.

Formosa, T. (2012). The role of FACT in making and breaking nucleosomes. Biochim. Biophys. Acta *1819*, 247–255.

Frank, S.R., Parisi, T., Taubert, S., Fernandez, P., Fuchs, M., Chan, H.-M., Livingston, D.M., and Amati, B. (2003). MYC recruits the TIP60 histone acetyltransferase complex to chromatin. EMBO Rep. *4*, 575–580.

Gallant, P., Shiio, Y., Cheng, P.F., Parkhurst, S.M., and Eisenman, R.N. (1996). Myc and Max homologs in Drosophila. Science *274*, 1523–1527.

Gareau, J.R., and Lima, C.D. (2010). The SUMO pathway: emerging mechanisms that shape specificity, conjugation and recognition. Nat. Rev. Mol. Cell Biol. *11*, 861–871.

Gartel, A.L., Ye, X., Goufman, E., Shianov, P., Hay, N., Najmabadi, F., and Tyner, A.L. (2001). Myc represses the p21(WAF1/CIP1) promoter and interacts with Sp1/Sp3. Proc. Natl. Acad. Sci. U.S.a. *98*, 4510–4515.

Gaubatz, S., Imhof, A., Dosch, R., Werner, O., Mitchell, P., Buettner, R., and Eilers, M. (1995). Transcriptional activation by Myc is under negative control by the transcription factor AP-2. Embo J. *14*, 1508–1519.

Geiss-Friedlander, R., and Melchior, F. (2007). Concepts in sumoylation: a decade on. Nat. Rev. Mol. Cell Biol. *8*, 947–956.

Geng, F., and Tansey, W.P. (2012). Similar temporal and spatial recruitment of native 19S and 20S proteasome subunits to transcriptionally active chromatin. Proc. Natl. Acad. Sci. U.S.a. *109*, 6060–6065.

Geng, F., Wenzel, S., and Tansey, W.P. (2012). Ubiquitin and proteasomes in transcription. Annu. Rev. Biochem. *81*, 177–201.

Gillette, T.G., Gonzalez, F., Delahodde, A., Johnston, S.A., and Kodadek, T. (2004). Physical and functional association of RNA polymerase II and the proteasome. Proc. Natl. Acad. Sci. U.S.a. *101*, 5904–5909.

Goldknopf, I.L., Taylor, C.W., Baum, R.M., Yeoman, L.C., Olson, M.O., Prestayko, A.W., and Busch, H. (1975). Isolation and characterization of protein A24, a “histone-like” non-histone chromosomal protein. J. Biol. Chem. *250*, 7182–7187.

Gomez-Roman, N., Grandori, C., Eisenman, R.N., and White, R.J. (2003). Direct activation of RNA polymerase III transcription by c-Myc. Nature *421*, 290–294.

Gonzalez, F., Delahodde, A., Kodadek, T., and Johnston, S.A. (2002). Recruitment of a 19S proteasome subcomplex to an activated promoter. Science *296*, 548–550.

Grandori, C., Gomez-Roman, N., Felton-Edkins, Z.A., Ngouenet, C., Galloway, D.A., Eisenman, R.N., and White, R.J. (2005). c-Myc binds to human ribosomal DNA and stimulates transcription of rRNA genes by RNA polymerase I. Nat. Cell Biol. *7*, 311–318.

Gregory, M.A., and Hann, S.R. (2000). c-Myc proteolysis by the ubiquitin-proteasome pathway: stabilization of c-Myc in Burkitt's lymphoma cells. Mol. Cell. Biol. *20*, 2423–2435.

Gregory, M.A., Qi, Y., and Hann, S.R. (2003). Phosphorylation by glycogen synthase kinase-3 controls c-myc proteolysis and subnuclear localization. J. Biol. Chem. *278*, 51606–51612.

Grönroos, E., Hellman, U., Heldin, C.-H., and Ericsson, J. (2002). Control of Smad7 stability by competition between acetylation and ubiquitination. Mol. Cell *10*, 483–493.

Guccione, E., Martinato, F., Finocchiaro, G., Luzi, L., Tizzoni, L., Dall' Olio, V., Zardo, G., Nervi, C., Bernard, L., and Amati, B. (2006). Myc-binding-site recognition in the human genome is determined by chromatin context. Nat. Cell Biol. *8*, 764–770.

Hakem, A., Bohgaki, M., Lemmers, B., Tai, E., Salmena, L., Matysiak-Zablocki, E., Jung, Y.-S., Karaskova, J., Kaustov, L., Duan, S., et al. (2011). Role of Pirh2 in mediating the regulation of p53 and c-Myc. PLoS Genet. *7*, e1002360.

Hann, S.R., King, M.W., Bentley, D.L., Anderson, C.W., and Eisenman, R.N. (1988). A non-AUG translational initiation in c-myc exon 1 generates an N-terminally distinct protein whose synthesis is disrupted in Burkitt's lymphomas. Cell *52*, 185–195.

Hart, M., Concordet, J.P., Lassot, I., Albert, I., del los Santos, R., Durand, H., Perret, C., Rubinfeld, B., Margottin, F., Benarous, R., et al. (1999). The F-box protein beta-TrCP associates with phosphorylated beta-catenin and regulates its activity in the cell. Curr. Biol. *9*, 207–210.

Hatakeyama, S., Yada, M., Matsumoto, M., Ishida, N., and Nakayama, K.I. (2001). U box proteins as a new family of ubiquitin-protein ligases. J. Biol. Chem. *276*, 33111–33120.

He, T.C., Sparks, A.B., Rago, C., Hermeking, H., Zawel, L., da Costa, L.T., Morin, P.J., Vogelstein, B., and Kinzler, K.W. (1998). Identification of c-MYC as a target of the APC pathway. Science *281*, 1509–1512.

Heidemann, M., Hintermair, C., Voß, K., and Eick, D. (2013). Dynamic phosphorylation patterns of RNA polymerase II CTD during transcription. Biochim. Biophys. Acta *1829*, 55–62.

Hemann, M.T., Bric, A., Teruya-Feldstein, J., Herbst, A., Nilsson, J.A., Cordon-Cardo, C., Cleveland, J.L., Tansey, W.P., and Lowe, S.W. (2005). Evasion of the p53 tumour surveillance network by tumour-derived MYC mutants. Nature *436*, 807–811.

Henriksson, M., Bakardjiev, A., Klein, G., and Lüscher, B. (1993). Phosphorylation sites mapping in the N-terminal domain of c-myc modulate its transforming potential. Oncogene *8*, 3199–3209.

Herbst, A., Hemann, M.T., Tworkowski, K.A., Salghetti, S.E., Lowe, S.W., and Tansey, W.P. (2005). A conserved element in Myc that negatively regulates its proapoptotic activity. EMBO Rep. *6*, 177–183.

Herbst, A., Salghetti, S.E., Kim, S.Y., and Tansey, W.P. (2004). Multiple cell-type-specific elements regulate Myc protein stability. Oncogene *23*, 3863–3871.

Hershko, A., and Ciechanover, A. (1998). The ubiquitin system. Annu. Rev. Biochem. *67*, 425–479.

Hjerpe, R., Aillet, F., Lopitz-Otsoa, F., Lang, V., England, P., and Rodriguez, M.S. (2009). Efficient protection and isolation of ubiquitylated proteins using tandem ubiquitin-binding entities. EMBO Rep. *10*, 1250–1258.

Hock, A.K., Vigneron, A., and Vousden, K.H. (2014). Ubiquitin Specific Peptidase 42 (USP42) Functions to Deubiquitylate Histones and Regulate Transcriptional Activity. J. Biol. Chem.

Holland, A.J., Fachinetti, D., Han, J.S., and Cleveland, D.W. (2012). Inducible, reversible system for the rapid and complete degradation of proteins in mammalian cells. Proc. Natl. Acad. Sci. U.S.a. *109*, E3350–E3357.

Hoppe, T., Cassata, G., Barral, J.M., Springer, W., Hutagalung, A.H., Epstein, H.F., and Baumeister, R. (2004). Regulation of the myosin-directed chaperone UNC-45 by a novel E3/E4-multiubiquitylation complex in C. elegans. Cell *118*, 337–349.

Hou, D., Cenciarelli, C., Jensen, J.P., Nguygen, H.B., and Weissman, A.M. (1994). Activation-dependent ubiquitination of a T cell antigen receptor subunit on multiple intracellular lysines. J. Biol. Chem. *269*, 14244–14247.

Hurlin, P.J., Quéva, C., and Eisenman, R.N. (1997). Mnt, a novel Max-interacting protein is coexpressed with Myc in proliferating cells and mediates repression at Myc binding sites. Genes Dev. *11*, 44–58.

Hydbring, P., Bahram, F., Su, Y., Tronnersjö, S., Högstrand, K., Lehr, von der, N., Sharifi, H.R., Lilischkis, R., Hein, N., Wu, S., et al. (2010). Phosphorylation by Cdk2 is required for Myc to repress Ras-induced senescence in cotransformation. Proc. Natl. Acad. Sci. U.S.a. *107*, 58–63.

Ikeda, F., and Dikic, I. (2008). Atypical ubiquitin chains: new molecular signals. “Protein Modifications: Beyond the Usual Suspects” review series. EMBO Rep. *9*, 536–542.

Inoue, S., Hao, Z., Elia, A.J., Cescon, D., Zhou, L., Silvester, J., Snow, B., Harris, I.S., Sasaki, M., Li, W.Y., et al. (2013). Mule/Huwe1/Arf-BP1 suppresses Ras-driven tumorigenesis by preventing c-Myc/Miz1-mediated down-regulation of p21 and p15. Genes Dev. *27*, 1101–1114.

Inui, M., Manfrin, A., Mamidi, A., Martello, G., Morsut, L., Soligo, S., Enzo, E., Moro, S., Polo, S., Dupont, S., et al. (2011). USP15 is a deubiquitylating enzyme for receptor-activated SMADs. Nat. Cell Biol. *13*, 1368–1375.

Jang, M.K., Mochizuki, K., Zhou, M., Jeong, H.-S., Brady, J.N., and Ozato, K. (2005). The bromodomain protein Brd4 is a positive regulatory component of P-TEFb and stimulates RNA polymerase II-dependent transcription. Mol. Cell *19*, 523–534.

Jenkins, R.B., Qian, J., Lieber, M.M., and Bostwick, D.G. (1997). Detection of c-myc oncogene amplification and chromosomal anomalies in metastatic prostatic carcinoma by fluorescence in situ hybridization. Cancer Res. *57*, 524–531.

Jin, J., and Harper, J.W. (2003). A license to kill: transcriptional activation and enhanced turnover of Myc by the SCF(kp2) ubiquitin ligase. Cancer Cell *3*, 517–518.

Jin, J., Li, X., Gygi, S.P., and Harper, J.W. (2007). Dual E1 activation systems for ubiquitin differentially regulate E2 enzyme charging. Nature *447*, 1135–1138.

Kadota, M., Yang, H.H., Gomez, B., Sato, M., Clifford, R.J., Meerzaman, D., Dunn, B.K., Wakefield, L.M., and Lee, M.P. (2010). Delineating genetic alterations for tumor progression in the MCF10A series of breast cancer cell lines. PLoS ONE *5*, e9201.

Kaiser, P., Flick, K., Wittenberg, C., and Reed, S.I. (2000). Regulation of transcription by ubiquitination without proteolysis: Cdc34/SCF(Met30)-mediated inactivation of the transcription factor Met4. Cell *102*, 303–314.

Kalb, R., Latwiel, S., Baymaz, H.I., Jansen, P.W.T.C., Müller, C.W., Vermeulen, M., and Müller, J. (2014). Histone H2A monoubiquitination promotes histone H3 methylation in Polycomb repression. Nat. Struct. Mol. Biol. *21*, 569–571.

Kalkat, M., Chan, P.-K., Wasylishen, A.R., Srikumar, T., Kim, S.S., Ponzielli, R., Bazett-Jones, D.P., Raught, B., and Penn, L.Z. (2014). Identification of c-MYC SUMOylation by mass spectrometry. PLoS ONE *9*, e115337.

Kasinathan, S., Orsi, G.A., Zentner, G.E., Ahmad, K., and Henikoff, S. (2014). High-resolution mapping of transcription factor binding sites on native chromatin. Nat. Methods *11*, 203–209.

Kato, G.J., Barrett, J., Villa-Garcia, M., and Dang, C.V. (1990). An amino-terminal c-myc domain required for neoplastic transformation activates transcription. Mol. Cell. Biol. *10*, 5914–5920.

Kerscher, O., Felberbaum, R., and Hochstrasser, M. (2006). Modification of proteins by ubiquitin and ubiquitin-like proteins. Annu. Rev. Cell Dev. Biol. *22*, 159–180.

Kim, S.Y., Herbst, A., Tworkowski, K.A., Salghetti, S.E., and Tansey, W.P. (2003). Skp2 regulates Myc protein stability and activity. Mol. Cell *11*, 1177–1188.

Kim, W., Bennett, E.J., Huttlin, E.L., Guo, A., Li, J., Possemato, A., Sowa, M.E., Rad, R., Rush, J., Comb, M.J., et al. (2011). Systematic and quantitative assessment of the ubiquitin-modified proteome. Mol. Cell *44*, 325–340.

King, R.W., Glotzer, M., and Kirschner, M.W. (1996). Mutagenic analysis of the destruction signal of mitotic cyclins and structural characterization of ubiquitinated intermediates. Mol. Biol. Cell *7*, 1343–1357.

Kirkpatrick, D.S., Hathaway, N.A., Hanna, J., Elsasser, S., Rush, J., Finley, D., King, R.W., and Gygi, S.P. (2006). Quantitative analysis of in vitro ubiquitinated cyclin B1 reveals complex chain topology. Nat. Cell Biol. *8*, 700–710.

Koch, H.B., Zhang, R., Verdoodt, B., Bailey, A., Zhang, C.-D., Yates, J.R., Menssen, A., and Hermeking, H. (2007). Large-scale identification of c-MYC-associated proteins using a combined TAP/MudPIT approach. Cell Cycle *6*, 205–217.

Koegl, M., Hoppe, T., Schlenker, S., Ulrich, H.D., Mayer, T.U., and Jentsch, S. (1999). A novel ubiquitination factor, E4, is involved in multiubiquitin chain assembly. Cell *96*, 635–644.

Komander, D., and Rape, M. (2012). The ubiquitin code. Annu. Rev. Biochem. *81*, 203–229.

Komander, D., Clague, M.J., and Urbé, S. (2009). Breaking the chains: structure and function of the deubiquitinases. Nat. Rev. Mol. Cell Biol. *10*, 550–563.

Kress, T.R., Cannell, I.G., Brenkman, A.B., Samans, B., Gaestel, M., Roepman, P., Burgering, B.M., Bushell, M., Rosenwald, A., and Eilers, M. (2011). The MK5/PRAK kinase and Myc form a negative feedback loop that is disrupted during colorectal tumorigenesis. Mol. Cell *41*, 445–457.

Krogan, N.J., Dover, J., Wood, A., Schneider, J., Heidt, J., Boateng, M.A., Dean, K., Ryan, O.W., Golshani, A., Johnston, M., et al. (2003). The Paf1 complex is required for histone H3 methylation by COMPASS and Dot1p: linking transcriptional elongation to histone methylation. Mol. Cell *11*, 721–729.

Kuo, M.H., and Allis, C.D. (1999). In vivo cross-linking and immunoprecipitation for studying dynamic Protein:DNA associations in a chromatin environment. Methods *19*, 425–433.

Kuras, L., Rouillon, A., Lee, T., Barbey, R., Tyers, M., and Thomas, D. (2002). Dual regulation of the met4 transcription factor by ubiquitin-dependent degradation and inhibition of promoter recruitment. Mol. Cell *10*, 69–80.

Kurland, J.F., and Tansey, W.P. (2008). Myc-mediated transcriptional repression by recruitment of histone deacetylase. Cancer Res. *68*, 3624–3629.

Kwak, H., and Lis, J.T. (2013). Control of transcriptional elongation. Annu. Rev. Genet. *47*, 483–508.

Lee, D.H., and Goldberg, A.L. (1996). Selective inhibitors of the proteasome-dependent and vacuolar pathways of protein degradation in Saccharomyces cerevisiae. J. Biol. Chem. *271*, 27280–27284.

Lee, J., and Zhou, P. (2007). DCAFs, the missing link of the CUL4-DDB1 ubiquitin ligase. Mol. Cell *26*, 775–780.

Lee, L.A., Dolde, C., Barrett, J., Wu, C.S., and Dang, C.V. (1996). A link between c-Myc-mediated transcriptional repression and neoplastic transformation. J. Clin. Invest. *97*, 1687–1695.

Lehr, von der, N., Johansson, S., Wu, S., Bahram, F., Castell, A., Cetinkaya, C., Hydbring, P., Weidung, I., Nakayama, K., Nakayama, K.I., et al. (2003). The F-box protein Skp2 participates in c-Myc proteosomal degradation and acts as a cofactor for c-Myc-regulated transcription. Mol. Cell *11*, 1189–1200.

Levens, D. (2010). You Don't Muck with MYC. Genes Cancer *1*, 547–554.

Li, H., Handsaker, B., Wysoker, A., Fennell, T., Ruan, J., Homer, N., Marth, G., Abecasis, G., Durbin, R., 1000 Genome Project Data Processing Subgroup (2009). The Sequence Alignment/Map format and SAMtools. Bioinformatics *25*, 2078–2079.

Li, W., Bengtson, M.H., Ulbrich, A., Matsuda, A., Reddy, V.A., Orth, A., Chanda, S.K., Batalov, S., and Joazeiro, C.A.P. (2008). Genome-wide and functional annotation of human E3 ubiquitin ligases identifies MULAN, a mitochondrial E3 that regulates the organelle's dynamics and signaling. PLoS ONE *3*, e1487.

Li, Y., Choi, P.S., Casey, S.C., Dill, D.L., and Felsher, D.W. (2014). MYC through miR-17-92 suppresses specific target genes to maintain survival, autonomous proliferation, and a neoplastic state. Cancer Cell *26*, 262–272.

Lin, C.Y., Lovén, J., Rahl, P.B., Paranal, R.M., Burge, C.B., Bradner, J.E., Lee, T.I., and Young, R.A. (2012). Transcriptional amplification in tumor cells with elevated c-Myc. Cell *151*, 56–67.

Lipford, J.R., and Deshaies, R.J. (2003). Diverse roles for ubiquitin-dependent proteolysis in transcriptional activation. Nat. Cell Biol. *5*, 845–850.

Lipford, J.R., Smith, G.T., Chi, Y., and Deshaies, R.J. (2005). A putative stimulatory role for activator turnover in gene expression. Nature *438*, 113–116.

Liu, X., Tesfai, J., Evrard, Y.A., Dent, S.Y.R., and Martinez, E. (2003). c-Myc transformation domain recruits the human STAGA complex and requires TRRAP and GCN5 acetylase activity for transcription activation. J. Biol. Chem. *278*, 20405–20412.

Lorick, K.L., Jensen, J.P., Fang, S., Ong, A.M., Hatakeyama, S., and Weissman, A.M. (1999). RING fingers mediate ubiquitin-conjugating enzyme (E2)-dependent ubiquitination. Proc. Natl. Acad. Sci. U.S.a. *96*, 11364–11369.

Lovén, J., Hoke, H.A., Lin, C.Y., Lau, A., Orlando, D.A., Vakoc, C.R., Bradner, J.E., Lee, T.I., and Young, R.A. (2013). Selective inhibition of tumor oncogenes by disruption of super-enhancers. Cell *153*, 320–334.

Lu, K., Ye, W., Zhou, L., Collins, L.B., Chen, X., Gold, A., Ball, L.M., and Swenberg, J.A. (2010). Structural characterization of formaldehyde-induced cross-links between amino acids and deoxynucleosides and their oligomers. J. Am. Chem. Soc. *132*, 3388–3399.

Lu, Z., and Hunter, T. (2010). Ubiquitylation and proteasomal degradation of the p21(Cip1), p27(Kip1) and p57(Kip2) CDK inhibitors. Cell Cycle *9*, 2342–2352.

Lutterbach, B., and Hann, S.R. (1994). Hierarchical phosphorylation at N-terminal transformation-sensitive sites in c-Myc protein is regulated by mitogens and in mitosis. Mol. Cell. Biol. *14*, 5510–5522.

Lutterbach, B., and Hann, S.R. (1999). c-Myc transactivation domain-associated kinases: questionable role for map kinases in c-Myc phosphorylation. J. Cell. Biochem. *72*, 483–491.

Lüscher, B., Kuenzel, E.A., Krebs, E.G., and Eisenman, R.N. (1989). Myc oncoproteins are phosphorylated by casein kinase II. Embo J. *8*, 1111–1119.

McMahon, S.B., Van Buskirk, H.A., Dugan, K.A., Copeland, T.D., and Cole, M.D. (1998). The novel ATM-related protein TRRAP is an essential cofactor for the c-Myc and E2F oncoproteins. Cell *94*, 363–374.

McMahon, S.B., Wood, M.A., and Cole, M.D. (2000). The essential cofactor TRRAP recruits the histone acetyltransferase hGCN5 to c-Myc. Mol. Cell. Biol. *20*, 556–562.

Medlin, J., Scurry, A., Taylor, A., Zhang, F., Peterlin, B.M., and Murphy, S. (2005). P-TEFb is not an essential elongation factor for the intronless human U2 snRNA and histone H2b genes. Embo J. *24*, 4154–4165.

Meerbrey, K.L., Hu, G., Kessler, J.D., Roarty, K., Li, M.Z., Fang, J.E., Herschkowitz, J.I., Burrows, A.E., Ciccia, A., Sun, T., et al. (2011). The pINDUCER lentiviral toolkit for inducible RNA interference in vitro and in vivo. Proc. Natl. Acad. Sci. U.S.a. *108*, 3665–3670.

Meinnel, T., Peynot, P., and Giglione, C. (2005). Processed N-termini of mature proteins in higher eukaryotes and their major contribution to dynamic proteomics. Biochimie *87*, 701–712.

Métivier, R., Penot, G., Hübner, M.R., Reid, G., Brand, H., Kos, M., and Gannon, F. (2003). Estrogen receptor-alpha directs ordered, cyclical, and combinatorial recruitment of cofactors on a natural target promoter. Cell *115*, 751–763.

Minsky, N., Shema, E., Field, Y., Schuster, M., Segal, E., and Oren, M. (2008). Monoubiquitinated H2B is associated with the transcribed region of highly expressed genes in human cells. Nat. Cell Biol. *10*, 483–488.

Molinari, E., Gilman, M., and Natesan, S. (1999). Proteasome-mediated degradation of transcriptional activators correlates with activation domain potency in vivo. Embo J. *18*, 6439–6447.

Murakami, Y., Matsufuji, S., Kameji, T., Hayashi, S., Igarashi, K., Tamura, T., Tanaka, K., and Ichihara, A. (1992). Ornithine decarboxylase is degraded by the 26S proteasome without ubiquitination. Nature *360*, 597–599.

Muratani, M., Kung, C., Shokat, K.M., and Tansey, W.P. (2005). The F box protein Dsg1/Mdm30 is a transcriptional coactivator that stimulates Gal4 turnover and cotranscriptional mRNA processing. Cell *120*, 887–899.

Muthalagu, N., Junttila, M.R., Wiese, K.E., Wolf, E., Morton, J., Bauer, B., Evan, G.I., Eilers, M., and Murphy, D.J. (2014). BIM is the primary mediator of MYC-induced apoptosis in multiple solid tissues. Cell Rep *8*, 1347–1353.

Nakayama, K., Nagahama, H., Minamishima, Y.A., Matsumoto, M., Nakamichi, I., Kitagawa, K., Shirane, M., Tsunematsu, R., Tsukiyama, T., Ishida, N., et al. (2000). Targeted disruption of Skp2 results in accumulation of cyclin E and p27(Kip1), polyploidy and centrosome overduplication. Embo J. *19*, 2069–2081.

Nakayama, K., Nagahama, H., Minamishima, Y.A., Miyake, S., Ishida, N., Hatakeyama, S., Kitagawa, M., Iemura, S.-I., Natsume, T., and Nakayama, K.I. (2004). Skp2-mediated degradation of p27 regulates progression into mitosis. Dev. Cell *6*, 661–672.

Nau, M.M., Brooks, B.J., Battey, J., Sausville, E., Gazdar, A.F., Kirsch, I.R., McBride, O.W., Bertness, V., Hollis, G.F., and Minna, J.D. (1985). L-myc, a new myc-related gene amplified and expressed in human small cell lung cancer. Nature *318*, 69–73.

Ndoja, A., Cohen, R.E., and Yao, T. (2014). Ubiquitin signals proteolysis-independent stripping of transcription factors. Mol. Cell *53*, 893–903.

Nicol, J.W., Helt, G.A., Blanchard, S.G., Raja, A., and Loraine, A.E. (2009). The Integrated Genome Browser: free software for distribution and exploration of genome-scale datasets. Bioinformatics *25*, 2730–2731.

Nie, Z., Hu, G., Wei, G., Cui, K., Yamane, A., Resch, W., Wang, R., Green, D.R., Tessarollo, L., Casellas, R., et al. (2012). c-Myc is a universal amplifier of expressed genes in lymphocytes and embryonic stem cells. Cell *151*, 68–79.

Nishimura, K., Fukagawa, T., Takisawa, H., Kakimoto, T., and Kanemaki, M. (2009). An auxin-based degron system for the rapid depletion of proteins in nonplant cells. Nat. Methods *6*, 917–922.

Noguchi, K., Kitanaka, C., Yamana, H., Kokubu, A., Mochizuki, T., and Kuchino, Y. (1999). Regulation of c-Myc through phosphorylation at Ser-62 and Ser-71 by c-Jun N-terminal kinase. J. Biol. Chem. *274*, 32580–32587.

Old, J.B., Kratzat, S., Hoellein, A., Graf, S., Nilsson, J.A., Nilsson, L., Nakayama, K.I., Peschel, C., Cleveland, J.L., and Keller, U.B. (2010). Skp2 directs Myc-mediated suppression of p27Kip1 yet has modest effects on Myc-driven lymphomagenesis. Mol. Cancer Res. *8*, 353–362.

Pan, J., Deng, Q., Jiang, C., Wang, X., Niu, T., Li, H., Chen, T., Jin, J., Pan, W., Cai, X., et al. (2014). USP37 directly deubiquitinates and stabilizes c-Myc in lung cancer. Oncogene.

Patel, J.H., Du, Y., Ard, P.G., Phillips, C., Carella, B., Chen, C.-J., Rakowski, C., Chatterjee, C., Lieberman, P.M., Lane, W.S., et al. (2004). The c-MYC oncoprotein is a substrate of the acetyltransferases hGCN5/PCAF and TIP60. Mol. Cell. Biol. *24*, 10826–10834.

Paul, I., Ahmed, S.F., Bhowmik, A., Deb, S., and Ghosh, M.K. (2013). The ubiquitin ligase CHIP regulates c-Myc stability and transcriptional activity. Oncogene *32*, 1284–1295.

Pavri, R., Zhu, B., Li, G., Trojer, P., Mandal, S., Shilatifard, A., and Reinberg, D. (2006). Histone H2B monoubiquitination functions cooperatively with FACT to regulate elongation by RNA polymerase II. Cell *125*, 703–717.

Peng, J., Schwartz, D., Elias, J.E., Thoreen, C.C., Cheng, D., Marsischky, G., Roelofs, J., Finley, D., and Gygi, S.P. (2003). A proteomics approach to understanding protein ubiquitination. Nat. Biotechnol. *21*, 921–926.

Peter, S., Bultinck, J., Myant, K., Jaenicke, L.A., Walz, S., Müller, J., Gmachl, M., Treu, M., Boehmelt, G., Ade, C.P., et al. (2014). Tumor cell-specific inhibition of MYC function using small molecule inhibitors of the HUWE1 ubiquitin ligase. EMBO Mol Med.

Petroski, M.D., and Deshaies, R.J. (2005). Function and regulation of cullin-RING ubiquitin ligases. Nat. Rev. Mol. Cell Biol. *6*, 9–20.

Peukert, K., Staller, P., Schneider, A., Carmichael, G., Hänel, F., and Eilers, M. (1997). An alternative pathway for gene regulation by Myc. Embo J. *16*, 5672–5686.

Pickart, C.M. (2001). Mechanisms underlying ubiquitination. Annu. Rev. Biochem. *70*, 503–533.

Pickart, C.M., and Cohen, R.E. (2004). Proteasomes and their kin: proteases in the machine age. Nat. Rev. Mol. Cell Biol. *5*, 177–187.

Pickart, C.M., and Eddins, M.J. (2004). Ubiquitin: structures, functions, mechanisms. Biochim. Biophys. Acta *1695*, 55–72.

Popov, N., Schülein, C., Jaenicke, L.A., and Eilers, M. (2010). Ubiquitylation of the amino terminus of Myc by SCF(β-TrCP) antagonizes SCF(Fbw7)-mediated turnover. Nat. Cell Biol. *12*, 973–981.

Popov, N., Wanzel, M., Madiredjo, M., Zhang, D., Beijersbergen, R., Bernards, R., Moll, R., Elledge, S.J., and Eilers, M. (2007). The ubiquitin-specific protease USP28 is required for MYC stability. Nat. Cell Biol. *9*, 765–774.

Qiu, H., Hu, C., Gaur, N.A., and Hinnebusch, A.G. (2012). Pol II CTD kinases Bur1 and Kin28 promote Spt5 CTR-independent recruitment of Paf1 complex. Embo J. *31*, 3494–3505.

Quinlan, A.R., and Hall, I.M. (2010). BEDTools: a flexible suite of utilities for comparing genomic features. Bioinformatics *26*, 841–842.

Rahl, P.B., and Young, R.A. (2014). MYC and transcription elongation. Cold Spring Harb Perspect Med *4*, a020990.

Rahl, P.B., Lin, C.Y., Seila, A.C., Flynn, R.A., McCuine, S., Burge, C.B., Sharp, P.A., and Young, R.A. (2010). c-Myc regulates transcriptional pause release. Cell *141*, 432–445.

Rape, M., Hoppe, T., Gorr, I., Kalocay, M., Richly, H., and Jentsch, S. (2001). Mobilization of processed, membrane-tethered SPT23 transcription factor by CDC48(UFD1/NPL4), a ubiquitin-selective chaperone. Cell *107*, 667–677.

Reid, G., Hübner, M.R., Métivier, R., Brand, H., Denger, S., Manu, D., Beaudouin, J., Ellenberg, J., and Gannon, F. (2003). Cyclic, proteasome-mediated turnover of unliganded and liganded ERalpha on responsive promoters is an integral feature of estrogen signaling. Mol. Cell *11*, 695–707.

Rosenberg-Hasson, Y., Bercovich, Z., Ciechanover, A., and Kahana, C. (1989). Degradation of ornithine decarboxylase in mammalian cells is ATP dependent but ubiquitin independent. Eur. J. Biochem. *185*, 469–474.

Sabò, A., Doni, M., and Amati, B. (2014a). SUMOylation of Myc-family proteins. PLoS ONE *9*, e91072.

Sabò, A., Kress, T.R., Pelizzola, M., de Pretis, S., Gorski, M.M., Tesi, A., Morelli, M.J., Bora, P., Doni, M., Verrecchia, A., et al. (2014b). Selective transcriptional regulation by Myc in cellular growth control and lymphomagenesis. Nature *511*, 488–492.

Sachdeva, M., Zhu, S., Wu, F., Wu, H., Walia, V., Kumar, S., Elble, R., Watabe, K., and Mo, Y.-Y. (2009). p53 represses c-Myc through induction of the tumor suppressor miR-145. Proc. Natl. Acad. Sci. U.S.a. *106*, 3207–3212.

Salghetti, S.E., Caudy, A.A., Chenoweth, J.G., and Tansey, W.P. (2001). Regulation of transcriptional activation domain function by ubiquitin. Science *293*, 1651–1653.

Salghetti, S.E., Muratani, M., Wijnen, H., Futcher, B., and Tansey, W.P. (2000). Functional overlap of sequences that activate transcription and signal ubiquitin-mediated proteolysis. Proc. Natl. Acad. Sci. U.S.a. *97*, 3118–3123.

Sampson, V.B., Rong, N.H., Han, J., Yang, Q., Aris, V., Soteropoulos, P., Petrelli, N.J., Dunn, S.P., and Krueger, L.J. (2007). MicroRNA let-7a down-regulates MYC and reverts MYC-induced growth in Burkitt lymphoma cells. Cancer Res. *67*, 9762–9770.

Sanchez-Arévalo Lobo, V.J., Doni, M., Verrecchia, A., Sanulli, S., Fagà, G., Piontini, A., Bianchi, M., Conacci-Sorrell, M., Mazzarol, G., Peg, V., et al. (2013). Dual regulation of Myc by Abl. Oncogene *32*, 5261–5271.

Saponaro, M., Kantidakis, T., Mitter, R., Kelly, G.P., Heron, M., Williams, H., Söding, J., Stewart, A., and Svejstrup, J.Q. (2014). RECQL5 controls transcript elongation and suppresses genome instability associated with transcription stress. Cell *157*, 1037–1049.

Saunders, A., Core, L.J., and Lis, J.T. (2006). Breaking barriers to transcription elongation. Nat. Rev. Mol. Cell Biol. *7*, 557–567.

Schaub, F.X., and Cleveland, J.L. (2014). Tipping the MYC-MIZ1 balance: targeting the HUWE1 ubiquitin ligase selectively blocks MYC-activated genes. EMBO Mol Med.

Schwab, M., Alitalo, K., Klempnauer, K.H., Varmus, H.E., Bishop, J.M., Gilbert, F., Brodeur, G., Goldstein, M., and Trent, J. (1983). Amplified DNA with limited homology to myc cellular oncogene is shared by human neuroblastoma cell lines and a neuroblastoma tumour. Nature *305*, 245–248.

Schwamborn, J.C., Berezikov, E., and Knoblich, J.A. (2009). The TRIM-NHL protein TRIM32 activates microRNAs and prevents self-renewal in mouse neural progenitors. Cell *136*, 913–925.

Schwanhäusser, B., Busse, D., Li, N., Dittmar, G., Schuchhardt, J., Wolf, J., Chen, W., and Selbach, M. (2011). Global quantification of mammalian gene expression control. Nature *473*, 337–342.

Sears, R., Leone, G., DeGregori, J., and Nevins, J.R. (1999). Ras enhances Myc protein stability. Mol. Cell *3*, 169–179.

Sears, R., Nuckolls, F., Haura, E., Taya, Y., Tamai, K., and Nevins, J.R. (2000). Multiple Ras-dependent phosphorylation pathways regulate Myc protein stability. Genes Dev. *14*, 2501–2514.

Shandilya, J., and Roberts, S.G.E. (2012). The transcription cycle in eukaryotes: from productive initiation to RNA polymerase II recycling. Biochim. Biophys. Acta *1819*, 391–400.

Sheaff, R.J., Singer, J.D., Swanger, J., Smitherman, M., Roberts, J.M., and Clurman, B.E. (2000). Proteasomal turnover of p21Cip1 does not require p21Cip1 ubiquitination. Mol. Cell *5*, 403–410.

Sheiness, D., and Bishop, J.M. (1979). DNA and RNA from uninfected vertebrate cells contain nucleotide sequences related to the putative transforming gene of avian myelocytomatosis virus. J. Virol. *31*, 514–521.

Sikder, D., Johnston, S.A., and Kodadek, T. (2006). Widespread, but non-identical, association of proteasomal 19 and 20 S proteins with yeast chromatin. J. Biol. Chem. *281*, 27346–27355.

Sims, R.J., Belotserkovskaya, R., and Reinberg, D. (2004). Elongation by RNA polymerase II: the short and long of it. Genes Dev. *18*, 2437–2468.

Soule, H.D., Maloney, T.M., Wolman, S.R., Peterson, W.D., Brenz, R., McGrath, C.M., Russo, J., Pauley, R.J., Jones, R.F., and Brooks, S.C. (1990). Isolation and characterization of a spontaneously immortalized human breast epithelial cell line, MCF-10. Cancer Res. *50*, 6075–6086.

Staller, P., Peukert, K., Kiermaier, A., Seoane, J., Lukas, J., Karsunky, H., Möröy, T., Bartek, J., Massagué, J., Hänel, F., et al. (2001). Repression of p15INK4b expression by Myc through association with Miz-1. Nat. Cell Biol. *3*, 392–399.

Steiger, D., Furrer, M., Schwinkendorf, D., and Gallant, P. (2008). Max-independent functions of Myc in Drosophila melanogaster. Nat. Genet. *40*, 1084–1091.

Subramanian, A., Tamayo, P., Mootha, V.K., Mukherjee, S., Ebert, B.L., Gillette, M.A., Paulovich, A., Pomeroy, S.L., Golub, T.R., Lander, E.S., et al. (2005). Gene set enrichment analysis: a knowledge-based approach for interpreting genome-wide expression profiles. Proc. Natl. Acad. Sci. U.S.a. *102*, 15545–15550.

Sun, X.-X., He, X., Yin, L., Komada, M., Sears, R.C., and Dai, M.-S. (2015). The nucleolar ubiquitin-specific protease USP36 deubiquitinates and stabilizes c-Myc. Proc. Natl. Acad. Sci. U.S.a. *112*, 3734–3739.

Svejstrup, J.Q. (2004). The RNA polymerase II transcription cycle: cycling through chromatin. Biochim. Biophys. Acta *1677*, 64–73.

Tait, S.W.G., de Vries, E., Maas, C., Keller, A.M., D'Santos, C.S., and Borst, J. (2007). Apoptosis induction by Bid requires unconventional ubiquitination and degradation of its N-terminal fragment. J. Cell Biol. *179*, 1453–1466.

Taub, R., Kirsch, I., Morton, C., Lenoir, G., Swan, D., Tronick, S., Aaronson, S., and Leder, P. (1982). Translocation of the c-myc gene into the immunoglobulin heavy chain locus in human Burkitt lymphoma and murine plasmacytoma cells. Proc. Natl. Acad. Sci. U.S.a. *79*, 7837–7841.

Thomas, L.R., Wang, Q., Grieb, B.C., Phan, J., Foshage, A.M., Sun, Q., Olejniczak, E.T., Clark, T., Dey, S., Lorey, S., et al. (2015). Interaction with WDR5 Promotes Target Gene Recognition and Tumorigenesis by MYC. Mol. Cell.

Toews, J., Rogalski, J.C., Clark, T.J., and Kast, J. (2008). Mass spectrometric identification of formaldehyde-induced peptide modifications under in vivo protein cross-linking conditions. Anal. Chim. Acta *618*, 168–183.

Tomson, B.N., and Arndt, K.M. (2013). The many roles of the conserved eukaryotic Paf1 complex in regulating transcription, histone modifications, and disease states. Biochim. Biophys. Acta *1829*, 116–126.

Tworkowski, K.A., Salghetti, S.E., and Tansey, W.P. (2002). Stable and unstable pools of Myc protein exist in human cells. Oncogene *21*, 8515–8520.

van der Horst, A., de Vries-Smits, A.M.M., Brenkman, A.B., van Triest, M.H., van den Broek, N., Colland, F., Maurice, M.M., and Burgering, B.M.T. (2006). FOXO4 transcriptional activity is regulated by monoubiquitination and USP7/HAUSP. Nat. Cell Biol. *8*, 1064–1073.

Vervoorts, J., Lüscher-Firzlaff, J.M., Rottmann, S., Lilischkis, R., Walsemann, G., Dohmann, K., Austen, M., and Lüscher, B. (2003). Stimulation of c-MYC transcriptional activity and acetylation by recruitment of the cofactor CBP. EMBO Rep. *4*, 484–490.

Voges, D., Zwickl, P., and Baumeister, W. (1999). The 26S proteasome: a molecular machine designed for controlled proteolysis. Annu. Rev. Biochem. *68*, 1015–1068.

Walker, C.W., Boom, J.D., and Marsh, A.G. (1992). First non-vertebrate member of the myc gene family is seasonally expressed in an invertebrate testis. Oncogene *7*, 2007–2012.

Walz, S., Lorenzin, F., Morton, J., Wiese, K.E., Eyss, von, B., Herold, S., Rycak, L., Dumay-Odelot, H., Karim, S., Bartkuhn, M., et al. (2014). Activation and repression by oncogenic MYC shape tumour-specific gene expression profiles. Nature *511*, 483–487.

Wang, H., Wang, L., Erdjument-Bromage, H., Vidal, M., Tempst, P., Jones, R.S., and Zhang, Y. (2004). Role of histone H2A ubiquitination in Polycomb silencing. Nature *431*, 873–878.

Wang, X., and Hayes, J.J. (2008). Acetylation mimics within individual core histone tail domains indicate distinct roles in regulating the stability of higher-order chromatin structure. Mol. Cell. Biol. *28*, 227–236.

Wang, X., Cunningham, M., Zhang, X., Tokarz, S., Laraway, B., Troxell, M., and Sears, R.C. (2011). Phosphorylation regulates c-Myc's oncogenic activity in the mammary gland. Cancer Res. *71*, 925–936.

Wang, X., Muratani, M., Tansey, W.P., and Ptashne, M. (2010). Proteolytic instability and the action of nonclassical transcriptional activators. Curr. Biol. *20*, 868–871.

Wasylishen, A.R., Chan-Seng-Yue, M., Bros, C., Dingar, D., Tu, W.B., Kalkat, M., Chan, P.-K., Mullen, P.J., Huang, L., Meyer, N., et al. (2013). MYC phosphorylation at novel regulatory regions suppresses transforming activity. Cancer Res. *73*, 6504–6515.

Welcker, M., Orian, A., Grim, J.E., Grim, J.A., Eisenman, R.N., and Clurman, B.E. (2004a). A nucleolar isoform of the Fbw7 ubiquitin ligase regulates c-Myc and cell size. Curr. Biol. *14*, 1852–1857.

Welcker, M., Orian, A., Jin, J., Grim, J.E., Grim, J.A., Harper, J.W., Eisenman, R.N., and Clurman, B.E. (2004b). The Fbw7 tumor suppressor regulates glycogen synthase kinase 3 phosphorylation-dependent c-Myc protein degradation. Proc. Natl. Acad. Sci. U.S.a. *101*, 9085–9090.

Wierstra, I., and Alves, J. (2008). The c-myc promoter: still MysterY and challenge. Adv. Cancer Res. *99*, 113–333.

Wiese, K.E., Haikala, H.M., Eyss, von, B., Wolf, E., Esnault, C., Rosenwald, A., Treisman, R., Klefström, J., and Eilers, M. (2015). Repression of SRF target genes is critical for Myc-dependent apoptosis of epithelial cells. Embo J.

Wiese, K.E., Walz, S., Eyss, von, B., Wolf, E., Athineos, D., Sansom, O., and Eilers, M. (2013). The role of MIZ-1 in MYC-dependent tumorigenesis. Cold Spring Harb Perspect Med *3*, a014290.

Wilcox, A.J., and Laney, J.D. (2009). A ubiquitin-selective AAA-ATPase mediates transcriptional switching by remodelling a repressor-promoter DNA complex. Nat. Cell Biol. *11*, 1481–1486.

Wilson, M.D., Saponaro, M., Leidl, M.A., and Svejstrup, J.Q. (2012). MultiDsk: a ubiquitin-specific affinity resin. PLoS ONE *7*, e46398.

Wolf, E., Gebhardt, A., Kawauchi, D., Walz, S., Eyss, von, B., Wagner, N., Renninger, C., Krohne, G., Asan, E., Roussel, M.F., et al. (2013). Miz1 is required to maintain autophagic flux. Nat Commun *4*, 2535.

Wolf, E., Lin, C.Y., Eilers, M., and Levens, D.L. (2015). Taming of the beast: shaping Myc-dependent amplification. Trends Cell Biol. *25*, 241–248.

Wood, M.A., McMahon, S.B., and Cole, M.D. (2000). An ATPase/helicase complex is an essential cofactor for oncogenic transformation by c-Myc. Mol. Cell *5*, 321–330.

Worsham, M.J., Pals, G., Schouten, J.P., Miller, F., Tiwari, N., van Spaendonk, R., and Wolman, S.R. (2006). High-resolution mapping of molecular events associated with immortalization, transformation, and progression to breast cancer in the MCF10 model. Breast Cancer Res. Treat. *96*, 177–186.

Wu, R.-C., Feng, Q., Lonard, D.M., and O'Malley, B.W. (2007). SRC-3 coactivator functional lifetime is regulated by a phospho-dependent ubiquitin time clock. Cell *129*, 1125–1140.

Wyce, A., Xiao, T., Whelan, K.A., Kosman, C., Walter, W., Eick, D., Hughes, T.R., Krogan, N.J., Strahl, B.D., and Berger, S.L. (2007). H2B ubiquitylation acts as a barrier to Ctk1 nucleosomal recruitment prior to removal by Ubp8 within a SAGA-related complex. Mol. Cell *27*, 275–288.

Xu, W. (2015). Personal communication.

Yada, M., Hatakeyama, S., Kamura, T., Nishiyama, M., Tsunematsu, R., Imaki, H., Ishida, N., Okumura, F., Nakayama, K., and Nakayama, K.I. (2004). Phosphorylation-dependent degradation of c-Myc is mediated by the F-box protein Fbw7. Embo J. *23*, 2116–2125.

Yamada, T., Yamaguchi, Y., Inukai, N., Okamoto, S., Mura, T., and Handa, H. (2006). P-TEFb-mediated phosphorylation of hSpt5 C-terminal repeats is critical for processive transcription elongation. Mol. Cell *21*, 227–237.

Yan, Q., Cho, E., Lockett, S., and Muegge, K. (2003). Association of Lsh, a regulator of DNA methylation, with pericentromeric heterochromatin is dependent on intact heterochromatin. Mol. Cell. Biol. *23*, 8416–8428.

Yang, Y., Do, H., Tian, X., Zhang, C., Liu, X., Dada, L.A., Sznajder, J.I., and Liu, J. (2010). E3 ubiquitin ligase Mule ubiquitinates Miz1 and is required for TNFalpha-induced JNK activation. Proc. Natl. Acad. Sci. U.S.a. *107*, 13444–13449.

Yang, Z., Yik, J.H.N., Chen, R., He, N., Jang, M.K., Ozato, K., and Zhou, Q. (2005). Recruitment of P-TEFb for stimulation of transcriptional elongation by the bromodomain protein Brd4. Mol. Cell *19*, 535–545.

Yeh, E., Cunningham, M., Arnold, H., Chasse, D., Monteith, T., Ivaldi, G., Hahn, W.C., Stukenberg, P.T., Shenolikar, S., Uchida, T., et al. (2004). A signalling pathway controlling c-Myc degradation that impacts oncogenic transformation of human cells. Nat. Cell Biol. *6*, 308–318.

Zhang, J., Kan, S., Huang, B., Hao, Z., Mak, T.W., and Zhong, Q. (2011). Mule determines the apoptotic response to HDAC inhibitors by targeted ubiquitination and destruction of HDAC2. Genes Dev. *25*, 2610–2618.

Zhang, K., Faiola, F., and Martinez, E. (2005). Six lysine residues on c-Myc are direct substrates for acetylation by p300. Biochem. Biophys. Res. Commun. *336*, 274–280.

Zhang, Q., Spears, E., Boone, D.N., Li, Z., Gregory, M.A., and Hann, S.R. (2013). Domain-specific c-Myc ubiquitylation controls c-Myc transcriptional and apoptotic activity. Proc. Natl. Acad. Sci. U.S.a. *110*, 978–983.

Zhang, X.-Y., Varthi, M., Sykes, S.M., Phillips, C., Warzecha, C., Zhu, W., Wyce, A., Thorne, A.W., Berger, S.L., and McMahon, S.B. (2008). The putative cancer stem cell marker USP22 is a subunit of the human SAGA complex required for activated transcription and cell-cycle progression. Mol. Cell *29*, 102–111.

Zhao, X., Heng, J.I.-T., Guardavaccaro, D., Jiang, R., Pagano, M., Guillemot, F., Iavarone, A., and Lasorella, A. (2008a). The HECT-domain ubiquitin ligase Huwe1 controls neural differentiation and proliferation by destabilizing the N-Myc oncoprotein. Nat. Cell Biol. *10*, 643–653.

Zhao, Y., Lang, G., Ito, S., Bonnet, J., Metzger, E., Sawatsubashi, S., Suzuki, E., Le Guezennec, X., Stunnenberg, H.G., Krasnov, A., et al. (2008b). A TFTC/STAGA module mediates histone H2A and H2B deubiquitination, coactivates nuclear receptors, and counteracts heterochromatin silencing. Mol. Cell *29*, 92–101.

Zheng, N., Schulman, B.A., Song, L., Miller, J.J., Jeffrey, P.D., Wang, P., Chu, C., Koepp, D.M., Elledge, S.J., Pagano, M., et al. (2002). Structure of the Cul1-Rbx1-Skp1-F boxSkp2 SCF ubiquitin ligase complex. Nature *416*, 703–709.

Zhou, Q., and Yik, J.H.N. (2006). The Yin and Yang of P-TEFb regulation: implications for human immunodeficiency virus gene expression and global control of cell growth and differentiation. Microbiol. Mol. Biol. Rev. *70*, 646–659.

Zhu, B., Mandal, S.S., Pham, A.-D., Zheng, Y., Erdjument-Bromage, H., Batra, S.K., Tempst, P., and Reinberg, D. (2005). The human PAF complex coordinates transcription with events downstream of RNA synthesis. Genes Dev. *19*, 1668–1673.

Zhu, L. (2010). Skp2 knockout reduces cell proliferation and mouse body size: and prevents cancer? Cell Res. *20*, 605–607.

7 Appendix

7.1 Abbreviations

Prefixes

p	pico
n	nano
µ	micro
m	milli
c	centi
k	kilo

Units

°C	degree celsius
A	ampere
Da	dalton
g	gram
h	hour
l	liter
m	meter
min	minute
M	mol/l
s	second
U	unit
v/v	volumer per volume
w/v	weight per volume

Other Abbreviations

A	adenine
A	alanine, Ala
aa	amino acid
APS	ammoniumpersulfate
ATCC	American type culture collection

ATP	adenosin-5'-triphosphate
b2M	β2-microglobulin
BET	bromodomain and extra-terminal
bp	basepairs
BR	basic region
BrdU	5-bromo-2-deoxyuridine
BSA	bovine serum albumine
C	cytosine
cDNA	complementary DNA
CDK	cyclin-dependent kinase
CDS	coding sequence
ChIP	chromatin immunoprecipitation
ChIP-Seq	chromatin immunoprecipiation followed by deep-sequening
CHX	cycloheximide
CMV	cyctomegalovirus
CUL	cullin
CRL	cullin-RING ligase
Ctrl	control
ddH_2O	bidestilled water
DMEM	Dulbecco's Modified Eagle-Medium
DMSO	dimethylsulfoxide
DNA	deoxyribonucleic acid
dNTPs	deoxyribonucleoside-5'-triphosphate (dATP, dCTP, dGTP, dTTP)
DTT	dithiothreitol
DUB	deubiquitinating enzyme
E	glutamic acid, Glu
E1	ubiquitin-activating enzyme
E2	ubiquitin-conjugating enzyme
E3	ubiquitin ligase
E4	ubiquitin-chain elongation factor
Eμ	immunoglobulin heavy chain enhancer
E.coli	*Escherichia coli*
EDTA	ethylendiamintetraacetate

ECL	enhanced chemoluminescence
e.g.	exempli gratia, for example
EGF	epidermal growth factor
FBS	fetal bovine serum
FC	fold change
FDR	false discovery rate
Fig.	figure
g	rcf, relative centrifugal force
G	guanine
GFP	green fluorescent protein
GTP	guanosine-5'-triphosphate
HLH	helix-loop-helix
HECT	homologous to the E6-AP carboxl terminus
HRP	horseradish peroxidase
hygro	hygromycin
IgG	immunoglobulin
IF	immunofluorescence
IP	immunoprecipitation
IRES	internal ribosomal entry site
K	lysine, Lys
LB	lysogeny broth
LZ	leucine zipper
mRNA	messenger RNA
NEM	N-ethylmaleimide
NES	normalized enrichment score
NLS	nuclear localization signal
NP-40	Nonidet P-40
NTA	nitrilotriacetic acid
p	phospho
P	proline, Pro
PAGE	polyacrylamide-gelelectrophoresis
PBS	phosphate-buffered saline
PCR	polymerase chain reaction

PEI	polyethylenimin
PEST	proline-, glutamate-, serine-, threonine-rich region
PI	propidiumiodide
PIC	preinitiation complex
PMSF	phenylmethylsulfonyl fluoride
PVDF	polyvinylidene difluoride
qPCR	quantitative PCR
R	arginine, Arg
RING	really interesting new gene
RNA	ribonucleic acid
RNAPII	RNA polymerase II
RNase	ribonuclease
RPKM	reads per kilobase per million mapped reads
RT	room temperature
T	threonine, Thr
$t_{1/2}$	half-life
TBE	Tris-borate EDTA buffer
TBS	Tris-buffered saline
TBS-T	Tris-buffered saline with tween-20
TE	Tris-EDTA buffer
TEMED	N,N,N',N'-tetramethylethylendiamine
TNT	Tris-NaCl-Triton X100
TRD	transregulatory domain
Tris	Tris-(hydroxymethyl)-aminomethan
TRRAP	transactivation/ transformation-associated protein
S	serine, Ser
S	Svedberg
SCF complex	SKP1-CUL1-F-box containing complex
SD	standard deviation
SDS	sodium dodecyl sulfate
SDS-PAGE	SDS polyacrylamide gelelectrophoresis
SEM	standard error of the mean
siRNA	small interfering RNA

S-phase	synthesis phase
U	uridine
Ub	ubiquitin
UPS	ubiquitin-proteasome system
USP	ubiquitin-specific-protease
UTR	untranslated region
WT	wild type
Y	tyrosine, Tyr

7.2 Acknowledgements

First of all, I would like to thank Prof. Dr. Martin Eilers and Dr. Nikita Popov for supervising this thesis and for giving me the opportunity to work on this project. I am very grateful for their advice, constant support and motivation throughout this project.

I would also like to thank Prof. Dr. Hermann Schindelin for his support and commitment as a thesis committee member.

I thank Prof Dr. Thomas Sommer for being a member of my thesis committee and for providing the opportunity to present my project in his research group in Berlin. Thanks for the support beyond my diploma thesis!

I want to express my gratitude towards the Boehringer Ingelheim Fonds for their personal and financial support. Especially, I would like to thank the BIF for organizing the great summer schools in Hirschegg and the seminar week in Lautrach.

I would also like to thank the Graduate School of Life Sciences for providing soft skill courses and supporting the participation in conferences.

Many thanks to all former and current members of the Eilers, Gallant, Popov, Schulze and Wiegering lab for the amazing working atmosphere, fruitful discussions and technical help! I especially thank Renate Metz for her technical assistance and for helping me to harvest hundreds of cell culture dishes. Giacomo, Elmar, Carsten, Markus and Katrin – thanks for the coffee breaks, “Feierabendbiere” and all the fun we had together; thanks Christina, Anneli, Fra L, Maria, Fra D, Eva, Jiajia and Anne for the great time we had together, as well outside the lab.

Katrin, what would I have done without you? Thanks for cheering me up in hard times and the many laughs we had together!

I want to thank my family for their continuous encouragement, support and love! I simply cannot thank you enough! Finally, Björn, I would like to thank you not only for your contribution to this project with your bioinformatical skills but especially for supporting me in every possible way! Thanks for believing in me and finding always the right words! Without you this thesis would not have been what it is today!

7.3 Publications

Jaenicke LA*, von Eyss B*, Carstensen A, Xu W, Eilers M, Popov N. (2015) "Ubiquitin-dependent turnover of MYC promotes loading of the PAF complex on RNA Polymerase II to drive transcriptional elongation." Manuscript under review.
*authors contributed equally

von Eyss B, **Jaenicke LA**, Kortlever RM, Royla N, Wiese KE, Letschert S, Sauer M, Rosenwald A, Evan GI, Kempa S, Eilers M. (2015). "A MYC-driven change in mitochondrial dynamics limits YAP/TAZ function in mammary epithelial cells and breast cancer." *Cancer Cell*, Manuscript under review.

Schülein-Völk C, Wolf E, Zhu J, Xu W, Taranets L, Hellmann A, **Jaenicke LA**, Diefenbacher ME, Behrens A, Eilers M, Popov N. (2014). "Dual regulation of Fbw7 function an oncogenic transformation by Usp28." *Cell reports* 9(3): 1099-109.

Peter S, Bultinck J, Myant K, **Jaenicke LA**, Walz S, Müller J, Gmachl M, Treu M, Boehmelt G, Ade CP, Schmitz W, Wiegering A, Otto C, Popov N, Sansom O, Kraut N, Eilers M. (2014). "Tumor cell-specific inhibition of MYC function using small molecule inhibitors of the HUWE1 ubiquitin ligase." *EMBO Mol Med* 6(12): 1525-41

Diefenbacher ME, Popov N, Blake SM, Schülein-Völk C, Nye E, Spencer-Dene B, **Jaenicke LA**, Eilers M, Behrens A. (2014). "The deubiquitinase USP28 controls intestinal homeostasis and promotes colorectal cancer." *J Clin Invest* 124(8): 3407-18.

Jaenicke LA, Brendebach H, Selbach M, Hirsch C. (2011). "Yos9p assists in the degradation of certain non-glycosylated proteins from the endoplasmic reticulum." *Mol Biol Cell* 22(16): 2937-45.
(publication resulted from diploma thesis work)

Popov N, Schülein C, **Jaenicke LA**, Eilers M. (2010). "Ubiquitylation of the amino terminus of Myc by SCF(β-TrCP) antagonizes SCF(Fbw7)-mediated turnover." *Nat Cell Biol* 12(10): 973-81.

7.4 Curriculum vitae

7.5 Affidavit

I hereby confirm that my thesis entitled “Regulation of MYC Activity by the Ubiquitin-Proteasome System” is the result of my own work. I did not receive any help or support from commercial consultants. All sources and/or materials are listed and specified in the thesis.

Furthermore, I confirm that this thesis has not yet been submitted as part of another examination process neither in identical nor in similar form.

Place, Date

Signature